CMS physics technical design report, volume II: Physics performance

Appendix A. 95% CL limits and 5σ discoveries

A.1. Estimators of significance

Several methods exist to quantify the statistical "significance" of an expected signal at future experiments. Following the conventions in high energy physics, the term significance usually means the "number of standard deviations" an observed signal is above expected background fluctuations. It is understood implicitly that S should follow a Gaussian distribution with a standard deviation of one. In statistics, the determination of the sensitivity is a typical problem of hypothesis testing, aiming at the discrimination between a null-hypothesis H_0 stating that only background and no signal is present, and a alternative hypothesis H_1, which states the presence of a signal on top of the background. The "significance level" is the probability to find a value of a suitably constructed test statistic beyond a certain pre-specified critical value, beyond which the validity of H_1 is assumed. The significance level has to be converted into an equivalent number of Gaussian sigmas to arrive at the common terminology of a high-energy physicist.

Since a signal is usually searched for in many bins of a distribution, and in many channels, a very high value of the significance of a local excess of events must be demanded before an observed "peak" found somewhere in some distribution can be claimed to be an observation of a signal. If the position of the signal peak is not known a-priori and treated as a free parameter in searches for new physics, the probability of background fluctuations is much higher. This is quantified in a case study in Section A.2 below, and this aspect will need careful consideration in the near future before first data taking at the LHC. The general, somewhat arbitrary convention is that the value of S of a local signal excess should exceed five, meaning that the significance level, or the corresponding one-sided Gaussian probability that a local fluctuation of the background mimics a signal, is 2.9×10^{-7}.

Here, the recommendations for the procedures to be used for the studies presented in this document are summarised. The aim of many of these studies is the prediction of the average expected sensitivity to the observation of a new signal in a future experiment. The real experiment might be lucky, i.e. observe a higher significance than the average expectation, or a downward fluctuation of the expected signal could lead to a lower observed significance. The proposed methods have been checked in a large number of pseudo-experiments using Monte Carlo simulation in order to investigate whether the probability of a background fluctuation having produced the claimed significance of the discovery is properly described.

Counting methods use the number of signal events, s, and the number of background events, b, observed in some signal region to define the significance S. These event numbers can be turned into a significance, S_{cP}, by using either the Poisson distribution for small numbers of events, or, in the high-statistics limit, the Gaussian distribution, leading to

$$S_{c1} = \frac{s}{\sqrt{b}}. \tag{A.1}$$

The significance may also be obtained from the ratio of the likelihoods, $\mathcal{L}_1$ and $\mathcal{L}_0$, belonging to the hypothesis H_0 and H_1,

$$S_L = \sqrt{2 \ln Q}, \text{ with } Q = \frac{\mathcal{L}_0}{\mathcal{L}_1}. \tag{A.2}$$

This approach is theoretically well founded and is applicable also to the simple approach of the counting method, leading to

$$S_{cL} = \sqrt{2\left((s+b)\,\ln\left(1+\frac{s}{b}\right)-s\right)}, \tag{A.3}$$

which follows directly from the Poisson distribution. In the Gaussian limit of large numbers s and b, S_{cL} becomes equivalent to S_{c1}. The likelihood approach can be extended to include the full shapes of the signal and background distributions for the hypothesis H_0 and H_1, and the likelihood may be obtained from binned or unbinned likelihood fits of the background-only and the background-plus-signal hypotheses to the observed distributions of events.

Another estimator,

$$S_{c12} = 2\left(\sqrt{s+b}-\sqrt{b}\right), \tag{A.4}$$

has been suggested in the literature [79, 763]. The formula for S_{c12} is strictly only valid in the Gaussian limit, but tabulated values exist for small statistics.

The presence of systematic errors deserves some special care. Two cases must be separated clearly:

(a) If the background and signal contributions can be determined from the data, e.g. by extrapolating the background level into the signal region from sidebands, systematic errors may be irrelevant, and the systematic errors only influence our ability to predict the average expected sensitivity. In this case, simple propagation of the theoretical errors on s and b applied to the above formulae for the various significances is all that is needed.

(b) If systematic errors on the background will affect the determination of the signal in the real experiment, e.g. because an absolute prediction of the background level or a prediction of the background shape are needed, the theoretical uncertainty must be taken into account when estimating the sensitivity. This can be done by numerical convolution of the Poisson distribution, or the Gaussian distribution in the high-statistics limit, with the probability density function of the theoretical uncertainty. Numerical convolutions of the Poisson distribution with a theoretical error of a Gaussian shape, leading to a variant of S_{cP} including systematic errors, were used for this document [679]. Numerical convolutions of the Poisson distribution with a systematic error of a Gaussian shape, leading to a variant of S_{cP} including systematic errors, were used for this document. The program ScPf [679] computes the significance by Monte Carlo integration with the assumption of an additional Gaussian uncertainty Δb on b. The significance can be approximated by an extension of S_{c12}:

$$S_{c12s} = 2\left(\sqrt{s+b}-\sqrt{b}\right)\frac{b}{b+\Delta b^2}. \tag{A.5}$$

In the Gaussian limit it leads to

$$S_{c1} = s/\sqrt{b+\Delta b^2}. \tag{A.6}$$

The most crucial point in this context is a realistic description of the probability density function of the systematic theoretical uncertainty, which can be anything ranging from a flat distribution between $b \pm \Delta b$ to a pathological distribution with a significant non-Gaussian tail, but, in practice, is hardly ever known precisely.

The distribution of a significance estimator S in a series of experiments, its probability density function (p.d.f.), is of prime importance for the calculation of discovery probabilities in the presence of a real signal, or of fake probabilities due to fluctuations of the background. In the large-statistics limit, the likelihood-based significance estimators are expected to follow a χ^2-distribution with a number of degrees of freedom given by the difference in the number of free parameters between the alternative hypothesis and the null hypothesis [103]. When

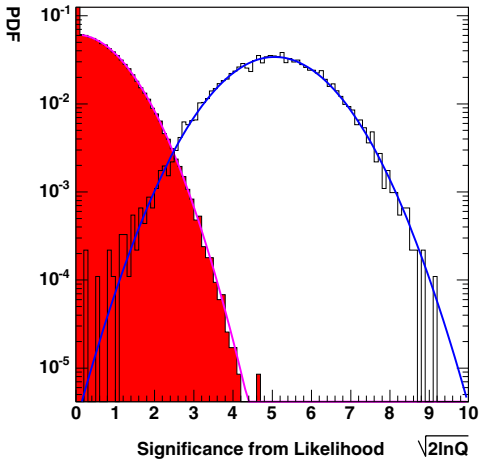

Figure A.1. Probability density functions of the estimator of significance S_L for small statistics (11 signal events over a background of 1.5 events). Filled histogram: pure background sample from 200 000 toy experiments, open histogram: background plus signal from 10 000 toy experiments. Gaussian fits are overlayed; the distribution of S_L for the background-only sample has a mean of -0.004 and a width of $\sigma = 1.0$, the background-plus-signal sample has a width of 1.1.

testing for the presence of a signal on top of background at a fixed peak position, $2 \ln Q = S_L^2$ is expected to follow a χ^2 distribution with one degree of freedom, i.e. a standard Gaussian distribution. All of the above estimators have been tested in a large number of toy experiments, see e.g. [60, 100, 102]. In particular the likelihood based estimators were found to be well-behaved, i.e. the distribution of the values of significance followed the expected behaviour already at moderate statistics, as is shown for one example in Fig. A.1. Good scaling with the square root of the integrated luminosity was also observed in these studies. On the other hand, the estimator S_{c1} cannot be considered a useful measure of significance at low statistics.

A quantitative comparison as a function of the number of background events for fixed values of $s/\sqrt{b}$ of the various estimators discussed above is shown in Fig. A.2. S_{cL} and S_{cP} are found to agree very well, while S_{c12} tends to slightly underestimate the significance, a result which was also verified in the above Monte Carlo studies with large samples of toy experiments. While S_{cL} and S_{cP} remain valid independent of the value of b, the simpler estimator S_{c1} can only be used for background levels larger than 50 events.

A.2. On the true significance of a local excess of events

In searching for new phenomena in a wide range of possible signal hypotheses (e.g. a narrow resonance of unknown mass over a broad range background), a special care must be exercised in evaluating the true significance of observing a local excess of events. In the past, this fact was given substantial scrutiny by statisticians (e.g. [764, 765]) and physicists (e.g., [766–770]) alike. The purpose of this Appendix is to quantify a possible scope of this effect on an example of a search for the Standard Model Higgs boson in the $H \to ZZ^{(*)} \to 4\mu$ decay channel. As the case study, we chose a counting experiment approach widely used in this volume.

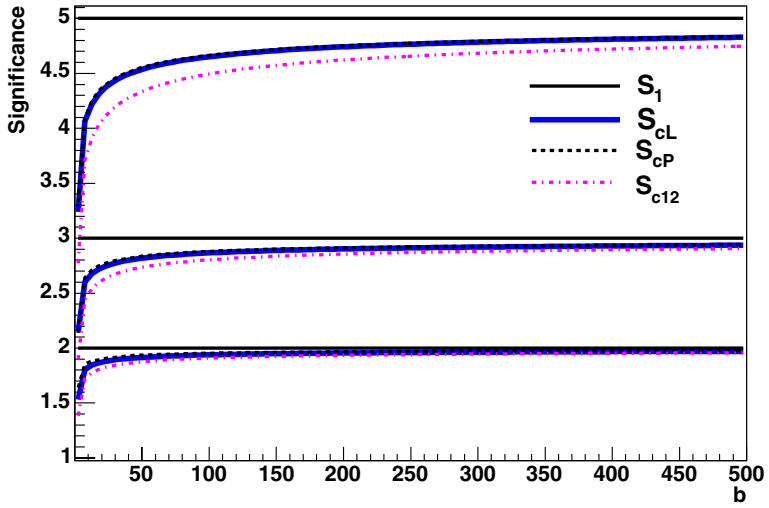

Figure A.2. Comparison of the various significance estimators as a function of the number of background events, b. The number of signal events was taken as $s = S_{c1}\sqrt{b}$, hence the constant black lines represent the value of S_{c1}. As can be seen, S_{cP} and S_{cL} agree perfectly, while S_{12} leads to slightly smaller values of significance. S_1 significantly overestimates the significance at small event numbers.

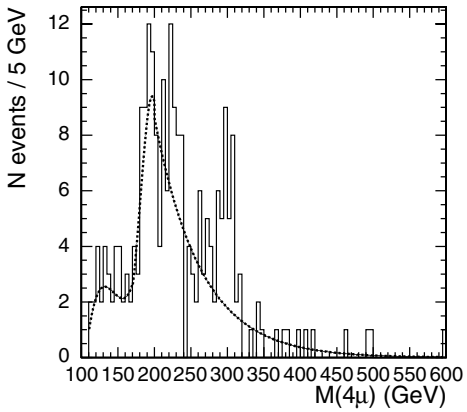

Figure A.3. The background *pdf* and an example of one pseudo-experiment with a statistical fluctuation appearing just like a signal.

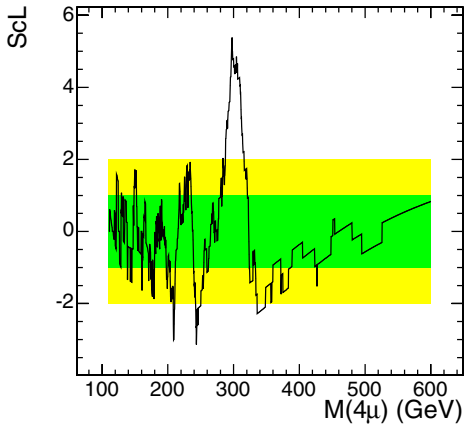

Figure A.4. Profile of the S_{cL} scan corresponding to the pseudo-experiment example shown on the left. Green (inner) and yellow (outer) bands denote $\pm 1\sigma$ and $\pm 2\sigma$ intervals. Spikes that can be seen are due to events coming in or dropping off the trial-window, a feature of low-statistics searches.

The dashed line in Fig. A.3 shows the expected 4μ invariant mass distribution for background at $\mathcal{L} = 30\,\text{fb}^{-1}$ after applying all the $m_{4\mu}$-dependent analysis cuts described in Sec. . Using this distribution, we played out $\sim 10^8$ pseudo-experiments; an example is shown in Fig. A.3. For each pseudo-experiment, we slid a *signal region window* across the spectrum looking for a local event excess over the expectation. The size of the window $\Delta m = w(m_{4\mu})$ was optimised and fixed *a priori* (about $\pm 2\sigma$) to give close to the best significance for a

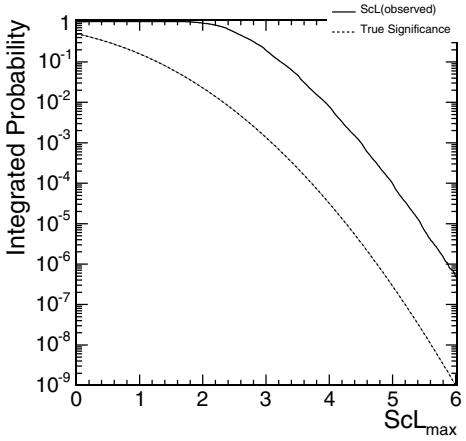

Figure A.5. S_{cL} cumulative probability density function.

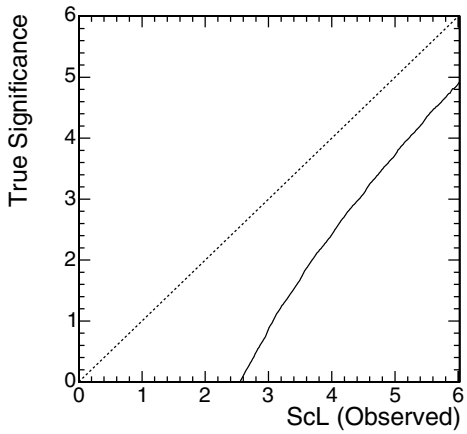

Figure A.6. Local significance "renormalisation" from an observed value to the true significance with a proper probabilistic interpretation.

resonance with a width corresponding to the experimental SM Higgs boson width $\sigma(m_{4\mu})$. The step of probing different values of $m_{4\mu}$ was "infinitesimally" small ($0.05\,\mathrm{GeV/c^2}$) in comparison to the Higgs boson width of more than $1\,\mathrm{GeV/c^2}$. The scanning was performed in *a priori* defined range of 115–600 $\mathrm{GeV/c^2}$.

We used a significance estimator $S_{cL} = \mathrm{sign}(s)\,\sqrt{2\,n_o \ln(1+s/b) - 2\,s}$, where b is the expected number of background events, n_o is the number of observed events, and the signal is defined as $s = n_o - b$. This estimator, based on the Log-Likelihood Ratio, is known to follow very closely the true Poisson significance, only slightly over-estimating it in the limit of small statistics [51]. Figure A.4 presents the results of such a scan for the pseudo-experiment shown in Fig. A.3. The maximum value of S_{cL}, S_{max}, and the corresponding mass of a "Higgs boson candidate" obtained in each pseudo-experiment were retained for further statistical studies.

After performing 10^8 pseudo-experiments, the differential probability density function for S_{max} and its corresponding cumulative probability function $P(S_{max} > S)$ (Fig. A.5) were calculated. From Fig. A.5, one can see that the frequency of observing some large values of S_{cL} (solid line) is much higher than its naive interpretation might imply (dashed line). If desired, the actual probability can be converted to the true significance. The result of such "renormalisation" is presented in Fig. A.6. One can clearly see that the required de-rating of significance is not negligible; in fact, it is larger than the effect of including all theoretical and instrumental systematic errors for this channel (see Section 3.1). More details on the various aspects of these studies can be found in [51].

There are ways of reducing the effect. A more detailed analysis of the shape of the $m_{4\mu}$ distribution will help somewhat. Using the predicted number of signal events $s = s_{theory}$ in the significance estimator to begin with and, then, for validating the statistical consistency of an excess $n_o - b$ with the expectation s_{theory} will reduce the effect further. One can also use a non-flat prior on the Higgs mass as it comes out from the precision electroweak measurements. Whether one will be able to bring the effect to a negligible level by using all these additional constraints on the signal hypotheses is yet to be seen. The purpose of this Appendix is not to give the final quantitative answer, but rather to assert that these studies must become an integral part of all future search analyses when multiple signal hypotheses are tried.

Appendix B. Systematic Errors

B.1. Theoretical uncertainties

The simulation of events at the LHC is complex and can be conventionally divided into different parts which either involve the description of the interesting physics process or the description of the initial scattering conditions and the physics environment.

The simulation of the hardest part of the physics process is done via matrix element (ME) calculations at a certain order in the coupling constants and continues with the parton showering (PS) of the resulting partons until a cut-off scale, over which the perturbative evolution stops and the fragmentation of the final partons takes on. This cut-off is often referred to as factorisation scale, because it is the scale at which the two processes (showering and fragmentation) are supposed to factorise.

The interesting event is accompanied by the so-called underlying event (UE), term which identifies all the remnant activity from the same proton-proton (p–p) interaction and whose definition often includes ISR as well, and the pile-up, composed by other minimum bias (MB) p–p interactions in the same bunch crossing (up to 25 at high luminosity at the LHC). Moreover, since the initial state is not defined in p–p collisions, a proper description of the proton parton density functions (PDFs) should be included in the calculations.

Each of these effects needs to be modelled to the best of our knowledge, and the associated uncertainties need to be determined and propagated to the physics measurements. Moreover, many of the sources are correlated: for instance, fragmentation and showering are obviously dependent on each other, and in turn they assume a certain description of the underlying event. The task of assessing systematics due to theory and modelling can therefore be a difficult one and can sometime contain a certain degree of arbitrariness.

In what follows we propose some guidelines for the estimation of errors coming from the above, trying to divide the systematics sources into wider categories as much uncorrelated as possible: QCD radiation, fragmentation description, PDFs, UE and MB.

In attributing systematic errors we believe that one should use motivated recipes, avoiding unrealistic scenarios which will lead to unnecessarily conservative errors or, much worse, totally arbitrary assumptions.

B.1.1. Hard process description and parametric uncertainties

The description of the hard process should be done with Monte Carlo tools which are best suited to the specific analysis. For instance, when precise description of hard gluon emission becomes an issue, then next-to-leading order (NLO) generator tools like MC@NLO [771], or higher leading order (LO) α_s generators like COMPHEP [43], MADGRAPH [81], ALPGEN [161], and SHERPA [194] should be considered. This is in general true for both the signal and the background description.

When adopting a ME tool, one should always keep in mind that its output is often (if not always) supposed to be interfaced to PS Monte Carlo such as HERWIG [196], PYTHIA [24] or ISAJET [672], that treat the soft radiation and the subsequent transition of the partons into observable hadrons. One of the most difficult problems is to eliminate double counting where jets can arise from both higher order ME calculations and from hard emission during the shower evolution. Much theoretical progress has been made recently in this field [772–775]. For what concerns the ME/PS matched description of multi-jet final states, a rich spectrum of processes is currently available in ALPGEN. However, adopting general purpose generators like PYTHIA can still be the best option for topologies that are better described in the Leading

Logarithm Approximation (LLA), for instance in the case of two leading jets and much softer secondary jets. The two different descriptions should be regarded as complementary.

In general, a sensible choice for the selection of the best generation tools can be driven by the HEPCODE data base [776]. However, comparison between different generators is recommended whenever applicable.

Each analysis needs then to make sure that other important effects (e.g. spin correlations in the final state, NLO ME corrections to top decays) are included in the generation mechanism. For example, TOPREX [44], as long with some of the Monte Carlo generators already introduced in this section, provides a correct treatment of top quark spin correlations in the final state. Neglecting some of these effects corresponds to introducing an error in the analysis that cannot be considered as coming from a theoretical uncertainty.

For both signal and backgrounds, missing higher orders are a delicate source of uncertainty. Formally, the associated error cannot be evaluated unless the higher order calculation is available. This is often not possible, unless extrapolating by using comparisons with analytical calculations of total or differential cross-sections at the next order, if available. One should keep in mind that simple K-factors are not always enough and that the inclusion of higher orders typically also involves distortions in differential distributions.

Moreover, one should not forget that any Standard Model calculation is performed in certain schemes and that the input parameters are subject to their experimental uncertainties; if the error on most of those and the choice of the renormalisation scheme are expected to give negligible effects in comparison with other uncertainties, this might not be so for the choice of the hard process scale, which we will discuss in the next section, and some of the input parameters.

Among the input parameters, by far the one known with less accuracy will be the top mass. The current uncertainty of about 2% [777] enters in the LO calculations for processes which involve top or Higgs production. For instance, the total $t\bar{t}$ cross-section is known to have a corresponding 10% uncertainty due to this [45]. As far as Higgs production (in association or not with tops) is concerned, gluon–gluon fusion proceeds via a top loop and therefore the total cross-section can have a strong dependence on the top mass when $m_H \approx 2m_t$. Analyses which include Higgs bosons or top are encouraged to estimate the dependence of the significant observables on the top mass itself. Effects of m_t variation on acceptances of these analyses should instead be negligible.

B.1.2. Hard process scale

The hard process under study drives the definition of the Q^2 scale, which directly enters in the parametrisation of PDFs and α_s, hence in the expression of the cross sections.

The dependence of the observables on the choice for the Q^2 hard process scale is unphysical and should be regarded as one important contribution to the total uncertainty in the theoretical predictions. The sensitivity of the predicted observables to such choice is expected to decrease with the increasing order in which the calculation is performed, and can be tested by changing the hard process scale parameters in the generation (where applicable) using a set of sound values according to the characteristics of the hard process.

A sensible choice for the hard process scale in $2 \to 1$ processes is often $\hat{s}$, which is the default in general purpose generators like PYTHIA. Alternative choices to quote theoretical uncertainties can be $0.25\hat{s}$ and $4.0\hat{s}$. In PYTHIA this can be obtained acting on PARP(34).

For $2 \to n$ processes, many reasonable alternatives for the Q^2 scale definition exist. The PYTHIA default (MSTP(32) = 8), corresponds to the average squared transverse mass of the outgoing objects. It is possible to test the sensitivity on the Q^2 scale switching to different options, for example trying $Q^2 = \hat{s}$ (MSTP(32) = 4 in PYTHIA).

B.1.3. PDF description

The parton distribution functions of interacting particles describe the probability density for partons undergoing hard scattering at the hard process scale Q^2 and taking a certain fraction x of the total particle momentum. Since the Q^2 evolution can be calculated perturbatively in the framework of QCD, PDFs measurements can be cross checked using heterogeneous DIS, Drell–Yan and jet data, and achieve predictivity for points where no direct measurements are available yet, for example in a large region of the (x,Q^2) space for p–p interactions at the LHC energy.

Various approaches are currently available to quote the PDFs of the proton, which propose different solutions for what concerns the functional form, the theoretical scheme, the order of the QCD global analysis (including possible QED corrections), and the samples of data retained in the fits: CTEQ [778], MRST [779], Botje [780], Alekhin [781], etc. The CTEQ and MRST PDFs, including Tevatron jet data in the fits, seem to be well suited for use in Monte Carlo simulations for the LHC.

The best way to evaluate theoretical uncertainties due to a certain proton PDFs is to vary the errors on the parameters of the PDF fit itself. With the Les Houches accord [95] PDF (LHAPDF) errors should be easily propagated via re-weighting to the final observables. However, errors are available only for NLO PDF, whereas in most of the cases only LO tools are available for the process calculation. Correctly performing evaluation of theoretical uncertainties in these cases requires some care. The proposed solution is to adopt CTEQxL (LO) for the reference predictions using CTEQxM (NLO) only to determine the errors.

For analyses which are known to be particularly sensitive to PDFs, like cross-section measurements, it would be also desirable to compare two different sets of PDFs (typically CTEQ vs MRST) taking then the maximum variation as an extra error. This is important since, even considering the error boundaries, different set of PDFs may not overlap in some region of the phase space.

The LHAGLUE interface [95] included from the most recent LHAPDF versions simplifies the use of the Les Houches accord PDF in PYTHIA by the switches MSTP(52) = 2, MSTP(51) = LHAPDF$_{id}$.

B.1.4. QCD radiation: the parton shower Monte Carlo

The showering algorithm is basically a numeric Markov-like implementation of the QCD dynamic in the LLA. After the generation of a given configuration at partonic level, the initial state radiation (ISR) and the final state radiation (FSR) are produced following unitary evolutions with probabilities defined by the showering algorithm.

The probability for a parton to radiate, generating a $1\rightarrow 2$ branching, are given by the Altarelli–Parisi equations [782], however various implementations of the showering algorithm exist in parton shower Monte Carlo, which mostly differ for the definition of the Q^2 evolution variable (virtuality scale) in the $1\rightarrow 2$ radiation branching and for the possible prescriptions limiting the phase space accessible to the radiation: PYTHIA, HERWIG, ARIADNE [783], ISAJET etc.

The virtuality scales for both ISR and FSR need to be matched to the hard process scale, the latter setting an upper limit on the former ones; such limit has to be considered in a flexible way, given the level of arbitrariness in the scale definitions. While this matching is somewhat guaranteed if one adopts the same simulation tool for both hard scattering and parton shower, a careful cross check is recommended in all other cases. In general, a critical judgement taking into account the hard process type is needed. Allowing a virtuality scale higher than the hard

process scale may give rise to double counting. This is the case of gg→gg processes with additional hard gluons added in the showering. However other processes are safer from this point of view, for instance the case of the $q\bar{q} \to Z$ process at LO.

Quantum interference effects in hadronic collisions have been observed by CDF [784] and DØ [785] studying the kinematical correlations between the third jet (regarded as the result of a soft branching in the LLA) and the second one. The implementation of the so called colour coherence in PS Monte Carlo is made in the limit of large number of colours and for soft and collinear emissions, restricting the phase space available to the radiation depending on the developed colour configuration. Different implementations of the colour coherence are available in HERWIG and PYTHIA, while ISAJET doesn't take into account such effects.

The theoretical uncertainty associated to the parton showering descriptions, includes what is normally referred to as ISR or FSR and their interference. In order to achieve practical examples for the recommended parton shower settings, we will consider PYTHIA as the default tool for showering from now on.

Turning OFF ISR and FSR (MSTP(61) = 0, MSTP(71) = 0 respectively) or even the interference part (MSTP(62) = 0, MSTP(67) = 0) is certainly a too crude approach and, to a large extent, a totally arbitrary procedure to assess a systematic error. We believe it is much more realistic to vary, according to sound boundaries, the switches regulating the amount and the strength of the radiation of the showering. These can correspond to Λ_{QCD} and the maximum virtuality scales up to which ISR stops and from which FSR starts. It would be important to switch the parameters consistently going from low to high values in both ISR and FSR.

Notice that the radiation parameters were typically fitted at LEP1 together with the fragmentation parameters, benefiting from a much simplified scenario where no ambiguity on the maximum virtuality scale applies, the only relevant energy scale of the problem being $\hat{s} = s$. One has to take into account that while for instance FSR accompanying heavy boson decays at the LHC can be directly related to the LEP experience, FSR in processes like $gg \to b\bar{b}$ entails additional uncertainties arising from the maximum allowed virtuality scale and ISR/FSR interference. On top of that, additional complications arise from the fact that ISR at hadron machines contributes to the description of the underlying event. Matching two different tunings of the same parameter (in particular PARP(67)) can be very subtle at the LHC.

These are the suggested settings in PYTHIA, which have been cross-checked with the ones adopted by the CDF experiment and also follow the prescription by the main author:

- Λ_{QCD}: PARP(61), PARP(72), PARJ(81) from 0.15 to 0.35 GeV consistently, symmetric with respect to 0.25. Notice that these settings have been optimised for the CTEQ6L PDFs. In general different ranges apply when changing PDFs. In order to give the user full control on these parameters the option MSTP(3) = 1 has to be set, otherwise Λ_{QCD} is assumed to be derived from the PDFs parametrisation.
- Q^2_{max}: PARP(67) from 0.25 to 4 and PARP(71) from 1 to 16 going from low to high emission in a correlated way. In doing so one should also make sure that the tuning of the underlying event is not changing at the same time. Possible re-tuning of the underlying event in different radiation scenarios may be needed, in particular for what concerns PARP(82).

B.1.5. Fragmentation

Perturbative QCD cannot provide the full description of the transition from primary quarks to observable hadrons, but only the part which involves large momentum transfer. The formation of final hadrons involves a range of interactions which goes above the Fermi scale and where

the strong coupling constant α_s increases above unity, making it necessary to describe this part in a non-perturbative way, normally referred to as fragmentation or hadronisation.

The non-perturbative description of fragmentation is realised via models, which need to be tuned to experimental data. The data correspond, typically, to event shapes and multiplicities at leptonic machines or to the inclusive jet shapes at hadronic machines. A comprehensive overview of the models can be found in [786].

Fragmentation is said to depend only on the factorisation scale if jet universality is assumed, i.e. assuming that jets fragment in the same way at hadron and lepton machines. Jet universality will be ultimately verified at the LHC; one should clarify whether instrumental effects and the LHC environment will have an impact on the final observables. For instance, the much larger fraction of gluon jets or the different description of the underlying event can change the values of the parameters that regulate the fragmentation. Moreover, for events with high multiplicity of jets it will also be crucial to properly describe fragmentation in conditions where large jet overlapping is to be expected and where inclusive tunings might not be ideal.

The consequence of jet universality is that, once the PS cut-off scale is fixed, the fragmentation description for light quarks should be universal, and the LEP/SLD tunings (or the Tevatron ones) could be used as they are for the LHC.

It is important to underline that the description of the non-perturbative part of the radiation also depends on the way the perturbative one is described. This means that one should not use a tuning of fragmentation done with LO(+LL) tools (typically PYTHIA at LEP) attached to perturbative calculation which are done at higher (or different) order.

B.1.5.1. Light quarks fragmentation. In the absence of LHC data, the best choice is therefore to use a model tuned to the LEP and SLD data [787–789]. It is important to choose the tuning in a consistent way from the same experiment, given that a combined LEP/SLD tuning has never been attempted. As a possibility, suggested by the major success in describing the data and by its extensive use in the experimental collaborations, is the use of PYTHIA, which uses the string (or Lund) fragmentation model [790]. The parameters that we consider more relevant in PYTHIA for the description of fragmentation are the following, where the central value is taken by the fit performed by the OPAL Collaboration, as an example:

PARJ(81) = 0.250
PARJ(82) = 1.90
PARJ(41) = 0.11
PARJ(42) = 0.52
PARJ(21) = 0.40

where PARJ(81) (Λ_{QCD}) and PARJ(82) (Q^2_{min}) refer to the radiation part. To properly evaluate a systematic error due to pure fragmentation one should vary only PARJ(42) and PARJ(21) by their respective errors (0.04 and 0.03 for OPAL). The variation should account for the proper parameter correlation if the effect is critical for the analysis. PARJ(41) is totally correlated to PARJ(42).

Alternatively, or additionally, it would also be important to compare PYTHIA with HERWIG with consistent tunings from LEP [787–789]; in doing so it is important to factorise the UE description (see next section) that can induce important differences in the results.

B.1.5.2. Heavy quarks fragmentation. The description of the heavy quarks fragmentation is important for top physics and for those processes with large b production in the final states. Exclusive channels are particularly influenced by the description of the fragmentation of the b quark.

The description of the fragmentation of the heavy quarks has been tuned to Z data at LEP and SLD[778, 791–793] (via a measurement of x_B and x_D) and $b\bar{b}$ data at the Tevatron, using different fragmentation functions like Lund, Bowler [794], Peterson [795], Kartvelishvili [796].

In the spirit of fragmentation universality the LEP/SLD tunings can be adopted for the LHC, but with much care. Significant differences among the fitted values in different experiment can point out that the factorisation scale used for the PS is not the same everywhere. One should make sure that the scale used is set consistently with the chosen fragmentation function parameters. This can be done by using the tuning from only one experiment, making sure to also use the main switches of the parton showering, (PARJ(81) and PARJ(82) in PYTHIA).

The fragmentation function that best describes heavy flavour data at LEP is Bowler. With the same OPAL tuning reported above the best fit of the Bowler parameters, a and $bm_\perp^2$, to data gives:

$bm_\perp^2 = 65^{+17}_{-14}$
$a = 15.0 \pm 2.3.$

The Bowler model would extend the string model to heavy flavours, describing the corrections in terms of the charm and bottom masses. Unfortunately, no tuning exists in the literature which is capable to describe at the same time light and heavy quark fragmentation, i.e. adopting universal parameters $a = \text{PARJ}(41)$ and $b = \text{PARJ}(42)$ for both light and heavy quarks.

Alternatively, the widely used Peterson function can be used, and its parameters are directly switchable in PYTHIA for just b and c fragmentation:

$\text{PARJ}(54) = -0.031 \pm 0.011$
$\text{PARJ}(55) = -0.0041 \pm 0.0004$

where the two parameters correspond, respectively, to ε_c and ε_b fitted in the OPAL tuning. The systematic can then be evaluated by varying the errors on the fitted parameters or by comparing with a different fragmentation function like Kartvelishvili, or Lund.

An important feature of the b fragmentation that should be considered by those analyses in the top sector sensitive to the details of the fragmentation, is the way the b fragments in top decays. At the LHC the b from a t is hadronising with a beam remnant, introducing potentially worrying differences with respect to the fragmentation at LEP. The main effects are presented in [797] and are known as *cluster collapse*, happening when a very low mass strings quark-remnant directly produces hadrons without fragmenting, hence enhancing the original flavour content, and *beam drag*, which is an angular distortion of hadron distribution toward the end of the string in the remnant. If, under reasonable assumptions on the transverse momentum in top events at the LHC, one can exclude to a large extent the importance of the first effect, beam drag could potentially introduce B meson production asymmetries, even though estimations are keeping the effect at the level of 1% at the LHC [797].

B.1.6. Minimum bias and underlying event

Multiple parton interaction models, extending the QCD perturbative picture to the soft regime, turn out to be particularly adequate to describe the physics of minimum bias and underlying event. Examples of these models are implemented in the general purpose simulation programs PYTHIA, HERWIG/JIMMY [193] and SHERPA. Other successful descriptions of underlying event and minimum bias at hadron colliders are achieved by alternative approaches like PHOJET [798], which rely on both perturbative QCD and Double Pomeron Models (DPM).

Huge progress in the phenomenological study of the underlying event in jet events have been achieved by the CDF experiment at Tevatron [799], using the multiplicity and transverse momentum spectra of charged tracks in different regions in the azimuth-pseudorapidity space defined with respect to the direction of the leading jet. Regions that receive contributions only by the underlying event have been identified. The average charged multiplicity per unit of pseudorapidity in these regions turns out to be significantly higher with respect to the one measured in minimum bias events. This effect, referred to as "pedestal effect", is well reproduced only by varying impact parameters models with correlated parton-parton interactions (MSTP(82) > 1 in PYTHIA). Simpler models are definitely ruled out.

The main problem of extrapolating the predictions of the multiple interactions models to the LHC is that some of the parameters are explicitly energy dependent, in particular the colour screening p_T cut-off (PARP(82) at the tuning energy PARP(89) in PYTHIA). The CDF tuning, often referred to as Tune-A, is not concentrating on this particular aspect. Other works [197, 800] have put more emphasis on this issue. However, one of their results is that currently only PYTHIA can be tuned to provide at the same time description of CDF and lower energy minimum bias data from UA5. One of these tunings can be summarised as follows:

- PARP(82) = 2.9
- PARP(83) = 0.5
- PAPR(84) = 0.4
- PARP(85) = 0.33
- PARP(86) = 0.66
- PARP(89) = 14000
- PARP(90) = 0.16
- PARP(91) = 1.0
- MSTP(81) = 1
- MSTP(82) = 4.

Sensible estimation of theoretical uncertainties arising from underlying event and minimum bias modelling can be performed assigning $\pm 3\sigma$ variations to the colour screening p_T cut-off parameter tuned on minimum bias CDF and UA5 data and extrapolated to the LHC energy [800], i.e. varying PARP(82) in the range [2.4–3.4], while keeping the other parameters listed above to their tuned values.

As a new tool for the description of UE and MB we would like to mention PYTHIA 6.3 [801], that allows for new interesting features, including the new p_T-ordered initial- and final-state showers and a new very sophisticated multiple interactions model that achieves description of colliding partons in the proton in terms of correlated multi-parton distribution functions of flavours, colours and longitudinal momenta. However, as stressed by the PYTHIA authors, the new model (PYEVNW) is still not so well explored. Therefore the old model (PYEVNT) is retained as the default choice, with full backward compatibility. Moreover, in the use of PYTHIA 6.3, one should be careful when switching to the new p_T-ordered showers and multiple interaction models, as their parameters are not tuned yet, in particular for what concerns the energy dependence, necessary to get meaningful extrapolations at the LHC energy.

B.1.7. Pile-up and LHC cross sections

The design parameters of the LHC at both low and high luminosity are such that, on top of possible signal events, additional minimum bias interactions are produced in the same beam crossing, the so-called pile-up effect.

Pile-up is a purely statistical effect. The number of minimum bias interactions generated in a single beam crossing is a Poissonian distribution that depends on the instantaneous luminosity, which varies of about a factor 2 during a LHC fill. Although luminosity variation is not arising from theoretical uncertainties, it is recommended to cross check the stability of the results against variation of the nominal luminosity.

An issue which can affect the pile-up is the definition of the minimum bias itself. The latter, indeed, may or may not include the diffractive and elastic contributions, with figures for the total cross section which can vary from 100 mb to 50 mb respectively. If the PYTHIA generator is adopted, these two different options correspond to MSEL 2 and MSEL 1, however, in order to get full control on the different contributions to the cross sections, one can use MSEL 2, setting MSTP(31) = 0, and providing explicit input through SIGT(0, 0, J), where the meaning of the index J is described below:

$J = 0$ Total cross section (reference value = 101.3 mb)
$J = 1$ Elastic cross section (reference value = 22.2 mb)
$J = 2$ Single diffractive cross section XB (reference value = 7.2 mb)
$J = 3$ Single diffractive cross section AX (reference value = 7.2 mb)
$J = 4$ Double diffractive cross section (reference value = 9.5 mb)
$J = 5$ Inelastic, non-diffractive cross section (reference value = 55.2 mb).

Where J = 0 has to correspond to the sum of the contributions for J = 1, . . . , 5. With respect to alternative cross section predictions [802], PYTHIA reference values for diffractive cross sections might be slightly shifted on the high side. A possible sound alternative could be to reduce the diffractive cross sections of around 30%, keeping constant the total cross section.

In order to assess the sensitivity of one analysis to the diffractive variations in the pile-up, at least the two options MSEL 1 and MSEL 2 should be tried. Diffractive contribution will in general result in few additional soft charged particles spiralling in the high magnetic fields of the LHC experiments. This effect is most likely to be relevant in the tracker detectors, where multiple hits in the same layer can be generated by the same track.

B.1.8. Decays

In contrast to the simple decay models available in the common PS Monte Carlo, alternative hadron decay models exist, for example EVTGEN [803], which have huge collections of exclusive hadron decays up to branching ratios as low as 10^{-4}.

EVTGEN follows the spin density matrix formalism and has an easily tuneable and upgradeable hadron decay data base which currently constitutes the largest and most refined collection of hadron decay models.

Comparison between the simple default decay models implemented in PS Monte Carlo and those available in EVTGEN should be recommended at least for analyses dealing with B hadrons or relying on b-tagging. However, since switching to a new hadron decay model could have a deep spin-offs on the exclusive description of the final states (multiplicity of kaons, pions, photons and muons, multiplicity of tracks reconstructed in secondary vertices) it might be worth to study also effects on trigger performances.

The LHC version of EVTGEN was initially provided by the LHCb experiment and is currently maintained by LCG Generator [804]. It comprises an interface to PYTHIA simulation that solves the technical problems of switching between the two different scenarios (i.e. hadron decays performed by PYTHIA, hadron decays performed by EVTGEN).

B.1.9. LHAPDF and PDF uncertainties

The detailed investigations of processes at LHC required a well understanding of the systematic theoretical uncertainties [201]. One of the important source of such errors is the parton distribution functions (PDFs).

The Les Houches Accord Parton Density Functions (LHAPDF) package [95] is designed to work with the different PDF sets[53]. In this approach a "fit" to the data is no longer described by a single PDF, but by a PDF set consisting of many individual PDF members. Indeed, PDFs are specified in a parameterised form at a fixed energy scale Q_0, such as

$$f(x, Q_0) = a_0 x^{a_1}(1-x)^{a_2}(1+a_3 x^{a_4}\ldots). \tag{B.1}$$

The PDFs at all higher Q are determined by NLO perturbative QCD evolution equations. The total number of PDF parameters (d) could be large (for example, for CTEQ parametrisation one has $d = 20$ [12]). Fitting procedure is used for evaluation an effective χ^2 function, which can be used to extract the "best fit" (the global minimum of χ^2) and also to explore the neighbourhood of the global minimum in order to quantify the uncertainties. As a result one has the "best-fit" PDF and $2d$ subsets of PDF [12, 95]:

$$f_0(x, Q),\ f_i^{\pm}(x, Q) = f\left(x, Q;\ \{a_i^{\pm}\}\right),\ \ i = 1, \ldots, d. \tag{B.2}$$

B.1.9.1. Master equations for calculating uncertainties. Let $X(\{a\})$ be any variable that depends on the PDFs. It can be a physical quantity such as the W production cross section, or a differential distribution.

Let $X_0 = X(\{a_0\})$ be the estimate for X calculated with the best-fit PDF and $X_i^{\pm}$ be the observable X calculated with i-th subset $f_i^{\pm}(x, Q)$.

Following to CTEQ6 collaboration one can estimate the variation of X by using a master formula [12]:

$$\Delta X = \sqrt{\sum_{i=1}^{d}\left(X_i^+ - X_i^-\right)^2}. \tag{B.3}$$

However, very often many X_i^+ and X_i^- have different magnitudes and even signs! This failure of the master formula is a result of the simple observation that the PDF set that minimises the uncertainty in a given observable X is not necessarily the same as the one that minimises the fit to the global data set.

The better estimator for the uncertainty of a generic observable X was proposed in [805]. It is defined as the maximum positive and negative errors on an observable X by

$$\begin{aligned}\Delta X_+ &= \sqrt{\textstyle\sum_{i=1}^{d}\left(\max[(X_i^+ - X_0),\ (X_i^- - X_0)\,,\ 0]\right)^2},\\ \Delta X_- &= \sqrt{\textstyle\sum_{i=1}^{d}\left(\max[(X_0 - X_i^+),\ (X_0 - X_i^-),\ 0]\right)^2}.\end{aligned} \tag{B.4}$$

In Eqs. (B.4) one sums the maximum deviations on the observable in each of the parameter directions, and hence retain both maximal sensitivity to the parameters that vary most and estimate the range of allowed values of the cross section. Note, that the errors in Table C.2 were evaluated with this Eq. (B.4).

[53] Note, at CMS it was recommended to use the CTEQ 5L set for PTDR simulation. Since there is only *one* CTEQ 5L PDF set (without corresponding subsets), it was recommended to use CTEQ 6M for evaluation of uncertainties due to PDFs for PTDR estimates and only in a special case can one use another sets (e.g. MRST).

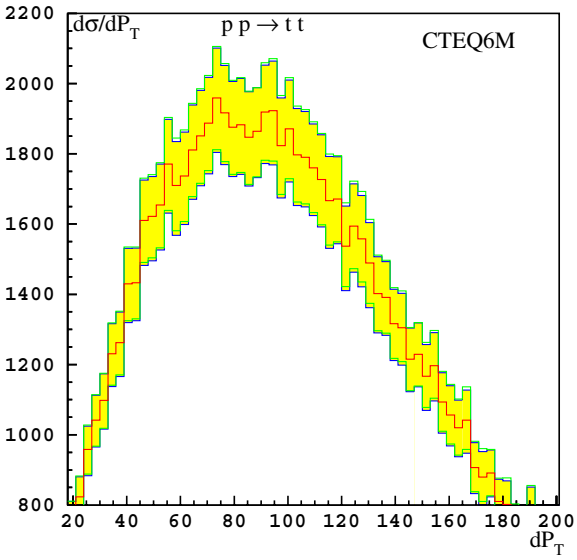

Figure B.1. $d\sigma/dP_{\mathrm{T}}$ distribution for $t\bar{t}$-pair production at LHC. The central histogram corresponds to the 'best-fit' of CTEQ6M PDF, while the shaded area represents the deviation due to PDF uncertainties.

Eq. (B.4 could also be used for calculations of differential distribution. Fig. B.1 presents the differential distribution $d\sigma/dP_{\mathrm{T}}$ for $t\bar{t}$-pair production at LHC.

B.1.9.2. How to calculate $X(\{a_i\})$. The most simple and straightforward method is to simulate a sample with the "best-fit" PDFs and then to repeat a such simulation $2d$ times with different $2d$ PDF subsets. As a results one gets $(1+2d)$ samples of *unweighted* events with *different* kinematics for each samples. Then use these samples to calculate $(1+2d)$ values for observable:

$$X_0 = \sum_{\text{events}} X_n(\{a_0\})), \quad X_i^{\pm} = \sum_{\text{events}} X_n(\{a_i^{\pm}\}), \quad i = 1, \ldots, d. \tag{B.5}$$

In practice, such method requires a large CPU-time and can be recommended only to be used for very few special cases, when a high accuracy is required.

In the second approach (*"re-weighting" method*) one needs to simulate only **one** sample with the 'best-fit' PDF. In doing so the additional weights, corresponding to all other PDF subsets are evaluated. This weight is the ratio of the parton luminosity [PDF($\{a_i\}$) – the product of PDFs] evaluated with PDF subset to the parton luminosity, calculated with the 'best-fit' PDF. As a result, for any n-event one has $2d$ additional weights:

$$w_{(0)} = 1(\text{best fit PDF}), \quad w_{(i)}^{\pm} = \frac{\text{PDF}(\{a_i^{\pm}\})_n}{\text{PDF}(\{a_0\})_n}; \quad w_{(i)}^{\pm} = \mathcal{O}(1). \tag{B.6}$$

The corresponding $(1+2d)$ values for observable X are evaluated as follows:

$$X_0 = \sum_{\text{events}} X_n(\{a_0\})), \quad X_i^{\pm} = \sum_{\text{events}} w_{(i)}^{\pm}\, X_n(\{a_0\}). \tag{B.7}$$

Contrary to the first method (see (B.5)) these $(1+2d)$ samples have the events with *different* weights, but with *identical* kinematics for each samples. Note, that all additional samples have

different "total number of events":

$$N_0 = \sum_{\text{events}} w_{(0)}(=1),\ N_i^{\pm} = \sum_{\text{events}} w_{(i)}^{\pm} \neq N_0,\ \text{and}\ N_i^{\pm} = \mathcal{O}(N_0). \tag{B.8}$$

Starting from CMKIN_6_0_0 version it is possible for each event the evaluation of the additional weights, corresponding to different PDF subsets (i.e. $w_{(i)}^{\pm}$, see (B.6)). This option is available for CMKIN run with PYTHIA-like generators (PYTHIA, MADGRAPH, COMPHEP, ALPGEN, TOPREX, STAGEN, etc) and HERWIG. This information is written in `/mc_param/` user block after all variables filled by CMKIN and a user (by using of `kis_xxx` routines).

B.2. Experimental uncertainties

The systematic uncertainties associated with the detector measurements contributing to an analysis are mostly covered in the corresponding chapters of Volume 1 of this Report [7] and are summarised here.

B.2.1. Luminosity uncertainty

As discussed in Chapter 8 of [7], the design goal for the precision of the luminosity measurement at CMS is 5%, which is assumed to be achieved after 1 fb^{-1} of data has been collected. For integrated luminosities of less than 1 fb^{-1}, it is assumed that the precision is limited to 10%. For studies based on 30 fb^{-1} or more in this Report, it is assumed that further improvement on the uncertainty can be achieved and a 3% uncertainty is assumed, via e.g. W, Z based luminosity measurements.

B.2.2. Track and vertex reconstruction uncertainties

The uncertainty in the silicon track reconstruction efficiency is taken to be 1% for all tracks. The primary vertex precision along the z coordinate is expected to be about 10 μm once 1 fb^{-1} has been collected. The transverse vertex precision is expected to be about 1 μm.

The effects of uncertainties on the alignment of silicon sensors on track and vertex reconstruction are studied using a dedicated software tool (Section 6.6.4 of [7]) that is able to displace tracker elements according to two scenarios: a "First Data Taking Scenario" with placement uncertainties as expected at LHC start-up from measurements using the laser alignment system for the strip tracker and from in-situ track-based alignment of the pixel detector, and a "Long Term Scenario" appropriate after the first few fb^{-1} have been collected and a complete track-based alignment has been carried out for all tracker elements.

The effect of the magnetic field uncertainty in the central region of CMS is expected to contribute a momentum scale uncertainty of 0.0003 GeV/c to $1/p_{\text{T}}$. When combined with the aggregate effect from alignment uncertainties, the overall momentum scale uncertainty is 0.0005 GeV/c at start-up.

B.2.3. Muon reconstruction uncertainties

As with the silicon tracker studies, a dedicated software tool has been developed (Section 3.2.2 of [7]) to study the effects of muon detector placement uncertainties on muon reconstruction. Two scenarios, a "First Data Taking Scenario" with placement uncertainties as expected at LHC start-up and a "Long Term Scenario" appropriate after the first few fb^{-1}, are available and used in analyses sensitive to the alignment precision of the muon detectors. The latter

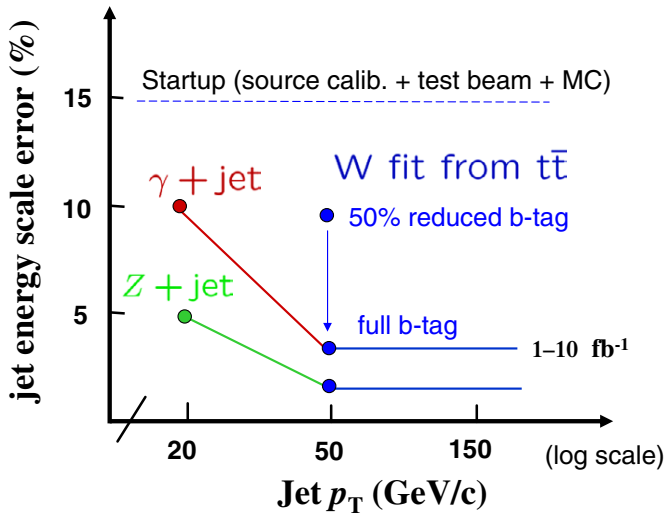

Figure B.2. Jet energy scale uncertainty is applied as a rescaling of the four-momentum of the reconstructed jet $p^{\mu,jet}_{scaled\pm} = (1 \pm \alpha) \cdot p^{\mu,jet}_{meas}$ where α is the percentage uncertainty plotted above.

scenario describes a detector alignment precision of 200 μm in the plane transverse to the beam axis using the laser alignment system and track-based alignment strategies.

The effect of magnetic field uncertainties on the muon momentum will be dominated by the uncertainty in the central region and its impact on the momentum scale determined by fits to the silicon tracker hits for muon momenta well below the TeV/c scale.

B.2.4. Electromagnetic calibration and energy scale uncertainties

The precision to which the ECAL crystals can be intercalibrated from a variety of techniques is discussed in Section 4.4 of [7], and ranges from 0.4–2.0% using about 5 fb^{-1} of *in situ* single isolated electron data. A software tool is used to apply calibration constants to the accuracy expected to be obtained with either 1 fb^{-1} or 10 fb^{-1} of integrated luminosity. The absolute energy scale can be determined using the Z mass constraint in $Z \rightarrow ee$ decays, and is expected to be measured to a precision of about 0.05%.

B.2.5. Jet and missing transverse energy uncertainties

The estimated systematic uncertainty on the jet energy scale is shown in Fig. B.2. At startup the accuracy of the jet energy scale relies on the understanding of single-particle test beam calibration and the level of agreement achieved in the data-to-Monte Carlo simulation comparisons of the detector response. The response of an individual tile or crystals is known to limited accuracy from source calibration in the HCAL and test stand measurements for crystals in the ECAL. Hence, given the limitations of the precalibration of the calorimeters, an overall uncertainty of 15% is expected for the "day-one" absolute energy scale. This applies equally for jet response and the energy scale uncertainty of the missing transverse energy.

In the first 1–10 fb^{-1} of data, the γ+ jet calibration [283] and the hadronic W boson mass calibration in top quark pair production events [287] are currently the best estimates for the accuracy on the absolute jet energy scale. The hadronic W jets in the selected

sample have a mean p_T that is approximately 50 GeV/c. A lowering of the jet selection threshold increases the effects of the offset correction from pile-up. The systematic on offset corrections and backgrounds puts the absolute jet energy scale at 3%. The jet reconstruction efficiencies are flat above 50 GeV/c, but drop in the low p_T region. The current estimate of the high p_T jet energy scale based on the hadronic W calibration is 3%. The calorimeter response curves that are required to extrapolate to high p_T are not expected to significantly increase the energy scale uncertainty beyond the 3% from the W calibration. In the low p_T region excluded from the hadronic W analysis, the absolute jet energy scale will be set by the γ+jet calibration which will extend down to 20 GeV. Below 20 GeV, only the single-particle calibration methods apply and these will have an accuracy of 10%. The recommended treatment for the jet energy systematic in this report is to apply an uncertainty according to this functional form:

$$\sigma_E^{jet}/E = \begin{cases} 10\% & p_T < 20\,\text{GeV/c} \\ 10\% - 7\% * (p_T - 20\,\text{GeV/c})/(30\,\text{GeV/c}) & 20\,\text{GeV/c} < p_T < 50\,\text{GeV/c} \\ 3\% & p_T > 50\,\text{GeV/c} \end{cases}.$$

It is expected that the Z+jet sample and further analysis of the hadronic W systematics will reduce the overall jet energy scale uncertainty, but these analyses remain under active study.

The low p_T region is particularly important for the missing transverse energy (MET) response. As the MET will have significant contributions from low p_T jets and unclustered energy, it is expected that the low p_T component of the MET will not be understood to better than 10% following the first 1–10 fb^{-1} of data. The recommended treatment of the MET energy scale uncertainty has two approaches (one simple and one more detailed). For a MET which is known to be dominated by low p_T jets and unclustered energy, an uncertainty of 10% should be applied to the components of the MET uncorrelated to the jet energy scale uncertainty of the jets. This is the simple approach and gives a conservative error on the MET. For events with reconstructed high p_T jets, the contributions to the MET uncertainty are correlated to the jet energy scale uncertainty of the high p_T jets. The recommended treatment of the MET uncertainty is to apply separate uncertainties on the low p_T and high p_T components of the MET. The MET is reconstructed as described in [147] and [148]. This gives a type-1 correction of the following form:

$$E^{\text{miss}}_{\text{Tx(y)}} = -\left[E^{\text{raw}}_{\text{Tx(y)}} + \sum_{\text{jets}} \left(p^{\text{corr. jet}}_{\text{Tx(y)}} - p^{\text{raw jet}}_{\text{Tx(y)}}\right)\right]$$

where $E^{\text{raw}}_{\text{Tx(y)}}$ is the sum over the raw calorimeter tower energies and the jet sum in the equation is over jets with a reconstructed p_T above a given jet p_T^{cut} selection cut, typically 20–25 GeV/c. The jet p_T is used in these formula to account for the angular separation of the towers included in the jet sum, contributing to the jet mass. Rewriting the above equation in this form

$$E^{\text{miss}}_{\text{Tx(y)}} = -\left[\left(E^{\text{raw}}_{\text{Tx(y)}} - \sum_{\text{jets}} p^{\text{raw jet}}_{\text{Tx(y)}}\right)_{\text{low } p_T} + \left(\sum_{\text{jet}} p^{\text{corr. jet}}_{\text{Tx(y)}}\right)_{\text{high } p_T}\right]$$

shows explicitly the low p_T (in the first set of brackets) and the high p_T components (second set of brackets) of the MET. The proposed systematics treatment is to vary the components of the low p_T MET by 10% scale uncertainty uncorrelated with the high p_T component and to vary the high p_T component according the jet energy scale uncertainty for the measured jets.

If a subset of the high p_T jets are identified as electromagnetic objects, isolated electrons or photons, then these EM-jets should be given EM-scale energy corrections which are closer to unity than hadronic jet corrections. The energy scale uncertainty on an EM-object will also be much lower than the jet energy scale systematic. Therefore, if the EM-objects are not removed from the jet list, the quoted energy scale uncertainty will be conservative relative to the lower errors associated with separate treatment of identified EM-objects.

In addition to the jet energy scale uncertainty, there are uncertainties on the jet resolution. At startup the jet resolution is estimated to be accurate to 20% of the quoted resolution based on the test-beam data and simulation studies. The dijet balancing resolution will be determined from data and will further constrain this uncertainty. It is expected that the systematics on the third jet veto and other selection criteria will limit the uncertainty on the jet resolution to 10% in the 1–10 fb^{-1} dataset. The recommended treatment for this systematic is to add an additional smearing to the jet energy which broadens the overall jet resolution by 10%. This can be done by throwing a Gaussian random number and adding an energy term which is 46% of the jet resolution. Therefore, the jet-by-jet event-by-event smearing should be done as follows:

$$E_T^{'\mathrm{jet}} = E_T^{\mathrm{jet}} + \mathrm{Gaus}[0,\ 0.46 * \sigma(E_T, \eta)] \tag{B.9}$$

where $\sigma(E_T, \eta)$ is the reference jet resolution which for the central barrel is given by (using Monte Carlo simulation derived jet calibrations where E_T^{MC} is equal to E_T^{rec} on average)

$$\sigma(E_T^{\mathrm{jet}}, |\eta| < 1.4) = (5.8\,\mathrm{GeV}) \oplus \left(1.25 * \sqrt{E_T^{\mathrm{jet}}}\right) \oplus 0.033 * E_T^{\mathrm{jet}} \tag{B.10}$$

(terms added in quadrature) and $\mathrm{Gaus}[0, 0.46 * \sigma(E_T, \eta)]$ is a randomly thrown sampling of a normal distribution per jet with a mean of zero and a width of 46% of the jet resolution and therefore $E_T^{'\mathrm{jet}}$ is the smeared jet energy to be used in the estimation of the jet resolution systematic uncertainty of the measurement. The 46% is chosen so that when added in quadrature to the nominal resolution gives an overall widening of the energy resolution of 10%. The resolutions of the endcap and forward jet regions are found in [165, Table 5]. These are

$$\sigma(E_T^{\mathrm{jet}}, 1.4 < |\eta| < 3.0) = (4.8\mathrm{GeV}) \oplus \left(0.89 * \sqrt{E_T^{\mathrm{jet}}}\right) \oplus 0.043 * E_T^{\mathrm{jet}}$$

$$\sigma(E_T^{\mathrm{jet}}, 3.0 < |\eta| < 5.0) = (3.8\mathrm{GeV}) \oplus 0.085 * E_T^{\mathrm{jet}}$$

where for these jet resolution fits the stochastic term in the forward region is small compared to the noise and constant terms (hence the missing $\sqrt{E_T^{\mathrm{jet}}}$ term for $3.0 < |\eta| < 5.0$). The shift in the +10% direction can be symmetrised to account for the −10% shift. Otherwise, the difference between the reconstructed and generated jet energies must be reduced by 10% in order to estimate the −10% uncertainty from the nominal Monte Carlo jet resolution. The jet resolution uncertainty is particularly important when searching for signals that are on a rapidly falling QCD multi-jet p_T spectrum.

B.2.6. Heavy-flavour tagging uncertainties

A strategy for measuring the b-tag efficiency using an enriched sample of b-jets from $\mathrm{t\bar{t}}$ events, and its estimated precision, is described in Section 12.2.8 of [7]. The relative uncertainty on the b-efficiency measurement is expected to be about 6% (4%) in the barrel and 10% (5%) in

the endcaps for 1 fb^{-1} (10 fb^{-1}) of integrated luminosity. These uncertainties correspond to a b-tag working point efficiency of 50%.

The light-quark (and gluon) mis-tag uncertainty is expected to be larger than the b efficiency uncertainty; however, for this Report a global uncertainty of 5% is assumed for the mis-tag uncertainty. As with the efficiency determination, it is important to identify strategies to measure the mis-tagging probabilities in data as well.

Likewise, a strategy to measure the uncertainty on the efficiency for identifying τ leptons is described in Section 12.1.4 of [7], and involves comparing the ratio of $\text{Z} \to \tau\tau \to \mu +$ jet to $\text{Z} \to \mu\mu$ events. With a 30 fb^{-1} data sample, the relative uncertainty on τ-tagging is estimated to be about 4%. A measurement of the τ misidentification probability can be determined from a sample of $\gamma+$ jet events, and with a 10 fb^{-1} data sample is expected to have an uncertainty at the level of 4–10%.

Appendix C. Monte Carlo Models and Generators

C.1. Introduction

This section presents a short description of the basic event generators used in CMS during preparation of the PTDR (see CMS "Generator Tools group" for details). A comprehensive review of the present Monte Carlo models and generators is given elsewhere [806]. Note that only MC generators used in CMS are described here, and a full description of several popular packages (like ISAJET or AcerMC, see [806]) is omitted.

There are several available Monte Carlo event generators for pp, pA and AA collisions, namely HERWIG [196], HIJING [807], ISAJET [672], PYTHIA [69] and SHERPA [808]. Each of these simulates a hadronic final state corresponding to some particular model of the underlying physics. The details of the implementation of the physics are different in each of these generators, however the underlying philosophy of the generators is the same.

The cross section values and the differential distribution for almost all processes are evalueated as follows:

$$\sigma(pp \to CX) = \sum_{ij} \int f_i^p(x_1, Q^2) f_j^p(x_2, Q^2) \hat{\sigma}(ij \to C) \mathrm{d}x_1 \mathrm{d}x_2, \qquad \text{(C.1)}$$

where $f_i^p(x, Q^2)$ are the Parton Distribution Functions (PDF) of ith parton, that carried a fraction x of the initial proton momentum at a scale (Q^2); $\sigma(ij \to C)$ is the cross section for the hard process (i.e. describing two partons, i and j, interaction).

A general scheme of event generation assumes the evaluation of the hard process (the cross section value, the incoming and outgoing particle's momenta and colours), then evolves the event through a parton showering and hadronisation step, and the decay of the unstable particles. The event information (stored in `/HEPEVT/` common block [69]) contains the momenta of the final hadrons, leptons and photons and positions of their decay vertexes. Typically such information contains also the characteristics (momenta, colours, `KF`-codes, mother's and daughter's relations) of all intermediate partons (quarks, gluons, gauge bosons, unstable physical particles, etc) that provide a trace-back the history of particle production inside of an event. By using an acceptance-rejection methods weighted events can be returned.

Parton showering is based on the expansion around the soft and collinear evolution limits and is often ascribed to either the initial or final state. The algorithm used by HERWIG and SHERPA also include some effects due to quantum interference. The events that have more energy in the parton process have more showering, and consequently more jet activity.

The collection of quarks and gluons must then be hadronised into mesons and baryons. This is done differently in each of the event generators, but is described by a set of (fragmentation) parameters that must be adjusted to agree with experimental results. HERWIG looks for colour singlet collections of quarks and gluons with low invariant mass and groups them together; this set then turns into hadrons. PYTHIA splits gluons into quark-anti-quark pairs and turns the resulting set of colour singlet quark-anti-quark pairs into hadrons via a string model. ISAJET simply fragments each quark independently paying no attention to the colour flow.

The dominant cross-section at the LHC consists of events with no hard scattering. There is little detailed theoretical understanding of these minimum-bias events and the event generators must rely on present data. These minimum-bias events are important at LHC, particularly at design luminosity, as they overlap with interesting hard-scattering events. The generators use a different approach in this case. HERWIG uses a parametrisation of data mainly from the CERN $p\bar{p}$ Collider. PYTHIA uses a mini-jet model where the jet cross-section is used at very low

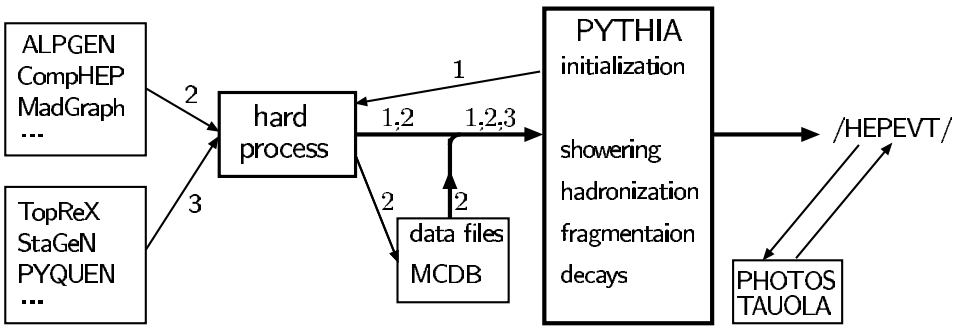

Figure C.1. Purely schematic data flow in PYTHIA and HERWIG.

transverse momenta, i.e the hard scattering process is extrapolated until it saturates the total cross-section. CMS has used the PYTHIA approach with dedicated modifications that agree with present data from Tevatron [69]. The model of the hadronic interactions implemented in the physics generator has a direct impact on physical observables such as jet multiplicity, their average transverse momentum, internal structure of the jets and their heavy flavour content. This led to the choice to use PYTHIA for most processes, allowing for a consistent set of signal and background events to be generated.

Table C.2 presents the predicted cross-section values for the basic SM processes, as used in the simulations for PTDR. The cross-section values (at leading order) were calculated by using PYTHIA 6.327 with `CTEQ5L` (default PDF for PTDR) and with `CTEQ6M` PDFs. α_s at 1st (2nd) order is used with `CTEQ5L` (`CTEQ6M`) PDFs. For `CTEQ6M` the quoted errors are related to the uncertainties due to PDFs (see Subsection B.1.9).

C.2. General scheme of generator usage in CMS

All event generators, included in CMS simulation software, can be separated into two groups.

The first group (HERWIG, HIJING, ISAJET, PYTHIA) provides the *full simulation* of events. The basic package explored in CMS is PYTHIA and only few specific processes were simulated with HERWIG or HIJING.

A purely schematic data flow in PYTHIA and HERWIG is presented in Fig. C.1.

After initialisation the package (HERWIG or PYTHIA) calls "hard process" routines (see "1" arrow lines in Fig. C.1). Then information (the momenta of initial and final partons, the colours and `KF`-codes) is passed to package for parton showering, hadronisation, fragmentation and decays of the unstable particles.

However, all these "full event simulation" generators have very limited number of the hard process matrix elements (typically for $2 \to 2$ reaction at LO). Therefore, several special generators are used for simulation of many other LO processes. In fact, such packages generate the hard processes kinematic quantities, such as masses and momenta, the spin, the colour connection, and the flavour of initial- and final-state partons. The information is stored in the "Les Houches" format [809] (`/HEPEUP/` common block) and is passed to full event simulation package like PYTHIA or HERWIG (see thick "output" line on Fig. C.1).

Three generators, namely ALPGEN [161], COMPHEP [355], and MADGRAPH [81, 493], are widely used for simulation of many processes, especially for the generation of the hard processes with multi-jet final states. For example, ALPGEN allows to generate $Q\bar{Q}$ pair

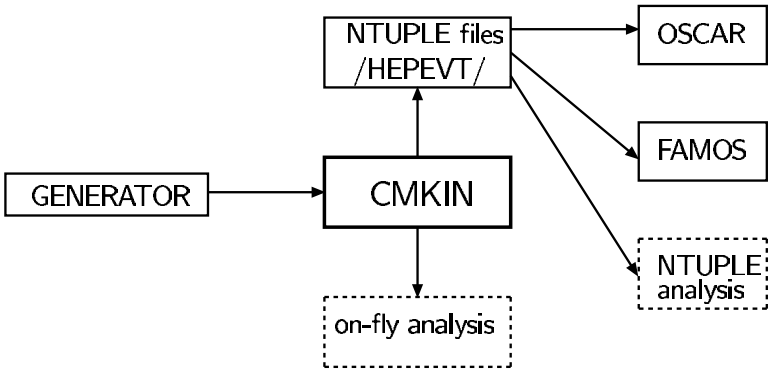

Figure C.2. Illustration of the CMKIN interface.

production with up to 6 jets. Due to the complexity of the matrix elements, describing the multi-jet processes, and a re-weighting procedure the generation of events is very CPU-time consuming. As a result, the information with kinematics is stored in the output files. (see "2" lines on Fig. C.1). Then, like in a generic PYTHIA process, such information is passed to PYTHIA (see thick "output" line on Fig. C.1).

There are several *"dedicated generators"*, TOPREX [44], STAGEN, SINGLETOP, COSMIC, SIMUB, PHASE, PYQUEN [810, 811], HYDJET [812], EDDE. These generators are used for simulation of several specific process (see below for a short description of these codes). The information with hard processes kinematic quantities is stored in `/HEPEUP/` common block [809] and is passed to the "full event simulation" package (see "3" lines on Fig. C.1).

After full simulation of event with PYTHIA or HERWIG the output information is stored in the `/HEPEVT/` common block. In addition two *special functionality* codes provide a better description of photon radiation from a charge final particles (PHOTOS [39]) and $\tau^{\pm}$-lepton decays (TAUOLA [155]). Typically, these codes read information from `/HEPEVT/` common, perform simulation and then add generated information (new particles) into the `/HEPEVT/` common block (see Fig. C.1).

C.3. CMKIN

Almost all generators available in CMS could be used with the CMKIN package. Now the CMKIN is used for OSCAR and FAMOS detector simulation input. This software package provides a common interface between physics event generators and CMS detector simulation (see Fig. C.2). It also provides an environment to make physics plots of generated events. CMKIN provides an interface to a number of physics generators like PYTHIA, ISAJET and HERWIG. It also offers the possibility to use different 'external generators' like ALPGEN [161], COMPHEP [355], MADGRAPH [81, 493] and TOPREX [44]. Cosmic muon simulation is available as well. Simple particle generation is also included, i.e. single and double particles as well as simple multi particle events. The interface is based on a common block `HEPEVT` - a HEP standard to store particle kinematics information for one event [69]. The `/HEPEVT/` common block is converted to HBOOK n-tuples. The event output format follows the `HEPEVT` standard and additional information can be included by the user in the block `/MC_PARAM/`.

There is a unified compilation script which is used as follows:

```
kine_make_ntpl.com <generator> [lhapdf]
```

where the first parameter can have one of the following values: *pythia*, *herwig*, *isajet*, *simple*, *single*, *double*, *simplemulti*, *cosmic*, *comphep*, *alpgen*, *madgraph*, *phase*, *toprex* or *stagen*. The optional second parameter *lhapdf* is given when the user wants to use `LHAPDF` library [95].

C.4. Full event simulation generators

C.4.1. PYTHIA

The PYTHIA package [69] is a general-purpose generator for hadronic events in pp, e $^{+}$e^{-} and ep colliders. It contains a subprocess library and generation machinery, initial- and final-state parton showers, underlying event, hadronisation and decays, and analysis tools. PYTHIA contains around 240 different $2 \to 2$ (and some $2 \to 1$ or $2 \to 3$) subprocesses, all at leading order. The subsequent decays of unstable resonances (W, Z, top, Higgs, SUSY, ...) brings up the partonic multiplicity, for many processes with full spin correlations in the decays. The external processes can be evolved through the showering and hadronisation (like internal ones).

The final-state shower is based on forward evolution in terms of a decreasing timelike virtuality m^2, with angular ordering imposed by veto. The framework is leading-log, but includes many NLL aspects such as energy–momentum conservation, $\alpha_s(p_\perp^2)$ and coherence. Further features include gluon polarisation effects and photon emission.

The initial-state shower is based on backward evolution, i.e. starting at the hard scattering and moving backwards in time to the shower initiators, in terms of a decreasing spacelike virtuality Q^2. Initial and final showers are matched to each other by maximum emission cones.

The composite nature of hadrons (and resolved photons) allows for several partons from each of the incoming hadrons to undergo scatterings. Such multiple parton–parton interactions are instrumental in building up the activity in the underlying event, in everything from charged multiplicity distributions and long-range correlations to minijets and jet pedestals. The interactions are described by perturbation theory, approximated by a set of more or less separate $2 \to 2$ scatterings; energy conservation and other effects introduce (anti)correlations. The scatterings are colour-connected with each other and with the beam remnants.

The Lund string model, used for hadronisation, is based on a picture with linear confinement, where (anti)quarks or other colour (anti)triplets are located at the ends of the string, and gluons are energy and momentum carrying kinks on the string. The string breaks by the production of new $q\overline{q}$ pairs, and a quark from one break can combine with an anti-quark from an adjacent one to form a colour singlet meson.

Unstable particles are allowed to decay. In cases where better decay models are available elsewhere, e.g. for $\tau^{\pm}$ with spin information or for B hadrons, such decays can be delegated to specialised packages.

At present the parameters from almost all PYTHIA common blocks (see `BLOCK DATA PYDATA`) could be set via data cards. With the CMKIN these parameters could be set in data card file with the following format (note, that only capital letters should be used):

PYTHIA	CMKIN	COMMENT
parameter		
MSEL = 6	MSEL6	$t\bar{t}$ production
one- *and* two-dimensional arrays		
CKIN(1) = 100	CKIN1 = 100	min.$\sqrt{\hat{s}}$
i.e. PMAS(6, 1) = 178	PMAS6, 1 = 178	top-quark mass

• *Common cards for* CMKIN

Below we present a list of PYTHIA parameters used for full event simulation for PTDR. Some of these parameters correspond to the old multiple interactions scenario, namely *Tune A* [813].

`MSTP(2)` = 1 : 1(first)/2(second) order running α_s
`MSTP(33)` = 0 : do not include of K-factors in hard cross sections
`MSTP(51)` = 7 : PDF set (here is CTEQ5L)
`MSTP(81)` = 1 : multiple parton interactions is switched ON
`MSTP(82)` = 4 : defines the multiple parton interactions model
`PARP(67)` = 1 : amount of initial-state radiation
`PARP(82)` = 1.9 : P_{T} cut-off for multi-parton interactions
`PARP(83)` = 0.5 : fraction of total hadronic matter in core
`PARP(84)` = 0.4 : radius of core
`PARP(85)` = 0.33 : gluon production mechanism in multiple interactions
`PARP(86)` = 0.66 : gluon prod. mechanism in multiple interactions
`PARP(88)` = 0.5
`PARP(89)` = 1000 : reference energy scale for which `PARP(82)` is set
`PARP(90)` = 0.160 : effective P_{T} cut − off = [PARP(82)/PARP(89)]**PARP(90)
`PARP(91)` = 1.0 : width of Gaussian primordial $k_{\perp}$ distribution inside hadron
`PARJ(71)` = 10 : maximum average $c\tau$ for particles allowed to decay
`MSTJ(11)` = 3 : choice of the fragmentation function
`MSTJ(22)` = 2 : allow to decay those unstable particles
`PMAS(5,1)` = 4.8 : the mass of the b-quark
`PMAS(6,1)` = 175.0 : the mass of the t-quark

C.4.2. HERWIG

HERWIG contains a wide range of Standard Model, Higgs and supersymmetric processes [196]. HERWIG uses the parton-shower approach for initial- and final-state QCD radiation, including colour coherence effects and azimuthal correlations both within and between the jets.

In the treatment of supersymmetric processes, HERWIG itself doesn't calculate the SUSY mass spectrum or decay rates, but reads in an input file containing the low-energy parameters (masses, couplings, decays, ...). This file can be written by hand or more conveniently be generated with the ISAWIG program. This program provides an interface to ISAJET (and therefore to all models in ISASUSY and ISASUGRA), to HDECAY (for NLO Higgs decays), and can also add R-parity violating decays.

Colour coherence effects of (initial and final) partons are taken into account in all hard subprocesses, including the production and decay of heavy quarks and supersymmetric particles. HERWIG uses the angular ordered parton shower algorithm which resumes both soft and collinear singularities. HERWIG includes spin correlation effects in the production and decay of top quarks, tau leptons and supersymmetric particles. For the SUSY decays, there is an option for using either the matrix elements (fast) or the full spin correlations. HERWIG uses a cluster hadronisation model based on non-perturbative gluon splitting, and a similar cluster model for soft and underlying hadronic events. This model gives a good agreement with the LEP data on event shapes, but does not fit the identified particle spectrum well.

C.4.3. ISAJET

ISAJET is a Monte Carlo program which simulates pp, $p\bar{p}$, e^+e^- interactions at high energies [672]. ISAJET is based on perturbative QCD plus phenomenological models for parton and beam jet fragmentation. At CMS ISAJET is used for calculations of SUSY parameters.

C.4.4. HIJING

Hard or semi-hard parton scatterings with transverse momentum of a few GeV/c are expected to dominate high energy heavy ion collisions. The HIJING (Heavy Ion Jet INteraction Generator) Monte Carlo model [807] was developed by M Gyulassy and X-N Wang with special emphasis on the role of minijets in pp, pA and AA reactions at collider energies.

Detailed systematic comparison of HIJING results with a very wide range of data demonstrates that a quantitative understanding of the interplay between soft string dynamics and hard QCD interaction has been achieved. In particular, HIJING reproduces many inclusive spectra two particle correlations, and can explain the observed flavour and multiplicity dependence of the average transverse momentum.

C.5. Tree level matrix element generators

C.5.1. ALPGEN

ALPGEN is designed for the generation of Standard Model processes in hadronic collisions, with emphasis on final states with large jet multiplicities [161]. It is based on the exact leading order evaluation of partonic matrix elements and t and gauge boson decays with helicity correlations. The code generates events in both a weighted and unweighted mode. Weighted generation allows for high-statistics parton-level studies. Unweighted events can be processed in an independent run through shower evolution and hadronisation programs.

The current available processes are:

- $W/Z/H\ Q\bar{Q} + N$ jets ($Q = c, b, t$) with $N \leqslant 4$
- $Q\bar{Q} + N$ jets, with $N \leqslant 6$
- $Q\bar{Q}Q'\bar{Q}' + N$ jets, with $N \leqslant 4$
- W + charm + N jets, with $N \leqslant 5$
- N jets, $W/Z + N$ jets, with $N \leqslant 6$
- $nW + mZ + lH + N$ jets, with $n + m + l + N \leqslant 8$, $N \leqslant 3$
- $N\gamma + M$ jets, with $N \geqslant 1$, $N + M \leqslant 8$ and $M \leqslant 6$
- $H + N$ jets ($N \leqslant 4$), with the Higgs produced via ggH vertex
- single top production.

C.5.2. COMPHEP

COMPHEP [814] is a package for evaluating Feynman diagrams, integrating over multi-particle phase space and generating events with a high level of automation. COMPHEP includes the Feynman rules for SM and several versions of MSSM (SUGRA, GMSB, MSSM with R-parity violation).

COMPHEP computes squared Feynman diagrams symbolically and then numerically calculates cross sections and distributions. After numerical computation one can generate the unweighted events with implemented colour flow information. The events are in the form of the Les Houches Accord event record [809] to be used in the PYTHIA program for showering and hadronisation.

COMPHEP allows for the computation of scattering processes with up to 6 particles and decay processes with up to 7 particles in the final state.

C.5.3. MADGRAPH *and* MADEVENT

MADEVENT [81] is a multi-purpose, tree-level event generator which is powered by the matrix element generator MADGRAPH [493]. Given a user process, MADGRAPH automatically generates the amplitudes for all the relevant subprocesses and produces the mappings for the integration over the phase space. This process-dependent information is packaged into MADEVENT, and a stand-alone code is produced. It allows the user to calculate cross sections and to obtain unweighted events automatically. Once the events have been generated – event information, (e.g. particle id's, momenta, spin, colour connections) is stored in the "Les Houches" format [809]. Events may be passed directly to a shower Monte Carlo program (interfaces are available for HERWIG and PYTHIA).

The limitation of the code are related to the maximum number of final state QCD particles. Currently, the package is limited to ten thousand diagrams per subprocess. So, for example, $W+5$ jets is close to its practical limit. At present, only the Standard Model Feynman rules are implemented and the user has to provide his/her own rules for beyond Standard Model physics, such as MSSM.

C.5.4. TOPREX

The event generator TOPREX [44] provides the simulation of several important processes in pp and $p\bar{p}$ collisions, not implemented in PYTHIA. In the matrix elements used in TOPREX the decays of the final t-quarks, $W^{\pm}$, Z and charged Higgs bosons are also included. The final top quark could decay into SM channel ($t \to qW^{+}$, $q = d, s, b$), b-quark and charged Higgs ($t \to bH^{+}$) and the channels with flavour changing neutral current (FCNC): $t \to u(c)V$, $V = g, \gamma, Z$. The implemented matrix elements take into account spin polarisations of the top quark, that provides a correct description of the differential distributions and correlations of the top quarks decay products.

C.6. Supplementary packages

C.6.1. PHOTOS

PHOTOS is a universal package to simulate QED photon radiative corrections [39]. The precision of the generation may in some cases be limited, in general it is not worse than the complete double bremsstrahlung in LL approximation. The infrared limit of the distributions is also correctly reproduced. The action of the algorithm consists of generating, with internally calculated probability, bremsstrahlung photon(s), which are later added to the `/HEPEVT/` record. Kinematic configurations are appropriately modified. Energy-momentum conservation is assured. When using PHOTOS, the QED bremsstrahlung of the principal generator must be switched off. For example in case of PYTHIA one has to use `MSTJ 41=1`.

C.6.2. TAUOLA

TAUOLA is a package for simulation of the $\tau^{\pm}$-lepton decays [155]. It uses the PHOTOS package to simulate radiative corrections in the decay. The TAUOLA interface is made with the PYTHIA generator. This interface evaluates also the position of τ-lepton decay (i.e. the information on the production vertex of the decay products of τ-lepton).

C.6.3. PYQUEN

The event generator PYQUEN (PYthia QUENched) [810, 811] provides the simulation of rescattering and energy loss of hard partons in dense QCD-matter (quark-gluon plasma) created in ultrarelativistic heavy ion collisions. The approach relies on an accumulative energy losses, when gluon radiation is associated with each scattering in expanding medium together including the interference effect by the modified radiation spectrum $dE/d\ell$ as a function of decreasing temperature T. The model is implemented as fast Monte Carlo tool, to modify standard PYTHIA jet event.

C.6.4. HYDJET

The event generator HYDJET [812] (HYDrodynamics + JETs) provides the fast simulation of heavy ion events at LHC energy including longitudinal, transverse and elliptic flow effects together with jet production and jet quenching (rescattering and energy loss of hard partons in dense QCD-matter, quark-gluon plasma). The model merges a fast generator of flow effects HYDRO [815] with PYTHIA (for jet production) and PYQUEN [810, 811] (for jet quenching) by simulating full heavy ion event as a superposition of soft, hydro-type state and hard multi-jets.

First of all, HYDJET calculates the number N^{hard} of hard nucleon-nucleon sub-collisions and number N^{part} nucleons-participants (at given impact parameter b of AA collision and minimum P_{T} of hard parton scattering) and generates the initial parton spectra by calling PYTHIA N^{hard} times (fragmentation off). After each jet parton affected by medium-induced rescattering and energy loss according with PYQUEN model. In the end of each PYTHIA sub-event adding new (in-medium emitted) gluons into PYTHIA parton list and rearrangements of partons to update string formation are performed. Then PYQUEN forms final hadrons with `PYEXEC` subroutine (fragmentation on). Finally, HYDJET calculates the multiplicity of soft, hydro-induced part of the event and add new particles in the end of the event record.

C.7. K-factors for dilepton production

Some event generators such as PYTHIA do not employ the most advanced matrix-element calculations. They must be reasonably fast since in most applications, many millions of events must be generated. Experimenters apply an *ad-hoc* correction or "kludge" called the K-factor so that the cross-section value used for, say, the production of muon pairs, is correct. This K-factor amounts to the ratio of a highly accurate cross-section calculation to a less accurate one, typically a leading-order calculation:

$$K_{\text{NLO}} = \frac{\sigma_{\text{NLO}}}{\sigma_{\text{LO}}} \qquad \text{and} \qquad K_{\text{NNLO}} = \frac{\sigma_{\text{NNLO}}}{\sigma_{\text{LO}}}.$$

Clearly the K-factor reflects the accuracy of the better theoretical calculation, and there can be significant differences between K_{NNLO} and K_{NLO}. The most significant contributions to the K-factor come from QCD radiative corrections are expected to be on the order of 10% or more. Usually one does not include electroweak radiative corrections in the K-factor.

We have examined the K-factor for the Drell–Yan production of charged lepton pairs, as well as the signal for new Z' neutral gauge bosons. The program PHOZPRMS is used to compute mass-dependent cross-sections [348], and a generalised version called WUWD is used to study Z' cross-sections [816]. We checked carefully the differential cross-section, $d\sigma/dM$ obtained from PHOZPRMS with the program RESBOS [817, 818] and found very good agreement. We use the MRST parton distribution functions [819] for these calculations. Very similar results are obtained using CTEQ6M [12].

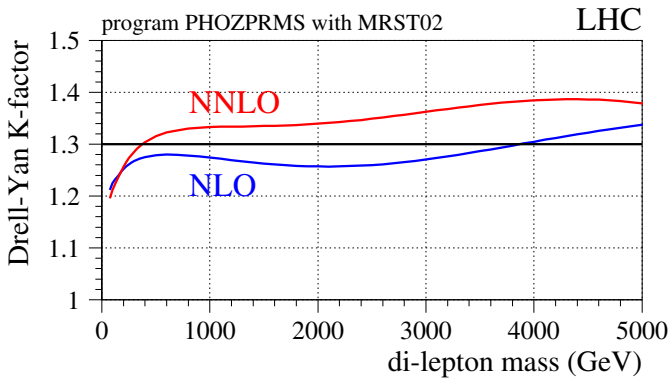

Figure C.3. K-factors as a function of mass for the LHC.

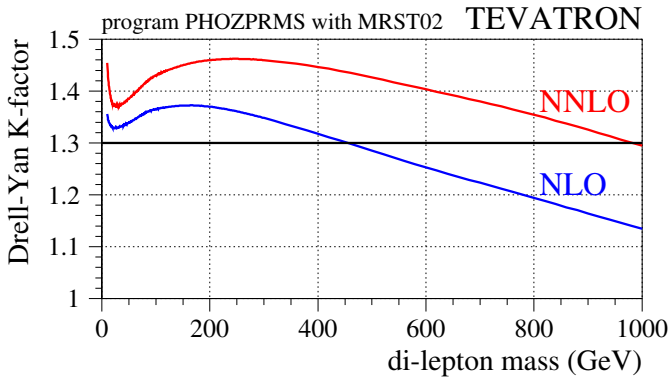

Figure C.4. K-factors as a function of mass for the Tevatron.

Usually experimenters use a constant value for the K-factor, but in fact this is not accurate. The variation of the K-factor with mass is substantial, as shown in Fig. C.3. (There is a similar, though different, variation in the K-factor for Drell–Yan production at the Tevatron – see Fig. C.4.) Notice that $K_{\mathrm{NLO}} \neq K_{\mathrm{NNLO}}$, in general, and the difference can be as large as 7%. A number of values for the K-factor are listed in Table C.1.

It is customary to take the difference $K_{\mathrm{NNLO}} - K_{\mathrm{NLO}}$ as a measure of the theoretical uncertainty due to missing higher orders. According to the results obtained with PHOZPRMS, this uncertainty is on the order of 5%. It is interesting to compare this to the uncertainty coming from the parton distribution functions (PDFs). We used the CTEQ6M set which contains "error" PDFs with which one can estimate this uncertainty [12]. The relative uncertainty of the Drell–Yan cross-section as a function of mass is shown in Fig. C.5. The positive and negative variations of the cross-section were summed separately. The error bands show the full uncertainty obtained from the twenty error-PDFs – no rescaling was done to take into account the fact that these error-PDF's correspond to 2σ variations of the PDF parameters. One sees that the PDF uncertainty varies from about 3% at low masses to 20% toward the upper reach of the LHC. Of course, these uncertainties will be reduces as data from HERA, the Tevatron and fixed-target experiments are used to improve the PDFs.

Table C.1. Values for K_{NNLO}, K_{NLO} and $K_{\mathrm{NNLO}}/K_{\mathrm{NLO}}$ as a function of mass.

mass (GeV/c^2)	K_{NNLO}	K_{NLO}	$K_{\mathrm{NNLO}}/K_{\mathrm{NLO}}$
100	1.212	1.225	0.989
200	1.256	1.252	1.003
300	1.286	1.268	1.014
400	1.303	1.275	1.022
600	1.323	1.280	1.033
800	1.330	1.278	1.040
1000	1.333	1.274	1.046
2000	1.339	1.257	1.065
3000	1.362	1.270	1.073
4000	1.385	1.304	1.061
5000	1.378	1.338	1.031

Table C.2. Leading order cross sections for some typical process at the LHC calculated by using PYTHIA 6.327 with `CTEQ5L` (default PDF for PTDR) and with `CTEQ6M` PDFs. P_0 denotes $\hat{p}_{\mathrm{T}}$-min. for the hard process.

process	cross section	comment	
$\sigma_{\mathrm{tot}}(pp \to X)$	110 ± 10 mb	different models	
$\sigma_{\mathrm{tot}}(pp \to X)$	$111.5 \pm 1.2^{+4.1}_{-2.1}$ mb	COMPETE Coll.	
process	`CTEQ5L`	`CTEQ6M`	comment
Z-boson	48.69 nb	$50.1^{+4.19\%}_{-4.76\%}$ nb	
$Z + \mathrm{jet}(g+q)$	13.94 nb	$12.73^{+3.16\%}_{-3.94\%}$ nb	$P_0 = 20$ GeV
$q\bar{q} \to Z\gamma$	44.21 pb	$46.7^{+3.93\%}_{-4.22\%}$ nb	$P_0 = 20$ GeV
$W^{\pm}$-boson	158.5 pb	$161.3^{+4.32\%}_{-4.93\%}$ nb	
$W^{\pm} + \mathrm{jet}(g+q)$	41.42 nb	$37.24^{+3.34\%}_{-4.10\%}$ nb	$P_0 = 20$ GeV
$W^{\pm}\gamma$	56.21 pb	$56.42^{+4.11\%}_{-4.38\%}$ nb	$P_0 = 20$ GeV
W^+W^-	69.69 pb	$75.0^{+3.87\%}_{-4.03\%}$ pb	
$W^{\pm}Z$	26.69 pb	$28.76^{+3.93\%}_{-4.08\%}$ pb	
$q\bar{q} \to ZZ$	11.10 pb	$10.78^{+4.02\%}_{-4.21\%}$ pb	
$WQ\bar{Q}$	$m_b = 4.8$ GeV, $m_c = 1.5$ GeV, TopReX		
$W^{\pm}c\bar{c}$	1215 pb	$1086^{+4.12\%}_{-4.53\%}$ pb	$M_{c\bar{c}} \geqslant 3.0$ GeV
$W^{\pm}c\bar{c}$	33.5 pb	$31.3^{+4.00\%}_{-4.18\%}$ pb	$M_{c\bar{c}} \geqslant 50$ GeV
$W^{\pm}b\bar{b}$	328 pb	$297^{+4.04\%}_{-4.37\%}$ pb	$M_{b\bar{b}} \geqslant 9.6$ GeV
$W^{\pm}b\bar{b}$	34.0 pb	$31.3^{+4.00\%}_{-4.18\%}$ pb	$M_{b\bar{b}} \geqslant 50$ GeV
$Zb\bar{b}, m_b = 4.62$ GeV	789.6 ± 3.66 pb	MCFM	$M_{b\bar{b}} \geqslant 9.24$ GeV
dijet processes	819 μb	$583^{+4.78\%}_{-6.02\%}$ μb	$P_0 = 20$ GeV
γ + jet	182 nb	$135^{+4.92\%}_{-6.14\%}$ nb	$P_0 = 20$ GeV
$\gamma\gamma$	164 pb	$137^{+4.62\%}_{-5.65\%}$ pb	$P_0 = 20$ GeV
$b\bar{b}, m_b = 4.8$ GeV	479 μb	$187^{+9.7\%}_{-13.2\%}$ μb	
$t\bar{t}, m_t = 175$ GeV	488 pb	$493^{+3.24\%}_{-3.31\%}$ pb	
$t\bar{t}, m_t = 175$ GeV	830 ± 90 pb	NLO+NNLO	
$t\bar{t}\,b\bar{b}$	10 pb		AcerMC 1.2
inclusive Higgs	$m_H = 150$ GeV	23.8 pb	
inclusive Higgs	$m_H = 500$ GeV	3.8 pb	

The variation of the K-factors with mass comes in part because of the Z-resonance. The size of the Z-peak relative to the continuum production of lepton pairs is therefore relevant. This relative size depends on the coupling of the Z-boson to the up and down quarks in

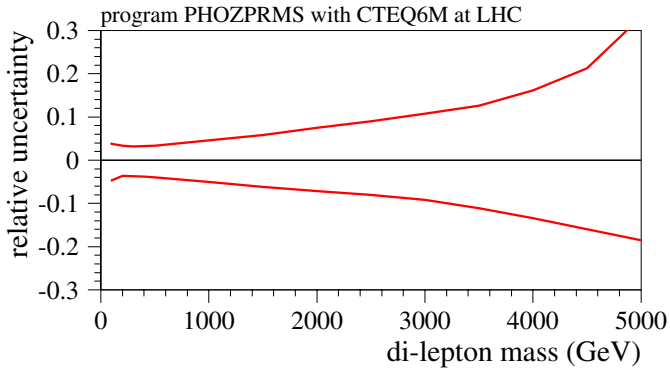

Figure C.5. Uncertainty from the parton distribution functions, evaluated using the CTEQ6M set.

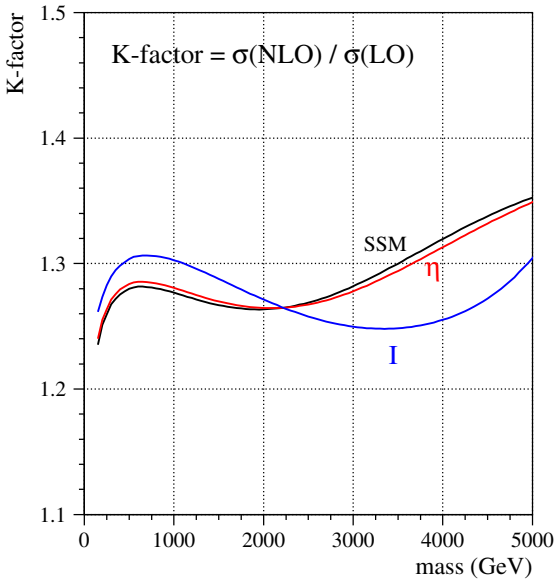

Figure C.6. K-factors as a function of mass of a new Z' resonance, for two cases: η and I (see text). The curve 'SSM' refers to a sequential Standard Model Z'.

the proton. There is practically no uncertainty on those couplings, and they are completely determined in the Standard Model. However, if a new Z' resonances is present, its couplings will not be known *a priori*. Thus it is interesting to consider to what extent the K-factor will depend on those couplings.

We have considered two examples of possible Z' resonances, and computed K_{NLO} as a function of the resonance mass, as shown in Fig. C.6. The first model, labelled "η," illustrates the case of a Z' which couples primarily to up-quarks, and the second one, labelled "I," couples mainly to down-quarks [816]. As is clear from the figure, the radiative corrections as a function of mass are quite different in these two extreme cases. Thus, there will be an ambiguity in the cross-section measurement of a new Z' resonance at the level of about 5% until the relative couplings of that Z' to up and down quarks can be established.

Appendix D. GARCON: Genetic Algorithm for Rectangular Cuts OptimizatioN

Typically HEP analysis has quite a few selection criteria (cuts) to optimise for example a significance of the "signal" over "background" events: transverse energy/momenta cuts, missing transverse energy, angular correlations, isolation and impact parameters, etc. In such cases simple scan over multi-dimensional cuts space (especially when done on top of a scan over theoretical predictions parameters space like for SUSY e.g.) leads to CPU time demand varying from days to many years... One of the alternative methods, which solves the issue is to employ a Genetic Algorithm (GA), see e.g. [820–822].

We wrote a code, GARCON [63], which automatically performs an optimisation and results stability verification effectively trying $\sim 10^{50}$ cut set parameters/values permutations for millions of input events in hours time. Examples of analyses are presented in this Physics TDR; see, for example, Sections 3.1, 8.4.1, 13.6, 13.7, 13.14 and recent papers [51, 317, 675, 676].

The GARCON program among many other features allows user:

- to select an optimisation function among known significance estimators, as well as to define user's own formula, which may be as simple as signal to background ratio, or a complicated one including different systematic uncertainties separately on different signal and background processes, different weights per event and so on;
- to define a precision of the optimisation;
- to restrict the optimisation using different kind of requirements, such us minimum number of signal/background events to survive after final cuts, variables/processes to be used for a particular optimisation run, number of optimisations inside one run to ensure that optimisation converges/finds not just a local maximum(s), but a global one as well (in case of a complicated phase space);
- to automatically verify results stability.

GARCON, like GA-based programs in general, exploits evolution-kind algorithms and uses evolution-like terms:

- Individual is a set of qualities, which are to be optimised in a particular environment or set of requirements. In HEP analysis case Individual is a set of lower and upper rectangular cut values for each of variables under study/optimization.
- Environment or set of requirements of evolutionary process in HEP analysis case is a Quality Function (QF) used for optimisation of individuals. The better QF value the better is an Individual. Quality Function may be as simple as $S/\sqrt{B}$, where S is a number of signal events and B is a total number of background events after cuts, or almost of any degree of complexity, including systematic uncertainties on different backgrounds, etc.
- A given number of individuals constitute a Community, which is involved in evolution process.
- Each individual involved in the evolution: breeding with possibility of mutation of new individuals, death, etc. The higher is the QF of a particular individual, the more chances this individual has to participate in breeding of new individuals and the longer it lives (participates in more breeding cycles, etc.), thus improving community as a whole.
- Breeding in HEP analysis example is a producing of a new individual with qualities (set of min/max cut values) taken in a defined way from two "parent" individuals.
- Death of an individual happens, when it passes over an age limit for it's quality: the bigger it's quality, the more it lives.

- Cataclysmic Updates may happen in evolution after a long period of stagnation in evolution, at this time the whole community gets renewed and gets another chance to evolve to even better quality level. In HEP analysis case it corresponds to a chance to find another local and ultimately a global maximum in terms of quality function. Obviously, the more complicated phase space of cut variables is used the more chances exist that there are several local maximums in quality function optimisation.
- There are some other algorithms involved into GAs. For example mutation of a new individual. In this case newly "born" individual has not just qualities of its "parents", but also some variations, which in terms of HEP analysis example helps evolution to find a global maximum, with less chances to fall into a local one. There are also random creation mechanisms serving the same purpose.

There is nothing special involved in GARCON input preparation. One would need to prepare a set of arrays for each background and a signal process of cut variable values for optimisation. Similar to what is needed to have to perform a classical eye-balling cut optimisation.

In comparison to other automatised optimisation methods GARCON output is transparent to user: it just says what rectangular cut values are optimal and recommended in an analysis. Interpretation of these cut values is absolutely the same as with eye-balling cuts when one selects a set of rectangular cut values for each variable in a "classical" way by eye.

All-in-all it is a simple yet powerful ready-to-use tool with flexible and transparent optimisation and verification parameters setup. It is publicly available along with a paper on it [63] consisting of an example case study and user's manual.

Appendix E. Online Selection

E.1. Introduction

The CMS trigger menu depends upon the luminosity delivered by the LHC and the available bandwidth between and out of the systems. The LHC luminosity is expected to start at $\mathcal{L} = 10^{32}\,\mathrm{cm}^{-2}\,\mathrm{s}^{-1}$ in 2007 and gradually rise to $\mathcal{L} = 10^{34}\,\mathrm{cm}^{-2}\,\mathrm{s}^{-1}$ by 2010. The CMS data acquisition can be operated with one to eight slices of Event Filter Farms that execute High-Level Trigger (HLT) algorithms. It is expected that we start with one slice in 2007, allowing a bandwidth of 12.5 kHz between Level-1 and HLT, and build up to the full eight slices by 2010, when the Level-1 to HLT bandwidth can be raised to 100 kHz. It is assumed that the data logging capability after the HLT selection will remain constant at a rate between 100 Hz to 150 Hz[54]. The Level-1 and HLT algorithms will be configured to operate with the lowest possible thresholds making the best use of the available bandwidth.

Here we focus solely on trigger studies for $\mathcal{L} = 2 \times 10^{33}\,\mathrm{cm}^{-2}\,\mathrm{s}^{-1}$. The scenario of operation assumes that CMS uses four DAQ slices capable of 50 kHz. While the actual choice of trigger thresholds, especially at HLT, depends strongly upon the physics of interest at the time of operation, we propose here an example set of trigger menus within the constraints of the data acquisition system. An effort has been made to optimise the Level-1 and HLT thresholds coherently, taking into account possible bandwidth limitations.

The structure of this note is as follows: first we overview the object-identification algorithms used for these studies. The emphasis is given to the changes that have been introduced since a similar study was performed in the DAQ TDR [76]. We then introduce a series of new trigger paths, aiming at increasing the event yield for various physics analyses. The central idea is to exploit various multi-object (or *cross-channel*) triggers in an attempt to improve the rejection and, at the same time, lower the kinematic thresholds of the corresponding objects. We finally present the performance of the triggers, and we calculate the overlap among them and the total HLT output rate.

E.2. Description of trigger tools

E.2.1. Level-1 reconstruction

There have been no significant changes in the Level-1 algorithms since the DAQ TDR. We have introduced an H_{T} algorithm which sums the corrected jet E_{T} of all the jets found above a programmable threshold, within $|\eta| < 5$. It does not account for E_{T} carried by muons and neutrinos.

The Level-1 strategy is the following: We have made an effort to keep the thresholds at the same levels, or even reduce them in order to be able to study cross-channel triggers (typically appearing with lower kinematic cuts). The notable exception is the tau triggers, where an increase in the HCAL noise and the usage of a new pile-up model in the simulation do affect the Level-1 τ identification tools, and therefore the related trigger rates. We have introduced additional Level-1 conditions for all HLT paths. The determination of thresholds and prescales is a compromise between the desire to distribute reasonably the available L1 bandwidth to the various triggers, and the need to optimise the L1 and HLT thresholds coherently in well-defined trigger paths.

[54] At the time of the writing of this document, several scenarios for the HLT output rate, the disk requirements for the storage manager and the associated cost are under discussion.

E.2.2. HLT reconstruction

Well defined Level-1 terms are used in order to obtain triggers whose behaviour and efficiency can be studied with real data. We have replaced some of the Level-1 conditions with respect to the DAQ TDR with new Level-1 terms when this leads to more reasonable trigger paths or triggers that are more stable and carry less of a bias. The optimisation of the thresholds for the various triggers has been a compromise between the physics needs of the CMS experiment and the total HLT rate available. This study serves only as an intermediate step in a long-term trigger study project. Further improvements in the reconstruction tools, better optimisation of the thresholds, implementation of additional triggers and a CMS-wide discussion of the allocation of the HLT bandwidth to the physics groups according to the priorities of the experiment, are foreseen.

A general and detailed description of the HLT system can be found in Ref. [76]. Here we summarise the recent modifications of the HLT tools, and the expected changes in the rates of the various triggers with respect to the earlier studies.

- **Muons:** The muon algorithm has not changed, with the exception of the drift-tube local reconstruction and segment building. Therefore, no significant changes in the rates of single- and dimuon trigger paths are expected. The option of constructing muon triggers without isolation has been added.
- **Electrons–Photons.** Here the most important change is that all saturated trigger towers at Level-1 are now considered isolated. This increases both the signal efficiency and the background. At HLT, the photon rate can be reduced by increasing the thresholds or by applying some isolation cuts. For the electrons the options include a matching with pixel lines and tracks, as well as isolation requirements in the hadron calorimeter and the tracker. A study of the algorithm optimisation can be found in Ref. [7]. An improvement of the rejection power of the electron–photon algorithms is achieved with a simultaneous decrease of the HLT thresholds. Similar enhancements are expected for cross-channel triggers where one of the objects under consideration is an electron or a photon.
- **Jets and $\boldsymbol{E_{\mathrm{T}}^{\mathrm{miss}}}$.** The main jet-finder algorithm (Iterative Cone with $R = 0.5$) has not been modified. Some optimisations of the tower thresholds have been added, and the jet corrections have been updated ("Scheme C"). Similarly, there are no major algorithm changes for $E_{\mathrm{T}}^{\mathrm{miss}}$, however it has been ensured that all triggers including a $E_{\mathrm{T}}^{\mathrm{miss}}$ object do not have any off-line corrections applied. Another improvement that has been recently introduced is the ability to construct *acoplanar* triggers by combining two jets, or a jet and a $E_{\mathrm{T}}^{\mathrm{miss}}$ object that do not lie "back-to-back" Details of the physics algorithms can be found in Refs. [165] and [148].
- ***b*-jets.** The algorithm now uses muon information for fast rejection. Further improvements have been made for faster decisions and for an increased efficiency in fully hadronic final states. The documentation for the b-jet HLT algorithm can be found in Ref. [290].
- **Taus:** The HLT τ algorithm has not changed. However, the increase in the Level-1 rate does propagate into the HLT. The isolation parameters for the electromagnetic calorimeter and the tracker have been tuned after recent studies performed by the Higgs group, described in Ref. [280]. The overall rate for τ-related triggers is expected to be slightly increased.

A new addition to the HLT reconstruction tools is the H_{T} algorithm. It sums the corrected jet E_{T} of all the $E_{\mathrm{T}} > 5\,\mathrm{GeV}$ jets found within $|\eta| < 5$, along with the energy of the $p_{\mathrm{T}} > 5\,\mathrm{GeV/c}$ HLT muons found in the event, and the $E_{\mathrm{T}}^{\mathrm{miss}}$ computed using the calorimeter deposits. It is meant to be driven off the corresponding L1 H_{T} term.

E.3. Triggering with forward detectors

E.3.1. Objective

We discuss[55] the feasibility of a special forward detectors trigger stream, with target output rate of $\mathcal{O}(1)$ kHz at L1 and $\mathcal{O}(1)$ Hz on the HLT, as well as the potential of the already foreseen CMS L1 trigger streams for retaining events with diffractive processes.

The proposed forward detectors trigger stream combines the information of the central CMS detector with that from detectors further downstream of the CMS IP. The forward detectors considered are the TOTEM T1 and T2 tracker telescopes as well as the TOTEM Roman Pot (RP) detectors up to 220 m downstream of CMS [823, 824]. Information from TOTEM will be available to the CMS L1 trigger. We also consider detectors at a distance of 420 m, in the cryogenic region of the LHC ring, currently being studied by the FP420 project [254].

Topologically, diffractive events are characterised by a gap in the rapidity distribution of final-state hadrons. In addition, the fractional momentum loss, ξ, of diffractively scattered protons peaks at $\xi = 0$ ("diffractive peak"). The TOTEM RP detectors will permit to measure protons in the region $0.2 > \xi > 0.02$. Detectors at a distance of 420 m from the IP would provide a coverage of $0.02 > \xi > 0.002$, complementary to that of the TOTEM detectors, but cannot be included in the Level-1 trigger without an increase in the Level-1 latency of 3.2 μs (though a special, long latency running mode might be feasible at lower luminosities).

The studies discussed in the following assume that the RP detectors are 100% efficient in detecting all particles that emerge at a distance of at least $10\,\sigma_{\text{beam}} + 0.5$ mm from the beam axis (1.3 mm at 220 m, 4 mm at 420 m). Their acceptance was calculated for the nominal LHC optics ($\beta^* = 0.55$ m), version V6.5 [825, 826], and by way of a simulation program that tracks particles through the accelerator lattice [827]. LHC bunches with 25 ns spacing were assumed.

The results presented below do not depend on the specific hardware implementation of the TOTEM T1, T2 and RP detectors; they hold for any tracker system with the T1, T2 η coverage in conjunction with RPs at 220 m from the IP.

E.3.2. Level-1 trigger rates for forward detectors trigger stream

E.3.2.1. 2-Jet conditions. A particularly interesting and challenging diffractive channel is the central exclusive production of a Higgs Boson, $pp \to pHp$, with Higgs mass close to the current exclusion limit. The dominant decay of a SM Higgs Boson of mass $\sim$120 GeV/c^2 is into two b-quarks and generates 2 jets with at most 60 GeV/c transverse momentum each. In order to retain as large a signal fraction as possible, as low an E_{T} threshold as possible of the Level-1 2-jet trigger is desirable. In practice, the threshold value cannot be chosen much lower than 40 GeV per jet. The Level-1 trigger applies cuts on the calibrated E_{T} value of the jet. Thus, a threshold of 40 GeV corresponds to 20–25 GeV in reconstructed E_{T}, i.e. to values where noise starts becoming sizable.

For luminosities of $10^{32}\,\text{cm}^{-2}\text{s}^{-1}$ and above, the Level-1 rate from standard QCD processes for events with at least 2 central jets ($|\eta| < 2.5$) with $E_{\text{T}} > 40$ GeV exceeds by far the target output rate of $\mathcal{O}(1)$ kHz. Thus additional conditions need to be employed to reduce the rate from QCD processes. The efficacy of several conditions was investigated [247, 248, 828–830]. In the following, the corresponding rate reduction factors are always quoted with respect to the rate of QCD events that contain at least 2 central jets with $E_{\text{T}} > 40$ GeV per jet.

[55] These studies were carried out in collaboration with TOTEM.

Table E.1. Reduction of the rate from standard QCD processes for events with at least 2 central Level-1 jets with $E_T > 40$ GeV, achievable with requirements on the tracks seen in the RP detectors. Additional rate reductions can be achieved with the H_T condition and with a topological condition. Each of them yields, for all luminosities listed, an additional reduction by about a factor 2.

				Reduction when requiring track in RPs at					
				220 m		420 m	220 & 420 m (asymmetric)		420 & 420 m
Luminosity [$cm^{-2}\,s^{-1}$]	Pile-up events per BX	Level-1 2-jet rate [kHz] for $E_T > 40$ GeV	Total reduction needed		$\xi < 0.1$			$\xi < 0.1$	
1×10^{32}	0	2.6	2	370					
1×10^{33}	3.5	26	20	7	15	27	160	380	500
2×10^{33}	7	52	40	4	10	14	80	190	150
5×10^{33}	17.5	130	100	3	5	6	32	75	30
1×10^{34}	35	260	200	2	3	4	17	39	10

The QCD background events were generated with the Pythia Monte Carlo generator. In order to assess the effect when the signal is overlaid with pile-up, a sample of 500,000 pile-up events was generated with Pythia. This sample includes inelastic as well as elastic and single diffractive events. Pythia underestimates the number of final state protons in this sample. The correction to the Pythia leading proton spectrum described in [831] was used to obtain the results discussed in the following.

Given a Level-1 target rate for events with 2 central Level-1 jets of $\mathcal{O}(1)$ kHz, a total rate reduction between a factor 20 at $1 \times 10^{33}\,cm^{-2}\,s^{-1}$ and 200 at $1 \times 10^{34}\,cm^{-2}\,s^{-1}$ is necessary. Table E.1 summarises the situation for luminosities between $10^{32}\,cm^{-2}\,s^{-1}$ and $10^{34}\,cm^{-2}\,s^{-1}$, and for different RP detector conditions: a track at 220 m on one side of the IP (single-arm 220 m), without and with a cut on ξ; a track at 420 m on one side of the IP (single-arm 420 m); a track at 220 m and 420 m (asymmetric); a track at 420 m on both sides of the IP (double-arm 420 m). Because the detectors at 220 m and 420 m have complementary coverage in ξ, the asymmetric condition in effect selects events with two tracks of very different ξ value, in which one track is seen at 220 m on one side of the IP and a second track is seen on the other side at 420 m. If not by the L1 trigger, these asymmetric events can be selected by the HLT and are thus of highest interest. At luminosities where pile-up is present, the rate reduction achievable with the RP detector conditions decreases because of the diffractive component in the pile-up.

A collimator located in front of the LHC magnet Q5, planned to be operative at higher luminosities, will have an effect on the acceptance of the RP detectors resembling that of a ξ cut. This effect has not been taken into account in Table E.1.

Using T1 and T2 as vetoes in events with 2 central Level-1 jets was found to be effective only in the absence of pile-up [832].

In addition to the E_T values of individual Level-1 jets, the CMS Calorimeter Trigger has at its disposal the scalar sum, H_T, of the E_T values of all jets. Requiring that essentially all the E_T be concentrated in the two central Level-1 jets with highest E_T, i.e. $[E_T^1 + E_T^2]/H_T > 0.9$ (H_T condition), corresponds to imposing a rapidity gap of at least 2.5 units with respect to the beam direction. This condition reduces the rate of QCD events by approximately a factor 2, independent of the presence of pile-up and with only a small effect on the signal efficiency.

A further reduction of the QCD rate could be achieved with the help of a topological condition. The 2-jet system has to balance the total momentum component of the two protons along the beam axis. In signal events with asymmetric ξ values, the proton seen on one side

Table E.2. Estimated threshold values that result in a L1 output rate of ~ 1 kHz, for various conditions on central CMS detector quantities and on tracks seen in the RP detectors at 220 m and 420 m.

	L1 E_T or p_T threshold [GeV] at $\mathcal{O}(1)$ KHz L1 output rate for luminosity [cm^{-2} s^{-1}]			
L1 condition	1×10^{33}	2×10^{33}	5×10^{33}	1×10^{34}
1 Jet	115	135	160	190
2 Jet	90	105	130	150
1 Jet+220s	90	115	155	190
2 Jet+220s	65	90	125	150
1 Jet+220d	55	85	130	175
2 Jet+220d	30	60	100	140
1 Jet+220s(c)	70	90	150	185
2 Jet+220s(c)	60	70	115	145
1 Jet+220d(c)	30	65	110	155
2 Jet+220d(c)	20	45	85	125
1 Jet+420s	65	90	125	165
2 Jet+420s	45	70	100	130
1 Jet+420d	20	40	80	115
2 Jet+420d	< 10	30	60	90
1 μ+220s	12	16	23	> 100
1 μ + 220d	4	9	17	80
1 μ+220s(c)	–	11	22	100
1 μ+220d(c)	–	6	13	30
1 μ+420s	7	11	14	37
1 μ+420d	< 2	4	7	14

in the RP detectors at 220 m distance is the one with the larger ξ and thus has lost more of its initial momentum component along the beam axis. Hence the jets tend to be located in the same η-hemisphere as the RP detectors that detect this proton. A trigger condition requiring that $[\eta^{jet1} + \eta^{jet2}] \times \text{sign}(\eta^{220\,mRP}) > 0$ reduces the QCD background by a factor 2, independent of pile-up, and with no loss in signal efficiency.

A reduction of the QCD rate to levels compatible with a Level-1 output target rate of $\mathcal{O}(1)$ kHz by including RP detectors at a distance of 220 m from the CMS IP thus appears feasible for luminosities up to 2×10^{33} cm^{-2} s^{-1}, as long as a ξ cut can be administered in the L1 trigger.

E.3.2.2. Other conditions. The effect of combining already foreseen Level-1 trigger conditions with conditions on the RP detectors is illustrated in Table E.2 [829]. Single- and double-arm RP detector conditions are indicated with 's' and 'd' endings, respectively. Entries marked with a '(c)' indicate thresholds applicable if a cut on $\xi < 0.1$ is implemented for the RP detectors at 220 m. The jet conditions consider all Level-1 jets with $|\eta| < 5$.

A further rate reduction by approximately a factor two can be obtained at luminosities with negligible pile-up by imposing a rough large rapidity gap cut at L1. This was implemented by requiring that there be no forward jets, i.e. jets in the HF, in either hemisphere in the event.

E.3.3. Level-1 signal efficiencies

Of the Level-1 conditions discussed so far, only those based on the RP detectors have a significant impact on the signal efficiency. Of further interest is the question how many signal events are being retained by the already foreseen trigger streams, notably the muon trigger.

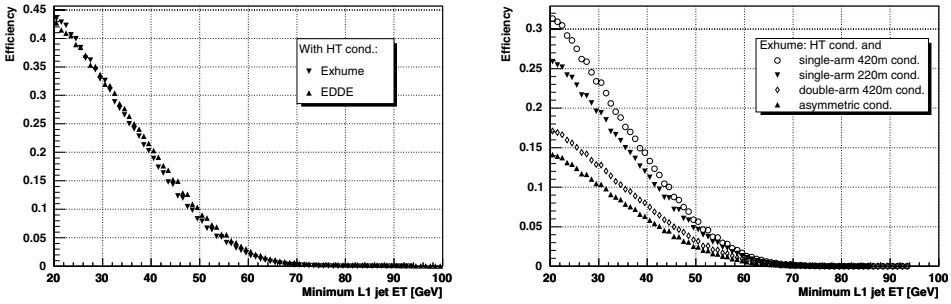

Figure E.1. L1 selection efficiency for $pp \to pHp$ and $H(120, \mathrm{GeV/c^2}) \to b\bar{b}$ as function of the E_T threshold value when at least 2 central Level-1 jets with E_T above threshold are required. All plots are for the non-pile-up case and the H_T condition has been applied. Left: Comparison between the EDDE and Exhume Monte Carlo generators, without applying any additional RP conditions. Right: Comparison of the effect of different RP conditions on the efficiency in the Exhume Monte Carlo sample.

E.3.3.1. Central exclusive Higgs production ($H(120\,\mathrm{GeV/c^2}) \to b\bar{b}$). In order to study the effect of the Level-1 trigger selection on the Higgs signal, signal samples of 100,000 events with central exclusive production of a Higgs Boson were generated with the Monte Carlo programs EDDE [261] (version 1.1) and Exhume [259] (version 1.0).

Figure E.1 shows the Level-1 selection efficiency as a function of the E_T threshold values when at least 2 central Level-1 jets with E_T above threshold are required [829]. For a threshold of 40 GeV per jet, Exhume and EDDE both yield an efficiency of about 20%. The plot on the right-hand side overlays the efficiency curves obtained with Exhume when the 2-jet condition is combines with RP detector conditions. With an E_T threshold of 40 GeV per jet, the single-arm 220 m (420 m) condition results in an efficiency of the order 12% (15%), the double-arm 420 m condition in one of 8% and the asymmetric condition in one of 6%. This also means that, even without the possibility of including the RP detectors at 420 m from the CMS IP in the Level-1 trigger, 6% of the signal events can be triggered on with the single-arm 220 m condition, but will have a track also in the 420 m detectors that can be used in the HLT.

An alternative trigger strategy is to exploit the relatively muon-rich final state from B-decays: about 20% of the events have at least a muon in the final state. Requiring at least one (two) L1 muon(s) with p_T above 14 GeV/c (3 GeV/c) yields an efficiency of 6% (2%). Demanding at least 1 muon and 1 jet, the latter with E_T >40 GeV, is a condition not yet foreseen in the CMS trigger tables. For a muon p_T threshold of 3 GeV/c, the rate at a luminosity of $10^{33}\,\mathrm{cm^{-2}}$ is slightly less than 3 kHz, and about half of the decays with muons in the final state (i.e. 9%) are retained [830].

E.3.3.2. Central exclusive Higgs production ($H(140\,\mathrm{GeV/c^2}) \to WW$). For SM Higgs Boson masses above 120 GeV/c^2, the $H \to WW$ branching ratio becomes sizable; in this case the final state contains high-p_T leptons that can be used for triggering. Efficiencies are in general high [830]. About 23% of the events have at least one muon in the final state. Approximately 70% of these (i.e. 16%) are retained by requiring at least one muon with a p_T threshold of 14 GeV/c. An extra $\approx$ 10% (i.e. 2%) would be retained by implementing the muon/jet slot discussed above with thresholds of 3 GeV/c on the muon p_T and 40 GeV on the jet E_T.

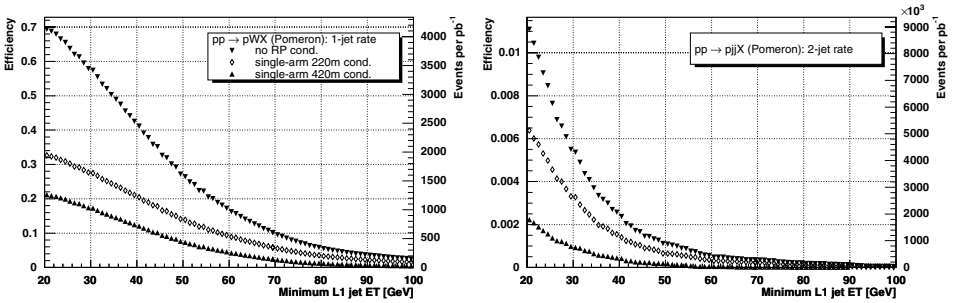

Figure E.2. L1 selection efficiency as function of the E_{T} threshold value for $pp \to pWX$ (left) and $pp \to pjjX$ (right), when at least one (left) or two (right) Level-1 jets ($|\eta| < 5$) above threshold are required. All plots are for the non-pile-up case.

E.3.3.3. Single diffractive hard processes. Double-Pomeron exchange processes constitute only a small part of the diffractive cross section. Hard single-diffraction, $pp \to pX$, where only one proton remains intact and the other is diffractively excited, have much higher cross sections than hard double-Pomeron exchange events. Efficiencies have been studied for $pp \to pX$, with X containing a W or a Z boson that decay to jets and to muons, as well as with X containing a dijet system. Samples of 100,000 signal events each were generated with the POMWIG Monte Carlo generator [833] (version 1.3).

For two example processes, Figure E.2 shows the efficiency as a function of the Level-1 threshold value, normalised to the number of events where for the diffractively scattered proton $0.001 < \xi < 0.2$ holds [829]. Three different trigger conditions are considered: trigger on central detector quantities alone (i), trigger on central detector quantities in conjunction (ii) with the single-arm 220 m condition, and (iii) with the single-arm 420 m condition. Also shown is the number of events expected to pass the L1 selection per pb^{-1} of LHC running. A significant part of events is retained when a proton is required in the 220 m RPs.

E.3.4. Effect of pile-up, beam-halo and beam-gas backgrounds

Pile-up effects are included in all rate and efficiency studies presented. In the 220 m stations, 0.055 protons/pile-up event are expected on average, in the 420 m stations, 0.012 protons/pile-up event. At a luminosity of $10^{34}\ \mathrm{cm}^{-2}\ \mathrm{s}^{-1}$, there are 35 pile-up events on average; this entails, on average, 2 extra tracks in the 220 m stations and less than one in the 420 m stations.

The effect from beam-halo and beam-gas events on the Level-1 rate is not yet included in the studies discussed here. Preliminary estimates suggest that they are chiefly a concern for any trigger condition based solely on the forward detectors. For any trigger condition that includes a requirement on central CMS detector quantities the size of their contribution is such that they do not lead to a significant increase of the Level-1 output rate.

E.3.5. HLT strategies

Jets are reconstructed at the HLT with an iterative cone ($R < 0.5$) algorithm. The Level-1 selection cuts are repeated with HLT quantities. The following conditions are imposed [829]:

(A) The event pass the single-arm 220 m Level-1 condition with $\xi < 0.1$ cut. As demonstrated in Table E.1, this condition reduces the Level-1 output rate to below $\mathcal{O}(1)$ kHz. Additional

Table E.3. Results of HLT selection.

HLT selection condition	A + B + C	A + B + D	A + B + C + E
HLT rate at 1×10^{33} cm^{-2} s^{-1}	15 Hz	20 Hz	< 1 Hz
line HLT rate at 2×10^{33} cm^{-2} s^{-1}	60 Hz	80 Hz	1 Hz
e Signal eff. $H(120)$ GeV/c$^2 \to b\bar{b}$	11%	7%	6%

rate reduction factors of ~ 300 (~ 1000) at $1(2) \times 10^{33}$ cm $^{-2}$ s $^{-1}$ are needed to reach the HLT target output rate of $\mathcal{O}(1)$ Hz.

(B) The two jets are back-to-back in the azimuthal angle ϕ ($2.8 < \Delta\phi < 3.48$ rad), and have $(E_{\mathrm{T}}^1 - E_{\mathrm{T}}^2)/(E_{\mathrm{T}}^1 + E_{\mathrm{T}}^2) < 0.4$, and $E_{\mathrm{T}} > 40$ GeV for each jet.

(C) The proton fractional momentum loss ξ is evaluated with the help of calorimeter quantities [834–836]:

$$\xi_{+-} = (1/\sqrt{s})\Sigma_i E_{Ti} \exp(\mp\eta_i), \tag{E.1}$$

where the sum runs over the two jets and the $+, -$ signs denote the two hemispheres. The result is compared with the ξ value measured by the RP detectors. At present, no simulation of the RP reconstruction is available. As estimate of the ξ resolution, 15% (10%) is assumed at 220 m (420 m). Events are rejected if the difference between the two values of ξ is larger than $2\,\sigma$.

(D) At least one of the two jets is b-tagged.

(E) A proton is seen at 420 m.

The case without pile-up presents no difficulty: essentially no QCD background events survive the selection. If conditions A+B+C are applied, the signal efficiency for $pp \to pHp$ with $H(120\ \mathrm{GeV/c^2}) \to b\bar{b}$ is at 11% essentially unchanged with respect to the Level-1 selection, but the HLT output rate exceeds the target output rate, see Table E.3. If b-tagging is required but no ξ matching (conditions A +B+D), the efficiency drops to 7%, without any improvement in the rate reduction. The combination of conditions A+B+C+E finally leads to the targeted HLT output rate of $\mathcal{O}(1)$ Hz, without any loss in signal efficiency compared to L1.

E.4. High-Level Trigger paths

We are starting with the DAQ-TDR trigger table as the baseline. This includes single- and double-triggers for the basic objects (e, γ, μ, τ) along with jets and b-jets. Some cross-channel triggers are also present. We are expanding the cross-channel "menu" by introducing additional triggers. We introduce an H_{T} algorithm, which we combine with other objects. We are also adding a series of central single-jets, non-isolated muons, and a diffractive trigger discussed earlier.

E.4.1. Level-1 conditions

Table E.4 summarises the Level-1 conditions used to drive all the trigger paths. A pseudo "L1 bit number" has been assigned for easy reference in the following sections.

E.4.2. Evolution of DAQ-TDR triggers

The trigger paths that have been studied in Ref. [76] have been inherited and constitute the "bulk" of this next iteration of the CMS Trigger Menu for $\mathcal{L} = 2 \times 10^{33}\,\mathrm{cm^{-2}\,s^{-1}}$.

Table E.4. Level-1 conditions used in High Level Trigger paths.

Level-1 bit #	Trigger	(GeV)	Prescale
0	Single μ	14	1
1	Double μ	3	1
2	Single isolated $e\gamma$	23	1
3	Double isolated $e\gamma$	11	1
4	Double $e\gamma$ (isolated/non-isolated)	19	1
8	Single central jet	177	1
9	Single forward jet	177	1
10	Single τ-jet	100	1
11	2 central jets	130	1
12	2 forward jets	130	1
13	2 τ-jets	66	1
14	3 central jets	86	1
15	3 forward jets	86	1
16	3 τ-jets	40	1
17	4 central jets	70	1
18	4 forward jets	70	1
19	4 τ-jets	30	1
26	(isolated) $e\gamma + \tau$	14, 52	1
31	H_{T}	300	1
32	$E_{\mathrm{T}}^{\mathrm{miss}}$	60	1
33	Single jet (central, forward or τ)	140	10
34	Single jet (central, forward or τ)	60	1 000
35	Single jet (central, forward or τ)	20	100 000
36	Single jet (central, forward or τ)	150	1
37	2 jets (central, forward or τ)	100	1
38	3 jets (central, forward or τ)	70	1
39	4 jets (central, forward or τ)	50	1

Modifications (optimisation of isolation cuts and thresholds) have been made for certain of the triggers, to reflect changes in the physics algorithms, or the improved understanding of the background from Monte Carlo (MC) simulations. The proposed Trigger Tables includes:

- **Muons.** The standard muon triggers include calorimeter-based isolation at L2, and both calorimeter and tracker isolation at L3. The p_{T} thresholds remain at 19 GeV/c for the single-muon and (7, 7) GeV/c for the dimuon trigger. A second set of relaxed single- and double-muons has been added with $p_{\mathrm{T}} > 37$ GeV and $p_{\mathrm{T}} > 10$ GeV, respectively. The main motivation here is Drell–Yan studies. In general, physics analyses that do not need a low p_{T} muon but do suffer from the isolation requirement on the muon. The reduced rejection caused by the removal of the isolation cuts is compensated by the higher-p_{T} thresholds on the muons, without affecting the event yield for the physics signal. The relaxed triggers have the advantage that the muons here are immune to radiative losses for the higher energy spectrum ($p_{\mathrm{T}} > 500$ GeV/c). Both isolated and relaxed triggers run off the corresponding non-isolated single- and double-muon bits at L1.
- **Electrons.** The p_{T} threshold remains at 26 GeV/c for the single electron trigger and has a new value of (12, 12) GeV/c for the dielectron trigger. An additional relaxed dielectron trigger appears with $p_{\mathrm{T}} > 19$ GeV/c. The single-electron and double-electron triggers run off the corresponding Level-1 bits.
- **Photons.** The new p_{T} thresholds are 80 GeV/c for the single-photon trigger and (30, 20) GeV/c for the diphoton trigger (both relaxed and non-relaxed flavours). A few prescaled

single- and double-photon triggers have also been introduced, for the purpose of studying trigger efficiencies. The photon HLT algorithms run off the corresponding Level-1 $e\gamma$ bits (single- and double-triggers).

- **Taus.** The single-τ trigger runs off the corresponding Level-1 bit. The double-τ trigger is driven by the `.OR.`-ing of the single- and double-τ trigger bits at L1. There is no explicit kinematic cut on the tau at HLT. There is, however, a match-to-track requirement in addition to the $p_{\mathrm{T}} > 100(66)\,\mathrm{GeV/c}$ L1 precondition for the inclusive (double) tau trigger. The single-τ has also a $E_{\mathrm{T}}^{\mathrm{miss}} > 65\,\mathrm{GeV}$ requirement at HLT.
- **Tau and electron.** The Level-1 condition is the corresponding τ+$e\gamma$ trigger. The p_{T} threshold remains at $16\,\mathrm{GeV/c}$ for the electron. There is no explicit p_{T} cut for the τ at HLT, but there is the match-to-track requirement for the τ candidate.
- **Jets.** The Level-1 conditions for the single-, double-, triple- and quadruple-jet triggers have been simplified considerably. Single jet triggers run off an `OR.` of a central-, forward- or tau-jet trigger at L1. Double-, triple- and quadruple-jet triggers use an `.OR.` of the all the Level-1 terms requiring the same number of jets or less. For example, the triple-jet trigger is driven by an `OR.` of the single-, double- and triple-jet Level-1 bits. In all cases, jets can be found in either the central or the forward region of the detector, and they include the τ candidates. The additional p_{T} cuts at HLT are: 400 (single), 350 (double), 195 (triple) and 80 (quadruple) GeV. The new double-jet trigger is expected to have a large overlap with the single-jet trigger path. However, it is useful for testing the additional bias introduced by the requirement for a second jet in the event. A series of prescaled triggers have also been introduced, which are discussed later (Sec. E.4.3.2).
- ***b*-jet.** This trigger is also based on the logical `.OR.` of the single-, double-, triple- and quadruple-jet Level-1 terms. At HLT, we have the additional requirement that the event is consistent with b-content. The E_{T} cut for the HLT jets is one of the following: 350 GeV if the event has one jet, 150 GeV if the event has three jets, or 55 GeV if the event has four jets.
- **Jet and $\boldsymbol{E}_{\mathbf{T}}^{\mathbf{miss}}$.** The E_{T} thresholds are 180 and 80 GeV, respectively. The Level-1 condition is a single $E_{\mathrm{T}}^{\mathrm{miss}}$ object above 60 GeV.

E.4.3. New triggers

E.4.3.1. Cross-channel triggers. The trigger studies presented in the DAQ TDR [76] have been the most comprehensive CMS effort to date to calculate rates for various trigger paths across many physics channels. For those studies the focus has been the optimisation of the rejection of the individual object-id algorithms (muon, electron, tau, etc.) rather than the combination of them into more powerful trigger tools. However, single (or even double) trigger objects are limited by the rate and, therefore, have their thresholds often higher than desired for many physics analyses. If the signal contains more than one trigger objects, using trigger paths combining different objects may yield a considerable gain by allowing lower trigger thresholds and higher efficiency. Cross-channel triggers can be much more stable and less prone to rate fluctuations from operating conditions. The correlations among trigger objects can help reduce difficult backgrounds and instrumental fakes. The additional advantage is that such cross-channel triggers have noticeably lower rates than the single trigger channels and therefore contribute fairly little to the overall bandwidth.

Some cross-channel triggers have already been considered and their rates estimated [76], such as $\tau + e$ and $\tau + E_{\mathrm{T}}^{\mathrm{miss}}$, motivated by the Higgs searches with hadronic decays of τ and leptons, and jet + $E_{\mathrm{T}}^{\mathrm{miss}}$, important for searches of super-symmetric particles. The new addition

to the Trigger Menu, expanding the scope of Higgs searches, is a combined $\tau + \mu$ trigger with p_T thresholds at 40 and 15 GeV/c, respectively. It is driven by the single-μ Level-1 bit.

We are presenting here a few additional cross-channel triggers, along with the physics motivation.

- A new category of triggers introduced here is the acoplanar dijet and jet+E_T^{miss} for SUSY signals. The gain is the lower thresholds that become possible because of the topology constraint. Possible biases should be studied, so these triggers are meant to run in parallel with the standard jet and jet + E_T^{miss} triggers without the acoplanarity requirements. We introduce a double-jet trigger with E_T thresholds at (200, 200) GeV and $|\Delta\phi| < 2.1$, and a new jet + E_T^{miss} trigger with E_T thresholds at (100, 80) GeV and $|\Delta\phi| < 2.1$. The former is driven by an `.OR.` of the single- and double-jet requirements at Level-1 (bits 36, 37). The latter is driven by a simple $E_T^{miss} > 60$ GeV Level-1 requirement.
- "$E_T^{miss} + X$" triggers. A combination of an E_T^{miss} object with an H_T cut, one (or more) jet or lepton may be the only way to access E_T^{miss}-enhanced triggers if there are problems (*e.g.* instrumental fakes) that prevent CMS from running an inclusive E_T^{miss} trigger. At this point we have implemented:
  - Multi-jets and E_T^{miss}. These will be useful for SUSY studies, just like the series of jet triggers. However, the additional E_T^{miss} requirement allows us to lower the thresholds on the jets, and therefore increase the sensitivity of the analyses. We introduce here a dijet + E_T^{miss} trigger with $E_T^{jet} > 155$ GeV, $E_T^{miss} > 80$ GeV, a triple − jet + E_T^{miss} trigger with $E_T^{jet} > 85$ GeV, $E_T^{miss} > 80$ GeV and a quadruple − jet + E_T^{miss} trigger with $E_T^{jet} > 35$ GeV, $E_T^{miss} > 80$ GeV. These all run off the single Level-1 requirement for $E_T^{miss} > 60$ GeV.
  - H_T + E_T^{miss} and H_T + e. It is difficult to contain the rate for an inclusive H_T trigger without any additional cuts. The requirement for a E_T^{miss} cut or an additional electron in the event allows us to access events with lower E_T^{miss} or softer electrons. This can give an increased efficiency for W+jets, top physics, SUSY cascades, and other similar physics channels. Here we propose an H_T + E_T^{miss} trigger with $H_T > 350$ GeV, $E_T^{miss} > 80$ GeV and an $H_T + e$ trigger with $H_T > 350$ GeV and $p_T > 20$GeV/c for the electron. They are both driven by the $E_T^{miss} > 60$ GeV condition at L1.

Some additional cross-channel triggers that have not been included in this Trigger Table iteration but should be considered in future trigger studies are:

- An $e + \mu$ trigger is of interest in many studies, for example:
  - $qqH, H \to \tau\tau \to 2\ell$, with an expected gain thanks to the lower lepton thresholds compared to the single-electron and single-muon trigger paths,
  - many SUSY decays including leptons in the final state,
  - top measurements in the double leptonic channel ($t\bar{t} \to b\bar{b}\ell\nu\ell\nu$), gaining sensitivity at the lower p_T spectrum, and
  - $B_s \to \ell\ell$, to allow for the lepton-number-violating channel to be studied.
- $E_T^{miss} + \ell$. The idea here is to exploit the presence of a W boson or a top decay in many channels. This could be used in many SM channels where lowering the lepton threshold extends the range of the measurement. For example:
  - top measurement in the double leptonic and semi-leptonic channels,
  - single top production, and
  - W measurements.

  Furthermore, this is a typical signature of an event containing super-symmetric particles.

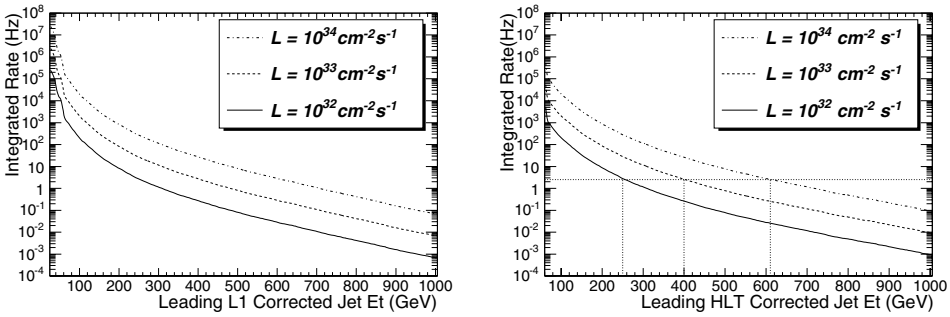

Figure E.3. The integrated trigger rates at Level-1 (left) and HLT (right) above the E_{T} thresholds for the highest E_{T} jet is plotted versus the E_{T} threshold for three luminosity scenarios: $\mathcal{L} = 10^{32}\,\mathrm{cm}^{-2}\,\mathrm{s}^{-1}$ (solid), and $\mathcal{L} = 10^{33}\,\mathrm{cm}^{-2}\,\mathrm{s}^{-1}$ (dashed), and $\mathcal{L} = 10^{34}\,\mathrm{cm}^{-2}\,\mathrm{s}^{-1}$ (dot-dashed). HLT thresholds that give 2.5 Hz are shown by vertical dotted lines.

- Triggers combining a lepton and a jet, or a lepton and a b-jet could be of interest for top measurements. The ℓ + jet signature is also very common in super-symmetric events.
- Finally, a combination of a lepton and a photon ($e+\gamma$ and $\mu+\gamma$) is ideal for Flavour Changing Neutral Current analyses, exploiting the extraordinary capabilities of CMS in detecting photons. These triggers allow to lower the thresholds on the lepton and the photon, increasing the event yield compared to the single-e, μ or γ trigger paths.

E.4.3.2. Single jet triggers. In this section we propose the single jet trigger paths. These have been driven by the needs of the inclusive jet and dijet analysis. The full study can be found in Ref. [118]. Here we summarise conclusions, along with a short description of the strategy for adjusting thresholds and prescales as the luminosity changes. This study looks at the evolution of the single-jet triggers for various luminosities. It serves as an example of how to preserve the long-term continuity of the triggers used for physics analyses. It is, therefore, interesting and instructive beyond the strict scope of the single-jet trigger suite.

To measure jet spectra down to low jet E_{T} and dijet mass requires multiple triggers, of roughly equal total rate, and with appropriately chosen E_{T} thresholds and prescales. In Fig. E.3 we show estimates of the Level-1 and HLT single jet trigger rates vs. corrected jet E_{T}. In Table E.5 we show the single jet trigger paths from Level-1 to HLT including thresholds, prescales and estimates of the rates. We find that the maximum allowed HLT rate is the constraining factor for triggering on jets. For luminosity $\mathcal{L} = 10^{32}\,\mathrm{cm}^{-2}\,\mathrm{s}^{-1}$, $\mathcal{L} = 10^{33}\,\mathrm{cm}^{-2}\,\mathrm{s}^{-1}$ and $\mathcal{L} = 10^{34}\,\mathrm{cm}^{-2}\,\mathrm{s}^{-1}$ the highest E_{T} threshold at HLT was chosen to give a rate of roughly 2.5 Hz, as illustrated in Fig. E.3, so that four triggers would saturate an allowed jet rate of roughly 10 Hz at HLT.

The highest E_{T} threshold in each scenario is not prescaled. Lower thresholds are prescaled and are chosen at roughly half the E_{T} of the next highest threshold. This allows reasonable statistics in the overlap between the two samples, necessary for measuring trigger efficiencies and producing a continuous jet spectrum. Note that the total L1 jet rate required is only around 0.3 KHz, a small fraction of the Level-1 total bandwidth. Since we are limited by HLT, not L1, for each trigger path the Level-1 thresholds are chosen low enough to have a Level-1 trigger efficiency of more than 95% at the corresponding HLT threshold in the path, as shown in Figure E.4. This strategy utilizes ten times more bandwidth at L1 than at HLT to insure that all of the resulting HLT sample has high enough trigger efficiency to be useful for analysis.

Table E.5. Single jet trigger table showing path names, trigger thresholds in corrected E_T, prescales, and estimated rates at Level-1 and HLT for four different luminosity scenarios.

Path	L1				HLT	
	E_T Cut (GeV)	Unpres. Rate (KHz)	Prescale (N)	Presc. Rate (KHz)	E_T Cut GeV)	Rate (Hz)
Single Jet Triggers in Scenario 1: $\mathcal{L} = 10^{32}$ cm^{-2} s^{-1}						
High	140	0.044	1	0.044	250	2.8
Med	60	3.9	40	0.097	120	2.4
Low	25	2.9×10^2	2,000	0.146	60	2.8
Single Jet Triggers in Scenario 2: $\mathcal{L} = 10^{33}$ cm^{-2} s^{-1}						
Ultra	270	0.019	1	0.019	400	2.6
High	140	0.44	10	0.044	250	2.8
Med	60	39	400	0.097	120	2.4
Low	25	2.9×10^3	20,000	0.146	60	2.8
Single Jet Triggers in Scenario 3: $\mathcal{L} = 2 \times 10^{33}$ cm^{-2} s^{-1}						
Ultra	270	0.038	1	0.038	400	5.2
High	140	0.88	20	0.044	250	2.8
Med	60	78	800	0.097	120	2.4
Low	25	5.8×10^3	40,000	0.146	60	2.8
Single Jet Triggers in Scenario 4: $\mathcal{L} = 10^{34}$ cm^{-2} s^{-1}						
Super	450	0.014	1	0.014	600	2.8
Ultra	270	0.19	10	0.019	400	2.6
High	140	4.4	100	0.044	250	2.8
Med	60	3.9×10^2	4,000	0.097	120	2.4
Low	25	2.9×10^4	200,000	0.146	60	2.8

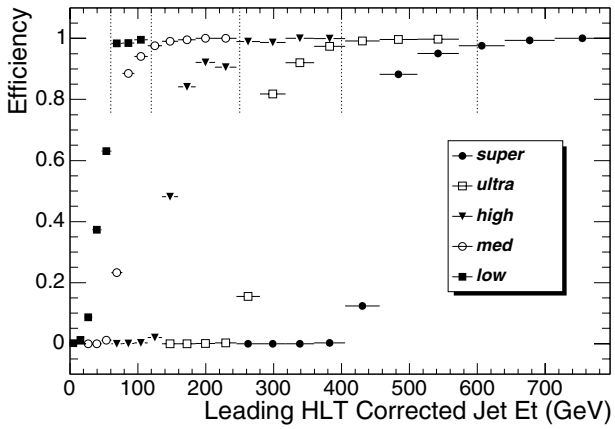

Figure E.4. The efficiency for passing the Level-1 jet trigger is shown as a function of HLT corrected jet E_T for each of the trigger paths shown in table E.5. The Level-1 thresholds were chosen to give an efficiency of greater than 95% at the corresponding HLT threshold.

Table E.5 illustrates a trigger strategy to maintain the continuity of jet analysis as the luminosity increases over a time span of years. The most important feature is that each luminosity scenario maintains the thresholds introduced in the previous scenario, allowing

combination of trigger samples over time. For the prescaled thresholds, we may increase the prescales, either in discrete steps or dynamically, to maintain the allowed HLT rate with increasing luminosity. However, to maintain maximum sensitivity to new physics, the highest E_T threshold must never be prescaled. For example, in table E.5 when the luminosity increases by only a factor of 2 from $\mathcal{L} = 10^{33}\,\mathrm{cm}^{-2}\,\mathrm{s}^{-1}$ to $\mathcal{L} = 2 \times 10^{33}\,\mathrm{cm}^{-2}\,\mathrm{s}^{-1}$, we double the prescales on the prescaled triggers but don't change either the threshold or the prescale of the highest E_T trigger labelled Ultra. This allows us to maintain stability of the single jet trigger thresholds, and analyses that depend on them, with only modest increases in the total rate for single jets. When the HLT rate in the unprescaled trigger becomes intolerably high, a higher E_T threshold unprescaled trigger is introduced, and the old unprescaled trigger can then be prescaled as necessary.

For the particular case of single-jet triggers: To commission the calorimeters, or perform a one-time jet study, it may be desirable to have more jets. If we want to write more than roughly 10 Hz of single jets at HLT, we can still use the same suite of single-jets, but lower the prescales to obtain more jets at low E_T. This is preferable to moving the threshold for the unprescaled trigger, or any of the triggers, and ending up with a special trigger that is only applicable for a given running period and difficult to combine with other samples.

For $\mathcal{L} = 2 \times 10^{33}\,\mathrm{cm}^{-2}\,\mathrm{s}^{-1}$, the suggested jet thresholds have been studied again in the scope of the global High-Level trigger analysis (Sec. E.5) and new Level-1 prescales and rates have been determined. For the trigger table proposed in this study, we have chosen four triggers, with E_T thresholds of 400, 250, 120 and 60 GeV, amd prescales of 1, 10, 1000 and 100 000, respectively.

E.4.3.3. Other triggers. The remaining triggers that have been introduced since the DAQ TDR are:

- Inclusive E_T^{miss} trigger. As discussed earlier, this is a difficult trigger that is subject to the good understanding and control of the detector noise. We suggest here a single E_T^{miss} trigger with $E_T > 91\,\mathrm{GeV}$, driven by the $E_T^{miss} > 60\,\mathrm{GeV}$ L1 condition. This is just an indicative value, rather on the low side, as E_T^{miss} rates appear lower compared to Ref. [76]. It is foreseen that additional E_T^{miss} triggers with different thresholds and prescales will be introduced in the future.
- Diffractive trigger. This trigger is different than all others described earlier in that it uses the TOTEM detector [823, 824]. At Level-1 we ask for two central jets with $E_T > 40\,\mathrm{GeV}$, along with a proton tagged with the 220 m Roman Pot. At HLT, a similar dijet cut and a "back-to-back" azimuthal condition are applied. We also require that we have a consistent measurement of the proton energy loss ξ in the two hemispheres (within 2 σ, measured at the Roman Pots). A final condition for a tagged proton seen by the 420 m Roman Pot brings the HLT rate down to $\mathcal{O}(1)$ Hz. This trigger is discussed in detail in Sec. E.3.

E.5. Performance

The performance of the trigger system is studied by using simulated data that has been digitised with appropriate pileup[56], taking into account both the inelastic (55.2 mb) and the diffractive (24.1 mb) cross sections. To reduce the amount of simulation time, about 50 million

[56] We have estimated the average number of in-time interactions per bunch crossing to be 5 for $\mathcal{L} = 2 \times 10^{33}\,\mathrm{cm}^{-2}\,\mathrm{s}^{-1}$. Additional, out-of-time interactions have been ignored.

Table E.6. Description and sizes of MC Samples used for the trigger studies. The contribution to the HLT rate does not include pre-scaled triggers.

Sample description	Cuts (Momenta in GeV/c)	Cross section (mb)	# of events	HLT rate (Hz)
Minimum bias with in-time pile-up; $\langle$ # of interactions $\rangle = 5$	—	79.3	50 000 000	—
QCD	$\hat{p_T} \in [15, 20]$	1.46×10^{0}	49 491	
QCD	$\hat{p_T} \in [20, 30]$	6.32×10^{-1}	49 244	
QCD	$\hat{p_T} \in [30, 50]$	1.63×10^{-1}	49 742	
QCD	$\hat{p_T} \in [50, 80]$	2.16×10^{-2}	99 486	
QCD	$\hat{p_T} \in [80, 120]$	3.08×10^{-3}	96 238	
QCD	$\hat{p_T} \in [120, 170]$	4.94×10^{-4}	99 736	
QCD	$\hat{p_T} \in [170, 230]$	1.01×10^{-4}	99 226	
QCD	$\hat{p_T} \in [230, 300]$	2.45×10^{-5}	99 481	
QCD	$\hat{p_T} \in [300, 380]$	6.24×10^{-6}	98 739	
QCD	$\hat{p_T} \in [380, 470]$	1.78×10^{-6}	46 491	
QCD	$\hat{p_T} \in [470, 600]$	6.83×10^{-7}	47 496	
QCD	$\hat{p_T} \in [600, 800]$	2.04×10^{-7}	48 986	
QCD	$\hat{p_T} \in [800, 1000]$	3.51×10^{-8}	45 741	
	Partial total		930 099	55.3 ± 6.9
$W \to e\nu$	1 electron with $\lvert\eta\rvert < 2.7$, $p_T > 25$	7.9×10^{-6}	3 944	9.7 ± 0.2
$Z \to ee$	2 electrons with $\lvert\eta\rvert < 2.7$, $p_T > 5$	8.2×10^{-7}	4 000	1.4 ± 0.0
$pp \to$ jet(s) $+ \gamma$, $\hat{p_T} > 30$ GeV/c	jet: $p_T > 20$,γ: $p_T > 30$	2.5×10^{-6}	4 000	1.0 ± 0.0
$W \to \mu\nu$	1 muon with $\lvert\eta\rvert < 2.5$, $p_T > 14$	9.8×10^{-6}	4 000	14.0 ± 0.3
$Z \to \mu\mu$	2 muons with $\lvert\eta\rvert < 2.5$, $p_T > 20, 10$	7.9×10^{-7}	2 941	1.5 ± 0.0
$pp \to \mu + X$	1 muon with $p_T > 3$	2.4×10^{-2}	839 999	25.5 ± 1.2

minimum bias events were simulated and reused in random combinations. It was ensured that these events do not cause triggers by themselves to avoid over estimating the rates due to this reuse of events.

In the following sections we list trigger rates along with their statistical uncertainties. These take into account the luminosity-dependent weight of the events from the different samples, the corresponding cross sections and the $\hat{p_T}$ of the main interaction and the pile-up contribution. They do *not* take into account the uncertainties of these individual factors, i.e. no systematic effects are studied here.

The Level-1 calorimeter trigger object rate studies are performed using QCD data that has been generated in several bins of $\hat{p_T}$. A special event-weighting procedure has been applied to properly take into account the cross sections of the sub-samples. The Level-1 muon and E_T^{miss} rate studies are performed using a purely minimum bias sample.

The HLT rates are estimated using specially enriched samples. For the triggers invoking muons, electrons and photons we have used a minimum bias sample enriched in muons, as well as $W \to e/\mu\nu$, $Z \to ee/\mu\mu$ and jet(s) $+ \gamma$ MC datasets. For the triggers including jets we have used QCD samples. These samples also contribute to the electron and photon triggers. Events triggered exclusively with muons have been excluded from the QCD samples, to avoid double-counting with the muon-enriched sample. Table E.6 summarises the MC samples used for the trigger studies, and their corresponding contribution to the HLT rate. A more detailed breakdown of the contributions to the electron, photon and muon trigger rates from

Table E.7. Trigger table showing Level-1 rates for DAQ TDR chosen thresholds for $\mathcal{L} = 2 \times 10^{33}\,\mathrm{cm}^{-2}\,\mathrm{s}^{-1}$. Whenever the "95% efficiency point" is reported in DAQ TDR, we also give the actual kinematic threshold that has been applied.

Trigger	95% Eff. point	Threshold (GeV)	Rate (kHz)	Cumulative Rate (kHz)
Single $e\gamma$	29	23.4	3.38 ± 0.23	3.4 ± 0.2
Double $e\gamma$	17	11.5	0.85 ± 0.12	4.0 ± 0.3
Single μ	—	14	2.53 ± 0.20	6.5 ± 0.3
Double μ	—	3	4.05 ± 0.26	10.3 ± 0.4
Single τ	86	93	3.56 ± 0.24	9.7 ± 0.4
Double τ	59	66	1.97 ± 0.18	10.6 ± 0.4
1-, 3-, 4-jets	177, 86, 70	135, 58, 45	2.43 ± 0.20	11.9 ± 0.4
Jet + $E_{\mathrm{T}}^{\mathrm{miss}}$	—	88, 46	1.07 ± 0.13	12.2 ± 0.4
$e\gamma + \tau$	—	21, 45	3.64 ± 0.24	12.9 ± 0.5
	Level-1 Trigger Total			12.9 ± 0.5

the different samples is discussed later (Sec. E.5.3-rates). For our calculations, we have used the standard HLT physics algorithms (`ORCA/_8/_13/_3` [10]) for the implementation of all trigger paths. At the time of this writing, this includes the latest algorithms and jet calibrations. For the global evaluation of the trigger rates we have used the "HLT steering code"

E.5.1. Level-1 rates

The background at Level-1 is entirely dominated by strong interactions. The muon rates at Level-1 are dominated by low p_{T} muons which are reconstructed as high p_{T} muons due to limited resolution at the trigger level. For the electron/photon trigger the rate is dominated by jets that fragment to high E_{T} π^0 s. The jet rates are dominated by true jets in the QCD events. The $E_{\mathrm{T}}^{\mathrm{miss}}$ background is due to the limited energy resolution, and pile-up of minimum bias interactions.

We first produce a trigger table with Level-1 rates for DAQ TDR chosen thresholds for comparison. For the calculations we use a sample of 2 million minimum bias crossings with an average of 5 events per crossing, constructed from the minbias events, without reuse of events. The out-of-time pile-up is neglected. Even though there are small differences for the individual triggers, the integral rate is consistent with the rates reported in Ref. [76]. This comparison serves as a cross-check and is a necessary intermediate step before the introduction of new trigger terms. Table E.7 summarises the Level-1 rate calculations for the DAQ TDR triggers with the new MC samples. Besides the "95% efficiency points" (used throughout the DAQ TDR), the applied L1 thresholds are also given.

For the new trigger table: We select several thresholds for each trigger object type and quote corresponding rates and prescales for $\mathcal{L} = 2 \times 10^{33}\,\mathrm{cm}^{-2}\,\mathrm{s}^{-1}$. For the single objects we have added a series of prescaled triggers to determine the efficiency turn-on. For the multi-object triggers we have picked the lowest common threshold that is allowed for the allocated bandwidth. For the cross-channel triggers we have attempted to keep the lepton thresholds as low as possible, within the allocated bandwidth based on the physics needs of the experiment. The prescales are chosen such that the simulated rate at all times falls below the DAQ bandwidth taking into account a safety factor of 3. The total Level-1 rate for all triggers (including prescaled ones) is 22.6 ± 0.3 kHz.

Table E.8. Comparison of HLT bandwidth given to various trigger paths calculated in this study with the DAQ TDR. See text for details on different kinematic cuts and changes in the HLT algorithms.

Trigger	DAQ TDR Rate (Hz)	New Rate (Hz)
Inclusive e	33.0	23.5 ± 6.7
e-e	1.0	1.0 ± 0.1
Relaxed e-e	1.0	1.3 ± 0.1
Inclusive γ	4.0	3.1 ± 0.2
γ-γ	5.0	1.6 ± 0.7
Relaxed γ-γ	5.0	1.2 ± 0.6
Inclusive μ	25.0	25.8 ± 0.8
μ-μ	4.0	4.8 ± 0.4
$\tau + E_{\mathrm{T}}^{\mathrm{miss}}$	1.0	0.5 ± 0.1
$\tau + e$	2.0	< 1.0
Double Pixel τ	1.0	4.1 ± 1.1
Double Tracker τ	1.0	6.0 ± 1.1
Single jet	1.0	4.8 ± 0.0
Triple jet	1.0	1.1 ± 0.0
Quadruple jet	7.0	8.9 ± 0.2
jet + $E_{\mathrm{T}}^{\mathrm{miss}}$	5.0	3.2 ± 0.1
b-jet (leading jet)	5.0	10.3 ± 0.3
b-jet (2^{nd} leading jet)	5.0	8.7 ± 0.3

E.5.2. Level-1 trigger object corrections

The trigger decisions are based on E_{T} of the objects reconstructed by various algorithms. Unfortunately, the energy deposition in the calorimeter and the size of the trigger towers, are not entirely uniform. We have used fits to the reconstructed-to-generated E_{T} ratios to correct for non-uniformity of the response for jets and electron/photon candidates found at all levels of trigger [830]. This correction procedure adjusts the mean response to the generated level.

The energy response of the calorimeters and the limited number of bits used in trigger calculations result in a finite resolution for the reconstructed trigger objects. Similarly, misalignments of the tracking systems and the limited number of patterns in the muon trigger look-up-tables also result in a finite resolution. To avoid systematic problems in understanding the trigger efficiency turn-on with the E_{T} of the trigger objects, it is envisioned that only data where high trigger efficiency is assured is used for analysis.

E.5.3. HLT rates

A rough comparison of the HLT bandwidth given to various triggers, calculated with the latest algorithms and the ones reported in Ref. [76] is shown in Table E.8. It must be noted that not only thresholds but also other cuts are different in the two trigger studies. Furthermore, additional changes in the HLT algorithms (summarised in Sec. E.2.2) must be taken into account. This comparison serves only as a consistency check. It reaffirms that despite the evolution of the CMS reconstruction algorithms over the years, trigger rates remain under control and that no major bandwidth changes are expected.

Table E.10 shows in a similar way the contributions to the single and double standard and relaxed muon rates from the various MC samples.

The contributions to the single and double electron and photon trigger rates at HLT from the various MC samples is given at Table E.9-egamma. The main contributions to the single

Table E.9. Contributions to the HLT rates for the electron and photon triggers from the various MC datasets.

Trigger	Threshold (GeV)	Rates (Hz)			
		QCD	$W \to e\nu$	$Z \to ee$	jet(s) + γ
Inclusive e	26	12.6 ± 6.7	9.7 ± 0.2	1.2 ± 0.0	—
e-e	12, 12	0.1 ± 0.1	—	1.0 ± 0.0	—
Relaxed e-e	19, 19	0.3 ± 0.1	—	1.0 ± 0.0	—
Inclusive γ	80	1.1 ± 0.2	—	—	2.0 ± 0.1
γ-γ	30, 20	1.3 ± 0.8	—	—	0.3 ± 0.0
Relaxed γ-γ	30, 20	0.9 ± 0.6	—	—	0.3 ± 0.0

Table E.10. Contributions to the HLT rates for the muon triggers from the various MC datasets.

Trigger	Threshold	Rates (Hz)		
	(GeV)	Enriched-μ sample	$W \to \mu\nu$	$Z \to \mu\mu$
Inclusive μ	19	10.9 ± 0.8	13.4 ± 0.3	1.5 ± 0.0
Relaxed μ	37	5.1 ± 0.5	5.7 ± 0.1	1.1 ± 0.0
μ-μ	7, 7	3.4 ± 0.4	—	1.3 ± 0.0
Relaxed μ-μ	10, 10	7.1 ± 0.5	—	1.4 ± 0.0

Table E.11. The Level-1 Trigger Menu at $\mathcal{L} = 2 \times 10^{33}\,\mathrm{cm}^{-2}\,\mathrm{s}^{-1}$. Individual and cumulative rates are given for the different trigger paths and selected kinematic thresholds.

Trigger	Level-1 Threshold (GeV)	Level-1 Rate (kHz)	Cumulative Level-1 Rate (kHz)
Inclusive $e\gamma$	22	4.2 ± 0.1	4.2 ± 0.1
Double $e\gamma$	11	1.1 ± 0.1	5.1 ± 0.1
Inclusive μ	14	2.7 ± 0.1	7.8 ± 0.2
Double μ	3	3.8 ± 0.1	11.4 ± 0.2
Inclusive τ	100	1.9 ± 0.1	13.0 ± 0.2
Double τ	66	1.8 ± 0.1	14.1 ± 0.2
1-,2-,3-,4-jets	150, 100, 70, 50	1.8 ± 0.1	14.8 ± 0.3
H_T	300	1.2 ± 0.1	15.0 ± 0.3
$E_\mathrm{T}^\mathrm{miss}$	60	0.3 ± 0.1	15.1 ± 0.3
H_T + $E_\mathrm{T}^\mathrm{miss}$	200, 40	0.7 ± 0.1	15.3 ± 0.3
jet + $E_\mathrm{T}^\mathrm{miss}$	100, 40	0.8 ± 0.1	15.4 ± 0.3
τ + $E_\mathrm{T}^\mathrm{miss}$	60, 40	2.7 ± 0.1	17.4 ± 0.3
μ + $E_\mathrm{T}^\mathrm{miss}$	5, 30	0.3 ± 0.1	17.6 ± 0.3
$e\gamma$ + $E_\mathrm{T}^\mathrm{miss}$	15, 30	0.7 ± 0.1	17.7 ± 0.3
μ + jet	7, 100	0.1 ± 0.1	17.8 ± 0.3
$e\gamma$ + jet	15, 100	0.6 ± 0.1	17.8 ± 0.3
μ + τ	7, 40	1.2 ± 0.1	18.4 ± 0.3
$e\gamma$ + τ	14, 52	5.4 ± 0.2	20.7 ± 0.3
$e\gamma$ + μ	15, 7	0.2 ± 0.1	20.7 ± 0.3
Prescaled			22.6 ± 0.3
	Total Level-1 Rate		22.6 ± 0.3

Table E.12. The High-Level Trigger Menu at $\mathcal{L} = 2 \times 10^{33}\,\mathrm{cm}^{-2}\,\mathrm{s}^{-1}$ for an output of approximately 120 Hz. The E_T values are the kinematic thresholds for the different trigger paths.

Trigger	Level-1 bits used	Level-1 Prescale	HLT Threshold (GeV)	HLT Rate (Hz)
Inclusive e	2	1	26	23.5 ± 6.7
e-e	3	1	12, 12	1.0 ± 0.1
Relaxed e-e	4	1	19, 19	1.3 ± 0.1
Inclusive γ	2	1	80	3.1 ± 0.2
γ-γ	3	1	30, 20	1.6 ± 0.7
Relaxed γ-γ	4	1	30, 20	1.2 ± 0.6
Inclusive μ	0	1	19	25.8 ± 0.8
Relaxed μ	0	1	37	11.9 ± 0.5
μ-μ	1	1	7, 7	4.8 ± 0.4
Relaxed μ-μ	1	1	10, 10	8.6 ± 0.6
$\tau + E_\mathrm{T}^\mathrm{miss}$	10	1	65 ($E_\mathrm{T}^\mathrm{miss}$)	0.5 ± 0.1
Pixel τ-τ	10, 13	1	—	4.1 ± 1.1
Tracker τ-τ	10, 13	1	—	6.0 ± 1.1
$\tau + e$	26	1	52, 16	< 1.0
$\tau + \mu$	0	1	40, 15	< 1.0
b-jet (leading jet)	36, 37, 38, 39	1	350, 150, 55 (see text)	10.3 ± 0.3
b-jet (2 nd leading jet)	36, 37, 38, 39	1	350, 150, 55 (see text)	8.7 ± 0.3
Single-jet	36	1	400	4.8 ± 0.0
Double-jet	36, 37	1	350	3.9 ± 0.0
Triple-jet	36, 37, 38	1	195	1.1 ± 0.0
Quadruple-jet	36, 37, 38, 39	1	80	8.9 ± 0.2
$E_\mathrm{T}^\mathrm{miss}$	32	1	91	2.5 ± 0.2
jet + $E_\mathrm{T}^\mathrm{miss}$	32	1	180, 80	3.2 ± 0.1
acoplanar 2 jets	36, 37	1	200, 200	0.2 ± 0.0
acoplanar jet + $E_\mathrm{T}^\mathrm{miss}$	32	1	100, 80	0.1 ± 0.0
2 jets + $E_\mathrm{T}^\mathrm{miss}$	32	1	155, 80	1.6 ± 0.0
3 jets + $E_\mathrm{T}^\mathrm{miss}$	32	1	85, 80	0.9 ± 0.1
4 jets + $E_\mathrm{T}^\mathrm{miss}$	32	1	35, 80	1.7 ± 0.2
Diffractive	Sec. E.3	1	40, 40	< 1.0
$H_\mathrm{T} + E_\mathrm{T}^\mathrm{miss}$	31	1	350, 80	5.6 ± 0.2
$H_\mathrm{T} + e$	31	1	350, 20	0.4 ± 0.1
Inclusive γ	2	400	23	0.3 ± 0.0
γ-γ	3	20	12, 12	2.5 ± 1.4
Relaxed γ-γ	4	20	19, 19	0.1 ± 0.0
Single-jet	33	10	250	5.2 ± 0.0
Single-jet	34	1 000	120	1.6 ± 0.0
Single-jet	35	100 000	60	0.4 ± 0.0
	Total HLT rate			119.3 ± 7.2

electron trigger come from the QCD and $W \to e\nu$ samples, whereas for the single photon trigger the primary source is the jet(s) + γ events.

E.5.4. Trigger tables

Table E.11 summarises the Level-1 triggers used in this study, their kinematic thresholds, the individual and cumulative rates. We have assumed a DAQ capability of 50 kHz, taking into account a safety factor of 3.

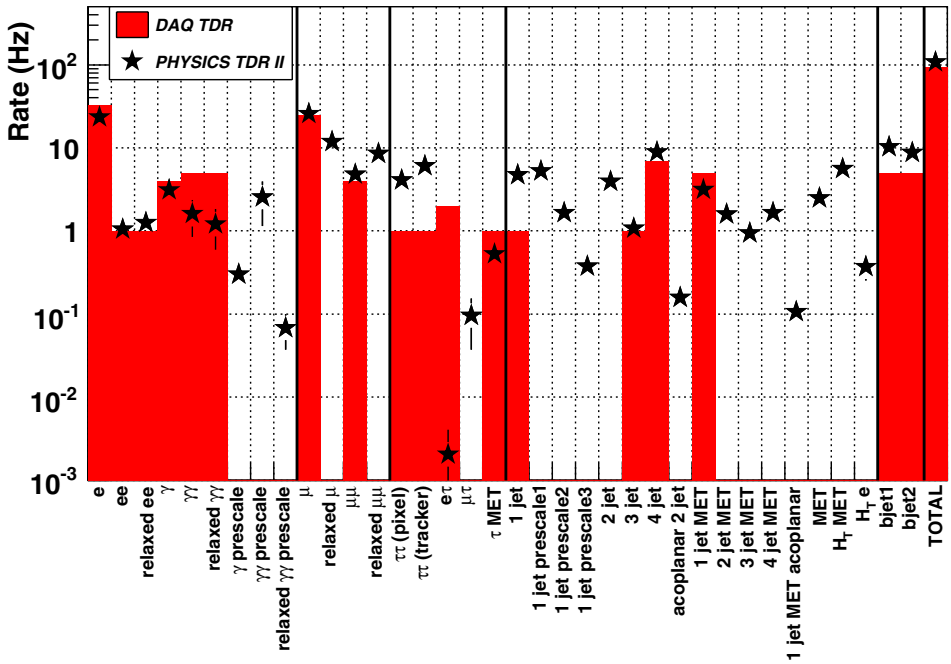

Figure E.5. Heuristic comparison of HLT bandwidth assigned to various trigger paths calculated in this study with the DAQ TDR. For the triggers introduced in this study the DAQ TDR entries appear empty. See text for details on different kinematic cuts and changes in the HLT algorithms.

Table E.12 gives the full list of trigger paths proposed for $\mathcal{L} = 2 \times 10^{33}\,\mathrm{cm}^{-2}\,\mathrm{s}^{-1}$ that have been described earlier for an HLT output rate of approximately 120 Hz.

Fig. E.5 shows a graphic representation of the HLT bandwidth assigned to all trigger paths presented in this study. For the triggers that appeared in the DAQ TDR, the corresponding rates are overlaid, in a heuristic comparison.

Glossary

ADC	Analog to Digital Converter
AdS	Anti de Sitter space
ALEPH	An experiment at LEP
ALICE	A Large Ion Collider Experiment at the LHC
ALPGEN	Monte Carlo event generator for multi-parton processes in hadronic collisions
ATLAS	A Toroidal LHC ApparatuS experiment
BMU	Barrel Muon system
BR	Branching Ratio
BX	Bunch Crossing
BXN	Bunch Crossing Number
CASTOR	Calorimeter in the forward region of CMS
CDF	Collider Detector Facility experiment at the FNAL Tevatron
CL	Confidence Level
CLHEP	Class Library for HEP
CMKIN	CMS Kinematics Package (legacy Fortran)
CMS	Compact Muon Solenoid experiment
CMSIM	CMS Simulation Package (legacy Fortran)
CMSSW	CMS Software framework
CPT	Computing, Physics, TriDAS and software projects of CMS
CPU	Central Processing Unit
CompHEP	Monte Carlo event generator for high-energy physics collisions
CSC	Cathode Strip Chamber muon system
CVS	Concurrent Versions System
DØ	Experiment at the FNAL Tevatron
DAQ	Data Acquisition
DELPHI	An experiment at LEP
DESY	Deutsches Elektronen SYnchrotron laboratory, Hamburg
DST	Data Summary Tape – a compact event format
DT	Drift Tube muon system
DY	Drell–Yan
EB	Electromagnetic Calorimeter (Barrel)
ECAL	Electromagnetic Calorimeter
ED	Extra Dimensions
EE	Electromagnetic Calorimeter (Endcap)
EM	Electromagnetic
EMU	Endcap Muon system
ES	Endcap preShower detector
EW	ElectroWeak
FAMOS	CMS Fast Simulation
FLUKA	Computer program for hadron shower calculations
FNAL	Fermi National Accelerator Laboratory, USA
FSR	Final State Radiation

Gb	Gigabit (10^9 bits)
GB	Gigabyte (10^9 bytes)
GCALOR	Computer program for hadron shower calculations
GEANT	Detector simulation framework and toolkit
GMSB	Gauge Mediated Symmetry Breaking
GUT	Grand Unified Theory
H1	An experiment at the DESY HERA collider
HAD	Hadronic
HCAL	Hadron Calorimeter
HB	Hadron Calorimeter (Barrel)
HE	Hadron Calorimeter (Endcap)
HEP	High Energy Physics
HEPEVT	HEP Event (generated event format)
HERA	Electron-proton collider at DESY
HERWIG	Hadron Emission Reactions With Interfering Gluons, a Monte Carlo event generator for high-energy physics collisions
HF	Hadron Calorimeter (Forward)
HI	Heavy Ion(s)
HIJING	Heavy Ion Jet INteraction Generator, Monte Carlo event generator for heavy-ion collisions
HLT	High-Level Trigger
HO	Hadron Calorimeter (Outer Barrel)
IGUANA	Interactive Graphics for User ANAlysis – used for the CMS Event Display Package
I/O	Input/Output
IP	Impact Parameter, also Impact Point or Internet Protocol
ISR	Initial State Radiation, also Intersecting Storage Ring collider at CERN
JES	Jet Energy Scale
Kalman Filter	Computational method for fitting tracks
kb	kilobit (10^3 bits)
kB	kilobytes (10^3 bytes)
L1	Level-1 hardware-based trigger
L3	An experiment at LEP
LCG	LHC Computing Grid (a common computing project)
LED	Large Extra Dimenstions, also Light Emitting Diode
LEP	Large Electron Positron collider at CERN
LHC	Large Hadron Collider
LHCb	Large Hadron Collider Beauty experiment
LHCC	LHC (review) Committee
LHEP	Physics model of GEANT4
LL	Leading Logarithm, also Log Likelihood
LO	Leading Order calculation
LOI	Letter Of Intent
LPC	LHC Physics Center, Fermilab
LS	Like-Sign
LSP	Lightest Supersymmetric Particle

Mb	Megabit (10^6 bits)
MB	Muon system (Barrel), also Mother Board or Megabyte (10^6 bytes)
MC	Monte Carlo simulation program/technique, also Mini-Crate of DT system
ME	Muon system (Endcap), also Matrix Element or Monitoring Element
MET	Missing Transverse Energy
metadata	Data describing characteristics of other data
MIP	Minimum Ionizing Particle
MSUGRA	Minimal SUper GRAvity model of supersymmetry
MSSM	Minimal SuperSymmetric Model
MTCC	Magnet Test Cosmic Challenge
ndf	number of degrees of freedom
NLO	Next-to-Leading Order calculation
NN	Neural Network
NNLO	Next-to-Next-to-Leading Order calculation
NS	Numbering Scheme
OO	Object Oriented
OPAL	An experiment at LEP
ORCA	Object-oriented Reconstruction for CMS Analysis
OS	Opposite-Sign, also Operating System
OSCAR	Object-oriented Simulation for CMS Analysis and Reconstruction
P5	Point 5 collision area of LHC
PAW	Physics Analysis Workstation (legacy interactive analysis application)
PB	Petabyte (10^5 bytes)
PC	Personal Computer
PD	Pixel Detector
PDF	Parton Density Function, also Probability Distribution Function (p.d.f.)
PRS	Physics Reconstruction and Selection groups
PS	Proton Synchrotron, also Parton Showers
PV	Primary Vertex
PYTHIA	Monte Carlo event generator for high-energy physics collisions
QCD	Quantum Chromodynamics
QED	Quantum Electrodynamics
QGSP	Physics model of GEANT4
RecHit	Reconstructed hit in a detector element
RHIC	Relativistic Heavy Ion Collider (at Brookhaven, USA)
RMS	Root Mean Square
ROOT	An object-oriented data analysis framework
RPC	Resistive Plate Chamber muon system

SLT	Soft Lepton Tag
SM	Standard Model, also SuperModule (ECAL) or Storage Manager (DAQ)
S/N	Signal to Noise ratio
SPS	Super Proton Synchrotron collider at CERN
SS	Same-Sign
SST	Silicon Strip Tracker
SUSY	SUperSYmmetry
SV	Secondary Vertex
T1, T2	Tracking telescopes of TOTEM
TAG	Event index information such as run/event number, trigger bits, etc.
Tb	Terabit (10^{12} bits)
TB	Terabyte (10^{12} bytes)
TDR	Technical Design Report
TEC	Tracker EndCap
TIB	Tracker Inner Barrel
TID	Tracker Inner Disks
TOB	Tracker Outer Barrel
TOTEM	Separate experiment at P5 for forward physics
TPD	Tracker Pixel Detector
TriDAS	Trigger and Data Acquisition project
UA1	An experiment at the CERN SPS collider
UA2	An experiment at the CERN SPS collider
UE	Underlying Event
UED	Universal Extra Dimensions
VBF	Vector Boson Fusion
VPT	Vacuum PhotoTriode
WWW	World Wide Web
ZDC	Zero Degree Calorimeter
ZEUS	An experiment at the DESY HERA collider

References

Blue font in the online PDF indicates links to full-text articles.

DOI numbers are given for some published articles, for which the full text may be accessed by prefixing the number with http://dx.doi.org/

CMS Notes are available at http://cms.cern.ch/iCMS/ unless otherwise noted.

[1] TLS Group 1995 The Large Hadron Collider Conceptual Design *CERN-AC-95-05 Preprint* hep-ph/0601012

[2] CMS Collaboration 1992 The Compact Muon Solenoid Letter of Intent *CERN/LHCC* 1992-3, LHCC/I 1

[3] CMS Collaboration 1994 The Compact Muon Solenoid Technical Proposal *CERN/LHCC* 94-38, LHCC/P1

[4] ATLAS and CMS Collaboration, Branson J G *et al* 2002 High transverse momentum physics at the Large Hadron Collider: The ATLAS and CMS Collaborations *Eur. Phys. J. direct* C **4** N1 (*Preprint* hep-ph/0110021)

[5] LHC/LC Study Group Collaboration, Weiglein G *et al* 2004 Physics interplay of the LHC and the ILC *Preprint* hep-ph/0410364

[6] Krasnikov N and Matveev V 2004 Search for new physics at LHC *Phys. Usp.* **47** 643 (*Preprint* hep-ph/0309200)

[7] CMS Collaboration 2006 The CMS Physics Technical Design Report, Volume 1 *CERN/LHCC* 2006-001, CMS TDR 8.1

[8] OSCAR: CMS Simulation Package Home Page http://cmsdoc.cern.ch/oscar

[9] GEANT4 Collaboration, Agostinelli S *et al* 2003 GEANT4: A simulation toolkit *Nucl. Instrum. Methods* A **506** 250–303

[10] ORCA: CMS reconstruction Package Site located at http://cmsdoc.cern.ch/orca

[11] CMS Collaboration, Acosta D *et al* 2006 CMS Physics Technical Design Report, Volume 1, Section 2.6: Fast simulation p 55 *CERN/LHCC* 2006-001

[12] Pumplin J *et al* 2002 New generation of parton distributions with uncertainties from global QCD analysis *J. High. Energy Phys.* JHEP07(2002)012 (*Preprint* hep-ph/0201195)

[13] Martin A D, Roberts R G, Stirling W J and Thorne R S 2002 MRST2001: Partons and alpha(s) from precise deep inelastic scattering and Tevatron jet data *Eur. Phys. J.* C **23** 73 (*Preprint* hep-ph/0110215)

[14] Alekhin S *et al* 2005 HERA and the LHC - A workshop on the implications of HERA for LHC physics: Proceedings Part A

[15] Seez C *et al* 1990 Photon decay modes of the intermediate mass Higgs *Proceedings of the Large Hadron Collider Workshop* (*Aachen, 4–9 October, 1990), CERN 90-10* volume II ed G Jarlskog and D Rein

[16] CMS Collaboration 1997 The Electromagnetic Calorimeter Technical Design Report *CERN/LHCC*, 97-033 CMS TDR 4, Addendum *CERN/LHCC* 2002-027

[17] Favara A and Pieri M 1997 Confidence Level Estimation and Analysis Optimization *Preprint* DFF 278/4/1997

[18] L3 Collaboration, Acciarri M *et al* 1997 Search for the Standard Model Higgs Boson in e^+e^- Interactions at 161 GeV $< \sqrt{s} <$ 172 GeV *Phys. Lett.* B **411** 373

[19] CMS Collaboration, Pieri M *et al* 2006 Inclusive search for the Higgs boson in the $H \to \gamma\gamma$ channel *CMS Note* AN 2006/112

[20] Spira M 1998 QCD effects in Higgs physics *Fortsch. Phys.* **46** 203–284 (*Preprint* hep-ph/9705337)

[21] Djouadi A, Kalinowski J and Spira M 1998 HDECAY: a program for Higgs boson decays in the Standard Model and its supersymmetric extension *Comput. Phys. Commun.* **108** 56–74 (doi:10.1016/S0010-4655(97)00123-9)

[22] CMS Collaboration, Dubinin M *et al* 2006 The vector boson fusion production with $H \to \gamma\gamma$ *CMS Note* 2006/097

[23] CMS Collaboration, Lethuillier M 2006 Search for SM Higgs boson with W/Z+H, H$\to 2\gamma$ channel *CMS Note* 2006/110

[24] Sjostrand T, Lonnblad L and Mrenna S 2001 PYTHIA 6.2: Physics and manual *Preprint* hep-ph/0108264

[25] CMSIM home page http://cmsdoc.cern.ch/cmsim/cmsim.html

[26] Giele W *et al* 2002 The QCD/SM working group: Summary report *Preprint* hep-ph/0204316

[27] Dobbs M *et al* 2004 The QCD/SM working group: Summary report *Preprint* hep-ph/0403100

[28] Binoth T 2000 Two photon background for Higgs boson searches at the LHC *Preprint* hep-ph/0005194

[29] Bern Z, Dixon L J and Schmidt C 2002 Isolating a light Higgs boson from the di-photon background at the LHC *Phys. Rev.* D **66** 074018 (*Preprint* hep-ph/0206194)

[30] Binoth T, Guillet J P, Pilon E and Werlen M 2002 A next-to-leading order study of photon pion and pion pair hadro-production in the light of the Higgs boson search at the LHC *Eur. Phys. J. Direct* C **4** (doi:10.1007/s1010502c0007)
[31] CMS Collaboration, Agostino L *et al* 2006 HLT Selection of Electrons and Photons *CMS Note* 2006/078
[32] CMS Collaboration, Meschi E *et al* 2001 Electron Reconstruction in the CMS Electromagnetic Calorimeter *CMS Note* 2001/034
[33] CMS Collaboration, Marinelli N 2006 Track Finding and Identification of Converted Photons *CMS Note* 2006/005
[34] CMS Collaboration, Litvin V *et al* 2002 The Rejection of Background to the HGG Process Using Isolation Criteria Based on Information from the Calorimeter and Tracker *CMS Note* 2002-030
[35] CMS Collaboration, Pieri M *et al* 2006 Distinguishing Isolated Photos from Jets *CMS Note* 2006/007
[36] The LEP Collaborations: ALEPH, DELPHI, L3 and OPAL1998 Lower Bound for the Standard Model Higgs Boson Mass from Combining the Results of the Four LEP Experiments *CERN EP* 98-046
[37] CMS Collaboration, Baffioni S *et al* 2006 Discovery potential for the SM Higgs boson in the $H \to ZZ^{(*)} \to e^+e^-e^+e^-$ decay channel *CMS Note* 2006/115
[38] Barberio E, van Eijk B and Was Z 1991 PHOTOS: A Universal Monte Carlo for QED radiative corrections in decays *Comput. Phys. Commun.* **66** 115–128
[39] Barberio E and Was Z 1994 PHOTOS: A Universal Monte Carlo for QED radiative corrections. Version 2.0 *Comput. Phys. Commun.* **79** 291–308 (doi:10.1016/0010-4655(94)90074-4)
[40] Spira M 1995 HIGLU: A Program for the Calculation of the Total Higgs Production Cross Section at Hadron Colliders via Gluon Fusion including QCD Corrections *Preprint* hep-ph/9510347
[41] Djouadi A, Kalinowski J and Spira M 1998 HDECAY: A Program for Higgs Boson Decays in the Standard Model and its Supersymmetric Extension *Comput. Phys. Commun.* **108** 56–74 (*Preprint* hep-ph/9704448)
[42] Zecher C *et al* 1994 Leptonic Signals from off-shell Z Boson Pairs at Hadron Colliders *Preprint* hep-ph/9404295
[43] CompHEP Collaboration, Boos E *et al* 2004 CompHEP 4.4: Automatic computations from Lagrangians to events *Nucl. Instrum. Meth.* A **534** 250–259 (*Preprint* hep-ph/0403113)
[44] Slabospitsky S R and Sonnenschein L 2002 TopReX generator (version 3.25): Short manual *Comput. Phys. Commun.* **148** 87–102 (doi:10.1016/S0010-4655(02)00471-X)
[45] Beneke M *et al* 2000 Top quark physics *Preprint* hep-ph/0003033
[46] CMS Collaboration, Baffioni S, Charlot C, Ferri F, Futyan D, Meridiani P, Puljak I, Rovelli C, Salerno R and Sirois Y 2006 Electron Reconstruction in CMS *CMS Note* 2006/040
[47] Abdullin S *et al* 2006 Study of PDF and QCD scale uncertainties in $H \to ZZ^{(*)} \to 4\mu$ events at the LHC *CMS Note* 2006/068 See also hep-ph/0604120, Les Houches Physics at TeV Colliders 2005, Standard Model and Higgs working group: Summary report. April 2006
[48] Meridiani P and Paramatti R 2006 Use of $Z \to e^+e^-$ events for ECAL calibration *CMS Note* 2006/039
[49] Bartsch V and Quast G 2006 Expected signal observability at future experiments *CMS Note* 2005-004
[50] Bityukov S and Krasnikov N 1998 New physics discovery potential in future experiments *Mod. Phys. Lett.* A **13** 3235–3249
[51] Abdullin S *et al* 2006 Search Strategy for the Standard Model Higgs Boson in the $H \to ZZ^{(*)} \to 4\mu$ Decay Channel using $M(4\mu)$-Dependent Cuts *CMS Note* 2006/122
[52] Karimaki V *et al* 2004 CMKIN v3 User's Guide *CMS IN* 2004-016
[53] Spira M 2005 'SM Higgs boson production cross sections at NLO' and 'SM Higgs boson BRs'Available at http://cmsdoc.cern.ch/~anikiten/cms-higgs/
[54] Particle Data Group, Eidelman S *et al* 2004 Review of Particle Physics *Phys. Lett.* B **592** 1 (doi:10.1016/j.physletb.2004.06.001)
Particle Data Group, Yao W-M *et al* 2006 Review of Particle Physics *J. Phys. G: Nucl. Part. Phys.* **33** 1 (doi:10.1088/0954-3899/33/1/001)
[55] Maltoni F 2005 Theoretical Issues and Aims at the Tevatron and LHC *Proceedings of the 1st Hadron Collider Physics Symposium (HCP 2005) (Les Diablerets, Switzerland 2005 July)* Available at http://hcp-2005.web.cern.ch/HCP-2005
[56] Campbell J M 2001 W/Z + B anti-B/jets at NLO using the Monte Carlo MCFM Talk given at 36th Rencontres de Moriond on QCD and Hadronic Interactions (*Les Arcs, France, 17–24 March 2001*) *Preprint* hep-ph/0105226
[57] Abdullin S *et al* 2006 Relative Contributions of t- and s-Channels to the $ZZ \to 4\mu$ Process *CMS Note* 2006/057, See also hep-ph/0604120, Les Houches Physics at TeV Colliders 2005, Standard Model and Higgs working group: Summary report. April 2006

[58] Bartalini P *et al* 2006 NLO vs. LO: kinematical differences for signal and background in the H $\rightarrow$ ZZ* $\rightarrow 4\mu$ analysis *CMS Note* 2006/130

[59] Acosta D *et al* 2006 Measuring Muon Reconstruction Efficiency from Data *CMS Note* 2006/060

[60] Aldaya M, Arce P, Caballero J, de la Cruz B, Garcia-Abia P, Hernandez J M, Josa M and Ruiz E 2006 Discovery potential and search strategy for the Standard Model Higgs boson in the $H \rightarrow ZZ^\star \rightarrow 4\mu$ decay channel using a mass-independent analysis *CMS Note* 2006/106

[61] Read A 2000 Modified Frequentist Analysis of Search Results (The CLs Method) *1st Workshop on Confidence Limits, CERN, Geneva CERN-EP* /2000-005

[62] LEP Working Group for Higgs boson searches Collaboration, Barate R *et al* 2003 Search for the standard model Higgs boson at LEP *Phys. Lett.* B **565** 61–75 (*Preprint* hep-ex/0306033)

[63] Abdullin S and Drozdetskiy A *et al* 2006 GARCON: Genetic Algorithm for Rectangular Cuts Optimization. User's manual for version 2.0 *Preprint* hep-ph/0605143 See also http://drozdets.home.cern.ch/drozdets/home/genetic/

[64] Abdullin S *et al* 2006 Sensitivity of the Muon Isolation Cut Efficiency to the Underlying Event Uncertainties *CMS Note* 2006/033, See also hep-ph/0604120, Les Houches Physics at TeV Colliders 2005, Standard Model and Higgs working group: Summary report. April 2006

[65] Aldaya M *et al* 2006 A method for determining the mass, cross-section and width of the Standard Model Higgs boson using the H $\rightarrow$ ZZ* $\rightarrow 4\mu$ decay channel *CMS Note* 2006/107

[66] Bartsch V Simulation of Silicon Sensors and Study of the Higgs Decay

[67] Dittmar M and Dreiner H 1997 How to find a Higgs boson with a mass between 155GeV to to 180GeV at the CERN LHC *Phys. Rev.* D **55** 167–172 (*Preprint* hep-ph/9608317) (doi:10.1103/PhysRevD.55.167)

[68] Dittmar M and Dreiner H 1997 LHC Higgs Search with $l^+\nu l^-\overline{\nu}$ final states *CMS Note* 1997/083

[69] Sjostrand T *et al* 2001 High-energy-physics event generation with PYTHIA 6.1 *Comput. Phys. Commun.* **135** 238–259 (doi:10.1016/S0010-4655(00)00236-8)

[70] Binoth T, Ciccolini M, Kauer N and Kramer M 2005 Gluon-induced W W background to Higgs boson searches at the LHC *J. High. Energy Phys.* JHEP03(2005)065 (*Preprint* hep-ph/0503094)

[71] Davatz G *et al* 2004 Effective k-factors for $H \rightarrow WW^{(*)} \rightarrow 2\mu 2\nu$ at the LHC *J. High. Energy Phys.* JHEP0405(2004)009 (*Preprint* hep-ph/0402218) (doi:10.1088/1126-6708/2004/05/009)

[72] Frixione S and Webber B R 2002 Matching NLO QCD computations and parton shower simulations *J. High. Energy Phys.* JHEP0206(2002)029 (*Preprint* hep-ph/0204244)

[73] Davatz G, Dittmar M and Giolo-Nicollerat A S 2006 Standard Model Higgs Discovery Potential of CMS in the $H \rightarrow WW^{(*)} \rightarrow l\nu l\nu$ Channel *CMS Note* 2006/047

[74] Campbell J M and Ellis R K 1999 An update on vector boson pair production at hadron colliders *Phys. Rev.* D **60** 113006 (doi:10.1103/PhysRevD.60.113006)

[75] Campbell J and Tramontano F 2005 Next-to-leading order corrections to Wt production and decay *Nucl. Phys.* B **726** 109–130 (doi:10.1016/j.nuclphysb.2005.08.015)

[76] CMS Collaboration 2002 The TriDAS Project Technical Design Report, Volume 2: Data Acquisition and High-Level Trigger *CERN/LHCC* 2002-26, CMS TDR 6.2

[77] Drollinger V, Gasparini U, Torassa E and Zanetti M 2006 Physics study of the Higgs decay chanel $H \rightarrow WW^{(*)} \rightarrow 2\mu 2\nu$ *CMS Note* 2006/055

[78] Chekanov S V 2002 Jet algorithms: a mini review *Proceedings of the 14th Topical Conference on Hadron Collider Physics (HCP 2002)* September-October (Karlsruhe, Germany)

[79] Bityukov S I and Krasnikov N V 2002 Uncertainties and discovery potential in planned experiments *CMS CR* 2002/05

[80] Davatz G, Giolo-Nicollerat A and Zanetti M 2006 Systematics uncertainties of the top background in the $H \rightarrow WW$ channel *CMS Note* 2006/048

[81] Maltoni F and Stelzer T 2003 MadEvent: Automatic event generation with MadGraph *J. High. Energy Phys.* JHEP02(2003)027 (doi:10.1088/1126-6708/2003/02/027)

[82] Kauer N 2004 Top background extrapolation for $H \rightarrow WW$ searches at the LHC *Preprint* hep-ph/0404045

[83] Lowette S, D'Hondt J, Heyninck J and Vanlaer P 2006 Offline Calibration of b-Jet Identification Efficiencies *CMS Note* 2006/013

[84] Drollinger V *et al* 2005 Modeling the production of W pairs at the LHC *CMS Note* 2005/024

[85] Anastasiou C *et al* 2004 High precision QCD at hadron colliders: Electroweak gauge boson rapidity distribution at NNLO *Phys. Rev.* D **69**

[86] Belotelov I *et al* 2006 Simulation of misalignment scenarios for CMS tracking devices *CMS Note* 2006-008

[87] Cvetic M and Langacker P 1996 Implications of abelian extended gauge structures from string models *Phys. Rev.* D **54** 3570–3579 (*Preprint* hep-ph/9511378)

[88] Cvetic M and Langacker P 1996 New gauge bosons from string models *Mod. Phys. Lett.* A **11** 1247–1262 (*Preprint* hep-ph/9602424)
[89] Leike A 1999 The phenomenology of extra neutral gauge bosons *Phys. Rept.* **317** 143–250 (*Preprint* hep-ph/9805494)
[90] Hill C T and Simmons E H 2003 Strong dynamics and electroweak symmetry breaking *Phys. Rept.* **381** 235–402 (*Preprint* hep-ph/0203079)
[91] Han T, Logan H, McElrath B and Wang L-T 2003 Phenomenology of the little Higgs model *Phys. Rev.* D **67** 095004 (doi:10.1103/PhysRevD.67.095004)
[92] Cvetic M and Godfrey S 1996 Discovery and identification of extra gauge bosons *Electroweak symmetry breaking and new physics at the TeV scale* ed T L Barlow and S Dawson (World Scientific) 383–415 *Preprint* hep-ph/9504216
[93] Godfrey S 2001 Update of discovery limits for extra neutral gauge bosons at hadron colliders *Proceedings of Snowmass 2001* (Snowmass, Colorado: June–July) p P344 *Preprint* hep-ph/0201093
[94] Randall L and Sundrum R 1999 A large mass hierarchy from a small extra dimension *Phys. Rev. Lett.* **83** 3370–3373 (doi:10.1103/PhysRevLett.83.3370)
[95] Whalley M R, Bourilkov D and Group R C 2005 The Les Houches accord PDFs (LHAPDF) and LHAGLUE *Preprint* hep-ph/0508110
[96] Rosner J L 1987 Off peak lepton asymmetries from new Zs *Phys. Rev.* D **35** 2244
[97] Rosner J L 1996 Forward-Backward asymmetries in hadronically produced lepton pairs *Phys. Rev.* D **54** 1078–1082 (*Preprint* hep-ph/9512299)
[98] Mohapatra R N, Goldstein S A and Money D (eds) 2002 *Unification and supersymmetry: The Frontiers of quark - lepton physics* 3rd ed. (Springer-Verlag)
[99] Belotelov I *et al* 2006 Influence of misalignment scenarios on muon reconstruction *CMS Note* 2006-017
[100] Cousins R, Mumford J and Valuev S 2005 Detection of Z' gauge bosons in the dimuon decay mode in CMS *CMS Note* 2005-002
[101] Cousins R, Mumford J and Valuev V 2006 Detection of Z′ gauge bosons in the dimuon decay mode in CMS *CMS CR* 2004/050
[102] Bartsch V and Quast G 2005 Expected signal observability at future experiments *CMS Note* 2005-004
[103] Wilks S S 1938 The large-sample distribution of the likelihood ratio for testing composite hypotheses *Annals of Math. Stat.* **9** 60
[104] Baur U, Brein O, Hollik W, Schappacher C and Wackeroth D 2002 Electroweak radiative corrections to neutral-current Drell–Yan processes at hadron colliders *Phys. Rev.* D **65** 033007 (*Preprint* hep-ph/0108274)
[105] Zykunov V 2005 Weak radiative corrections to Drell–Yan process for large invariant mass of di-lepton pair *Preprint* hep-ph/0509315
[106] De Roeck A and Slabospitsky S Evaluation of the PDF Uncertainties (in CMS) available at http://cmsdoc.cern.ch/cms/PRS/gentools/www/pdfuncert/uncert.html
[107] Cerminara G private communication
[108] Langacker P, Robinett R W and Rosner J L 1984 New heavy gauge bosons in pp and $p\bar{p}$ collisions *Phys. Rev.* D **30** 1470
[109] Rosner J L 1989 Observability of charge asymmetries for lepton pairs produced in present collider experiments *Phys. Lett.* B **221** 85
[110] Cheng T P and Li L F 1988 *Gauge theory of elementary particle physics* (Oxford University Press)
[111] Cousins R, Mumford J and Valuev V 2005 Measurement of Forward-Backward Asymmetry of Simulated and Reconstructed $Z' \to \mu^+\mu^-$ Events in CMS *CMS Note* 2005-022
[112] Dittmar M 1997 Neutral current interference in the TeV region: The experimental sensitivity at the LHC *Phys. Rev.* D **55** 161–166 (*Preprint* hep-ex/9606002)
[113] Wulz C-E 1996 Z' at LHC *Proceedings of the 1996 DPF/DPB Summer Study on New Directions in High-Energy Physics* available at http://www.slac.stanford.edu/pubs/snowmass96
[114] Collins J C and Soper D E 1977 Angular distribution of dileptons in high-energy hadron collisions *Phys. Rev.* D **16** 2219
[115] Allanach B C, Odagiri K, Parker M A and Webber B R 2000 Searching for narrow graviton resonances with the ATLAS detector at the Large Hadron Collider *J. High. Energy Phys.* JHEP09(2000)019 (*Preprint* hep-ph/0006114)
[116] Cousins R, Mumford J, Tucker J and Valuev V 2005 Spin discrimination of new heavy resonances at the LHC *J. High. Energy Phys.* JHEP11(2005)046 (doi:10.1088/1126-6708/2005/11/046)
[117] Belotelov I *et al* 2006 Search for Randall-Sandrum Graviton Decay into Muon Pairs *CMS Note* 2006/104
[118] Esen S and Harris R M 2006 Jet Triggers and Dijet Mass *CMS Note* 2006/069

[119] CMS Collaboration, Acosta D *et al* 2006 CMS Physics Technical Design Report, Volume 1, Section 11.3: Monte Carlo Corrections *CERN/LHCC*, 2006-001 p 409

[120] CDF Collaboration, Abe F *et al* 1997 Search for new particles decaying to dijets at CDF *Phys. Rev.* D **55** 5263–5268 (doi:10.1103/PhysRevD.55.R5263)

[121] DØ Collaboration, Abazov V M *et al* 2004 search for new particles in the two-jet decay channel with the DØdetector *Phys. Rev.* D **69** 111101 (*Preprint* hep-ex/0308033)

[122] DØ Collaboration, Abbott B *et al* 1999 The dijet mass spectrum and a search for quark compositeness in $\bar{p}p$ collisions at $\sqrt{s} = 1.8$-TeV *Phys. Rev. Lett.* **82** 2457–2462 (doi:10.1103/PhysRevLett.82.2457)

[123] Eichten E, Lane K D and Peskin M E 1983 New tests for quark and lepton substructure *Phys. Rev. Lett.* **50** 811–814 (doi:10.1103/PhysRevLett.50.811)

[124] Lane K D 1996 Electroweak and flavor dynamics at hadron colliders *Preprint* hep-ph/9605257

[125] CDF Collaboration, Abe F *et al* 1996 Measurement of dijet angular distributions at CDF *Phys. Rev. Lett.* **77** 5336–5341 (doi:10.1103/PhysRevLett.77.5336)

[126] CMS Collaboration, Acosta D *et al* 2006 CMS Physics Technical Design Report, Volume 1, Section 11.6.1: Data-driven calibration strategy *CERN/LHCC*, 2006-001 p 421

[127] CMS Collaboration, Acosta D *et al* 2006 CMS Physics Technical Design Report, Volume 1, Section 11.6.2: Dijet Balancing *CERN/LHCC*, 2006-001 p 422

[128] CDF Collaboration, Acosta D *et al* 2005 Measurement of the lifetime difference between B_s mass eigenstates *Phys. Rev. Lett.* **94** 101803 (*Preprint* hep-ex/0412057) (doi:10.1103/PhysRevLett.94.101803)

[129] DØ Collaboration 2006 Measurement of the lifetime difference in the B_s system *DØ Conference note 5052*

[130] Belkov A and Shulga S 2004 Studies of angular correlations in the decays $B_s^0 \to J/\psi\phi$ by using the SIMUB generator *Comput. Phys. Commun.* **156** 221–240 (*Preprint* hep-ph/0310096) (doi:10.1016/S0010-4655(03)00465-X)

[131] Dighe A S, Dunietz I and Fleischer R 1999 Extracting CKM phases and $B_s - \bar{B}_s$ mixing parameters from angular distributions of non-leptonic B decays *Eur. Phys. J.* C **6** 647–662 (doi:10.1007/s100529800954)

[132] Dighe A S, Dunietz I, Lipkin H J and Rosner J L 1996 Angular distributions and lifetime differences in $B_s \to J/\psi\phi$ decays *Phys. Lett.* B **369** 144–150 (doi:10.1016/0370-2693(95)01523-X)

[133] CDF Collaboration, Abe F *et al* 1997 Production of J/ψ mesons from χ_c meson decays in $p\bar{p}$ collisions at $\sqrt{s} = 1.8$ TeV *Phys. Rev. Lett.* **79** 578–583 (doi:10.1103/PhysRevLett.79.578)

[134] Cano-Coloma B and Sanchis-Lozano M A 1997 Charmonia production in hadron colliders and the extraction of colour-octet matrix elements *Nucl. Phys.* B **508** 753–767 (*Preprint* hep-ph/9706270) (doi:10.1016/S0550-3213(97)00660-3)

[135] Cucciarelli S, Konecki M, Kotlinski D and Todorov T 2006 Track reconstruction, primary vertex finding and seed generation with the Pixel Detector *CMS Note* 2006/026

[136] Prokofiev K and Speer T 2005 A kinematic fit and a decay chain reconstruction library *CERN Yellow Report* http://doc.cern.ch/yellowrep/2005/2005-002/p411.pdf, 2005-002 Proc. of the 2004 Conference for Computing in High-Energy and Nuclear Physics (CHEP 04) (Interlaken, Switzerland, 2004) available at http://indico.cern.ch

[137] Dunietz I, Fleischer R and Nierste U 2001 In pursuit of new physics with B_s decays *Phys. Rev.* D **63** 114015 (doi:10.1103/PhysRevD.63.114015)

[138] BABAR Collaboration, Aubert B *et al* 2005 Ambiguity-free measurement of $\cos(2\beta)$: Time-integrated and time-dependent angular analyses of $B \to J/\psi K\pi$ *Phys. Rev.* D **71** 032005 (doi:10.1103/PhysRevD.71.032005)

[139] Dunietz I, Quinn H, Snyder A, Toki W and Lipkin H J 1991 How to extract CP-violating asymmetries from angular correlations *Phys. Rev.* D **43** 2193–2208 (doi:10.1103/PhysRevD.43.2193)

[140] Vanlaer P *et al* 2006 Impact of CMS Silicon Tracker Misalignment on Track and Vertex Reconstruction *CMS Note* 2006/029

[141] Speer T *et al* 2006 Vertex Fitting in the CMS Tracker *CMS Note* 2006/032

[142] Heinemeyer S, Hollik W and Weiglein G 2000 FeynHiggs: A program for the calculation of the masses of the neutral CP-even Higgs bosons in the MSSM *Comput. Phys. Commun.* **124** 76–89 (*Preprint* hep-ph/9812320)

[143] Heinemeyer S, Hollik W and Weiglein G 1999 The masses of the neutral CP-even Higgs bosons in the MSSM: accurate analysis at the two-loop level *Eur. Phys. J.* C **9** 343–366 (*Preprint* hep-ph/9812472)

[144] Degrassi G, Heinemeyer S, Hollik W, Slavich P and Weiglein G 2003 Towards high-precision predictions for the MSSM Higgs sector *Eur. Phys. J.* C **28** 133–143 (*Preprint* hep-ph/0212020)

[145] Lehti S 2006 Study of bbZ as a benchmark for MSSM bbH *CMS Note* 2006/099

[146] Bagliesi G, Dutta S, Gennai S, Kalinowski A, Konecki M, Kotlinski D, Moortgat F, Nikitenko A, Wendland L and Wakefield S 2006 Tau jet reconstruction and tagging at high level trigger and off-line *CMS Note* 2006/028
[147] Kunori S, Kinnunen R and Nikitenko A 2001 Missing transverse energy measurement with jet energy correctioins *CMS Note* 2001/040
[148] Pi H *et al* 2006 Measurement of missing transverse energy with the CMS detector at the LHC *CMS Note* 2006/035
[149] Kalinowski A and Nikitenko A 2006 Measurement of the τ-tagging efficiency using the Z$\rightarrow \tau\tau \rightarrow \mu$ + hadrons + X events *CMS Note* 2006/074
[150] Gennai S, Nikitenko A and Wendland L 2006 Search for MSSM Heavy Neutral Higgs Boson in $\tau\tau \rightarrow$ two Jet Decay Mode *CMS Note* 2006/126
[151] Rizzi A, Palla F and Segneri G 2006 Track impact parameter based b-tagging with CMS *CMS Note* 2006/019
[152] Kalinowski A, Konecki M and Kotlinski D 2006 Search for MSSM Heavy Neutral Higgs Boson in $\tau\tau \rightarrow \mu$ + jet Decay Mode *CMS Note* 2006/105
[153] Kalinowski A, Konecki M and Kotliński D 2006 Search for MSSM heavy neutral Higgs boson in $\tau + \tau \rightarrow \mu +$ jet decay mode *CMS Note* 2006/105
[154] Kinnunen R and Lehti S 2006 Search for the Heavy Neutral MSSM Higgs Bosons with the H/A$\rightarrow \tau\tau \rightarrow$ Electron plus Jet Decay Mode *CMS Note* 2006/075
[155] Jadach S, Was Z, Decker R and Kuhn J H 1993 The tau decay library TAUOLA: Version 2.4 *Comput. Phys. Commun.* **76** 361–380 (doi:10.1016/0010-4655(93)90061-G)
[156] Giolo-Nicollerat A-S 2006 *CMS Note*
[157] Weiser C 2006 A Combined Secondary Vertex Based B-Tagging Algorithm in CMS *CMS Note* 2006/014
[158] Haywood S *et al* 1999 Electroweak physics *Preprint* hep-ph/0003275 In 'Standard Model Physics (and more) at the LHC', Geneva, 1999
[159] Chakraborty D, Konigsberg J and Rainwater D L 2003 Review of top quark physics *Ann. Rev. Nucl. Part. Sci.* **53** 301–351 (*Preprint* hep-ph/0303092)
[160] Benedetti D, Cucciarelli S, Hill C, Incandela J, Koay S, Riccardi C, Santocchia A, Schmidt A, Torre P and Weiser C 2006 Search for $H \rightarrow bb$ in association with a tt pair at CMS *CMS Note* 2006/119
[161] Mangano M L, Moretti M, Piccinini F, Pittau R and Polosa A D 2003 ALPGEN, a generator for hard multiparton processes in hadronic collisions *J. High. Energy Phys.* JHEP07(2003)001 (*Preprint* hep-ph/0206293) (doi:10.1088/1126-6708/2003/07/001)
[162] Beenakker W, Dittmaier S, Kraemer M, Pluemper B, Spira M and Zerwas P 2003 NLO QCD corrections to $t\bar{t}H$ production in hadron collisions *Nucl. Phys.* B **653** 151–203 (*Preprint* hep-ph/0211352)
[163] Roberfroid V *et al* 2006 Validation and status of the HLT Steering Code and default menu *CMS IN* 2006/001
[164] James E, Maravin Y, Mulders M and Neumeister N 2006 Muon Identification in CMS *CMS Note* 2006/010
[165] Heister A, Kodolova O, Konoplianikov V, Petrushanko S, Rohlf J, Tully C and Ulyanov A 2006 Measurement of Jets with the CMS Detector at the LHC *CMS Note* 2006/036
[166] Santocchia A 2006 Optimization of Jet Reconstruction Settings and Parton-Level Correction for the ttH Channel *CMS Note* 2006/059
[167] D'Hondt J, Lowette S, Buchmuller O, Cucciarelli S, Schilling F P, Spiropulu M, Mehdiabadi S, Benedetti D and Pape L 2006 Fitting of Event Topologies with External Kinematic Constraints in CMS *CMS Note* 2006/023
[168] Mangano M private communication
[169] Wang X-N and Gyulassy M 1991 HIJING: A Monte Carlo model for multiple jet production in p p, p A and A A collisions *Phys. Rev.* D **44** 3501–3516
[170] Bedjidian M *et al* 2004 Hard probes in heavy ion collisions at the LHC: heavy flavour physics *Preprint* hep-ph/0311048
[171] Eskola K J, Kolhinen V J and Salgado C A 1999 The scale dependent nuclear effects in parton distributions for practical applications *Eur. Phys. J.* C **9** 61–68 (*Preprint* hep-ph/9807297)
[172] Kodolova O, Bedjidian M and Petrouchanko S 1999 Dimuon reconstruction in heavy ion collisions using a detailed description of CMS geometry *CMS Note* 1999-004
[173] Bedjidian M and Kodolova O 2006 Quarkonia measurements in heavy-ion collisions in CMS *CMS Note* 2006/089
[174] Sterman G and Weinberg S 1977 Jets from Quantum Chromodynamics *Phys. Rev. Lett.* **39** 1436
[175] JADE Collaboration, Bartel W *et al* 1986 Experimental studies on multi-jet production in e^+e^+ annihilation at petra energies *Z. Phys.* C **33** 23
[176] JADE Bethke S *et al* 1988 Experimental investigation of the energy dependence of the strong coupling strength *Phys. Lett.* B **213** 235

[177] Catani S, Dokshitzer Y L, Olsson M, Turnock G and Webber B R 1991 New clustering algorithm for multi-jet cross-sections in e^+e^+ annihilation *Phys. Lett.* B **269** 432–438

[178] CDF Run II Collaboration, Abulencia A *et al* 2005 Measurement of the inclusive jet cross section in $p\bar{p}$ interactions at $\sqrt{s} = 1.96$ TeV using a cone-based jet algorithm *Preprint* hep-ex/0512020

[179] DØ, Collaboration, Strohmer R 2006 Inclusive jet cross-sections and dijet azimuthal decorrelations with DØ*PoS* HEP **2005** 051 (*Preprint* hep-ex/0601016)

[180] Butterworth J, Couchman J, Cox B and Waugh B 2003 KtJet: A C^{++} implementation of the K(T) clustering algorithm *Comput. Phys. Commun.* **153** 85–96 (*Preprint* hep-ph/0210022)

[181] ed U Baur, R K Ellis and D Zeppenfeld 2000 *QCD and Weak Boson Physics in Run II* (Batavia, IL, USA: FERMILAB) Prepared for Physics at Run II: QCD and Weak Boson Physics Workshop: Final General Meeting, Batavia, Illinois, 4–6 November, 1999

[182] Ellis S D, Huston J and Tonnesmann M 2001 On building better cone jet algorithms *eConf* C 010630 P513 (*Preprint* hep-ph/0111434)

[183] Wobisch M private communication

[184] Sjostrand T 1994 High-energy physics event generation with PYTHIA 5.7 and JETSET 7.4 *Comput. Phys. Commun.* **82** 74–90

[185] Nagy Z 2002 Three-jet cross sections in hadron hadron collisions at next-to-leading order *Phys. Rev. Lett.* **88** 122003 (*Preprint* hep-ph/0110315)

[186] Kluge T, Rabbertz K and Wobisch M fast NLO—fast pQCD calculations for hadron-induced processes To be published, available at http://hepforge.cedar.ac.uk/fastnlo

[187] Moretti S, Nolten M R and Ross D A 2005 Weak corrections and high E(T) jets at Tevatron *Preprint* hep-ph/0503152

[188] DØ Collaboration, Abazov V M *et al* 2002 The inclusive jet cross-section in p anti-p collisions at s**(1/2)=1.8-TeV using the k(T) algorithm *Phys. Lett.* B **525** 211–218 (*Preprint* hep-ex/0109041)

[189] DØ Collaboration, Abbott B *et al* 2001 High-p_{T} jets in $\bar{p}p$ collisions at $\sqrt{s} = 630$ GeV and 1800 GeV *Phys. Rev.* D **64** 032003 (doi:10.1103/PhysRevD.64.032003)

[190] CDF Collaboration, Affolder A A *et al* 2002 Charged jet evolution and the underlying event in proton anti-proton collisions at 1.8-TeV *Phys. Rev.* D **65** 092002

[191] CDF Collaboration, Acosta D *et al* 2004 The underlying event in hard interactions at the Tevatron anti-p p collider *Phys. Rev.* D **70** 072002 (*Preprint* hep-ex/0404004)

[192] Sjostrand T and van Zijl M 1987 A multiple interaction model for the event structure in hadron collisions *Phys. Rev.* D **36** 2019

[193] Butterworth J, Forshaw J R and Seymour M 1996 Multiparton interactions in photoproduction at HERA *Z. Phys.* C **72** 637–646 (*Preprint* hep-ph/9601371)

[194] Gleisberg T *et al* 2004 SHERPA 1.alpha, a proof-of-concept version *J. High. Energy Phys.* JHEP02(2004)056 (*Preprint* hep-ph/0311263)

[195] Bopp F W, Engel R and Ranft J 1998 Rapidity gaps and the PHOJET Monte Carlo *Preprint* hep-ph/9803437

[196] Corcella G *et al* 2001 HERWIG 6: An event generator for hadron emission reactions with interfering gluons (including supersymmetric processes) *J. High. Energy Phys.* JHEP01(2001)010 (*Preprint* hep-ph/0011363) (doi:10.1088/1126-6708/2001/01/010)

[197] Buttar C M, Clements D, Dawson I and Moraes A 2004 Simulations of minimum bias events and the underlying event, MC tuning and predictions for the LHC *Acta Phys. Polon.* B **35** 433–441

[198] CDF Collaboration, Field R 2005 Min-bias and the underlying event in Run 2 at CDF *Acta Phys. Polon.* B **36** 167–178

[199] Acosta D *et al* 2006 The underlying event at the LHC *CMS Note* 2006/067

[200] CDF Collaboration, Abe F *et al* 1991 Measurement of the Z-boson p_{T} distribution in $\bar{p}p$ collisions at $\sqrt{s} = 1.8$ TeV *Phys. Rev. Lett.* **67** 2937–2941 (doi:10.1103/PhysRevLett.67.2937)

[201] Bartalini P, Chierici R and De Roeck A 2005 Guidelines for the estimation of theoretical uncertainties at the LHC *CMS Note* 2005/013

[202] Adam W, Mangano B, Speer T and Todorov T 2006 Track reconstruction in the CMS tracker *CMS Note* 2006/041

[203] Andreev V P, Cline D.B and Otwinowski S 2006 Inclusive b quark production *CMS Note* 2006/120

[204] CDF Collaboration, Abe F *et al* 1993 Measurement of the bottom quark production cross section using semileptonic decay electrons in $p\bar{p}$ collisions at $\sqrt{s} = 1.8$ TeV *Phys. Rev. Lett.* **71** 500 (doi:10.1103/PhysRevLett.71.500)

[205] CDF Collaboration, Abe F *et al* 1994 Measurement of the B meson and b quark cross sections at $\sqrt{s} = 1.8$ TeV using the exclusive decay $B^0 \to J/\psi K^*(892)^0$ *Phys. Rev.* D **50** 4252 (doi:10.1103/PhysRevD.50.4252)

[206] CDF Collaboration, Abe F *et al* 1995 Measurement of the B Meson Differential Cross Section $d\sigma/dp_{\mathrm{T}}$ in $p\bar{p}$ Collisions at $\sqrt{s} = 1.8$ TeV *Phys. Rev. Lett.* **75** 1451 (doi:10.1103/PhysRevLett.75.1451)

[207] CDF Collaboration Abe F *et al* 2002 Measurement of the B^+ total cross section and B^+ differential cross section $d\sigma/dp_{\mathrm{T}}$ in $p\bar{p}$ collisions at $\sqrt{s} = 1.8$ TeV *Phys. Rev.* D **65** 052005 (doi:10.1103/PhysRevD.65.052005)

[208] CDF Collaboration, Abe F *et al* 2002 Measurement of the ratio of b quark production cross sections in $\bar{p}p$ collisions at $\sqrt{s} = 630$ GeV and $\sqrt{s} = 1800$ GeV *Phys. Rev.* D **66** 032002 (doi:10.1103/PhysRevD.66.032002)

[209] DØ Collaboration, Abachi S *et al* 1995 Inclusive μ and b-quark production cross-sections in $p\bar{p}$ collisions at $\sqrt{s} = 1.8$ TeV *Phys. Rev. Lett.* **74** 3548 (doi:10.1103/PhysRevLett.74.3548)

[210] DØ Collaboration, Abbott B *et al* 2000 The $b\bar{b}$ production cross section and angular correlations in $p\bar{p}$ collisions at $\sqrt{s} = 1.8$ TeV *Phys. Lett.* B **487** 264 (doi:10.1016/S0370-2693(00)00844-3)

[211] DØ Collaboration, Abbott B *et al* 2000 Cross section for b-Jet production in $\bar{p}p$ collisions at $\sqrt{s} = 1.8$ TeV *Phys. Rev. Lett.* **85** 5068 (doi:10.1103/PhysRevLett.85.5068)

[212] H1 Collaboration, Adloff C *et al* 1999 Measurement of open beauty production at HERA *Phys. Lett.* B **467** 156 (doi:10.1016/S0370-2693(99)01099-0)

[213] H1 Collaboration, Adloff C *et al* 2001 Erratum *Phys. Lett.* B **518** 331

[214] ZEUS Collaboration, Breitweg J *et al* 2001 Measurement of open beauty production in photoproduction at HERA *Eur. Phys. J.* C **18** 625–637 (doi:10.1007/s100520100571)

[215] H1 Collaboration, Aktas A *et al* 2005 Measurement of F2(c anti-c) and F2(b anti-b) at high Q**2 using the H1 vertex detector at HERA *Eur. Phys. J.* C **40** 349–359 (*Preprint* hep-ex/0411046)

[216] ZEUS Collaboration, Chekanov S *et al* 2004 Bottom photoproduction measured using decays into muons in dijet events in e p collisions at s**(1/2)=318 GeV *Phys. Rev.* D **70** 012008

[217] ZEUS Collaboration, Chekanov S *et al* 2004 Measurement of beauty production in deep inelastic scattering at HERA *Phys. Lett.* B **599** 173–189 (*Preprint* hep-ex/0405069)

[218] H1 Collaboration, Aktas A *et al* 2005 Measurement of beauty production at HERA using events with muons and jets *Eur. Phys. J.* C **41** 453–467 (*Preprint* hep-ex/0502010)

[219] L3 Collaboration, Acciarri M *et al* 2001 Measurements of the cross sections for open charm and beauty production in $\gamma\gamma$ collisions at $\sqrt{s} = 189$ GeV–202 GeV *Phys. Lett.* B **503** 10 (doi:10.1016/S0370-2693(01)00134-4)

[220] L3 Collaboration, Achard P *et al* 2005 Measurement of the cross section for open-beauty production in photon photon collisions at LEP *Phys. Lett.* B **619** 71

[221] Nason P, Dawson S and Ellis R K 1988 The total cross-section for the production of heavy quarks in hadronic collisions *Nucl. Phys.* B **303** 607

[222] Nason P, Dawson S and Ellis R K 1989 The one particle inclusive differential cross-section for heavy quark production in hadronic collisions *Nucl. Phys.* B **327** 49–92

[223] Beenakker W, Van Neerven W L, Meng R, Schuler G A and Smith J 1991 QCD corrections to heavy quark production in hadron-hadron collisions *Nucl. Phys.* B **351** 507–560 (doi:10.1016/S0550-3213(05)80032-X)

[224] Cacciari M, Frixione S, Mangano M L, Nason P and Ridolfi G 2004 QCD analysis of first b cross section data at 1.96-TeV *J. High. Energy Phys.* JHEP07(2004)033 (doi:10.1088/1126-6708/2004/07/033)

[225] Mangano M L 2005 The saga of bottom production in proton antiproton collisions *AIP Conf. Proc.* **753** 247–260 (*Preprint* hep-ph/0411020)

[226] Frixione S 2004 Bottom production *Preprint* hep-ph/0408317

[227] Weinberg S 1990 Unitarity vonstraints on CP nonconservation in Higgs exchange *Phys. Rev.* D **42** 860–866

[228] Lavoura L 1993 Maximal CP violation via Higgs boson exchange *Int. J. Mod. Phys.* A **8** 375–390

[229] Jenkins E, Luke M E, Manohar A V and Savage M J 1993 Semileptonic B_c decay and heavy quark spin symmetry *Nucl. Phys.* B **390** 463–473 (*Preprint* hep-ph/9204238)

[230] Kiselev V V, Kovalsky A E and Likhoded A K 2000 B_c decays and lifetime in QCD sum rules *Nucl. Phys.* B **585** 353–382 (doi:10.1016/S0550-3213(00)00386-2)

[231] Wu X-G, Chang C-H, Chen Y-Q and Fang Z-Y 2003 The meson B_c annihilation to leptons and inclusive light hadrons *Phys. Rev.* D **67** 094001 (doi:10.1103/PhysRevD.67.094001)

[232] Chang C-H and Chen Y-Q 1992 The Production of B_c or $\bar{B}_c$ meson associated with two heavy quark jets in Z^0 boson decay *Phys. Rev.* D **46** 3845–3855 (doi:10.1103/PhysRevD.46.3845)

[233] Chang C-H and Chen Y-Q 1993 Hadronic production of the B_c meson at TeV energies *Phys. Rev.* D **48** 4086 (doi:10.1103/PhysRevD.48.4086)

[234] Chang C-H, Chen Y-Q, Han G-P and Jiang H-T 1995 On hadronic production of the B_c meson *Phys. Lett.* B **364** 78 (doi:10.1016/0370-2693(95)01235-4)

[235] Chang C-H, Chen Y-Q and Oakes R J 1996 Comparative study of the hadronic production of B_c mesons *Phys. Rev.* D **54** 4344 (doi:10.1103/PhysRevD.54.4344)
[236] Chang C-H and Wu X-G 2004 Uncertainties in estimating hadronic production of the meson B/c and comparisons between TEVATRON and LHC *Eur. Phys. J.* C **38** 267–276 (doi:10.1140/epjc/s2004-02015-0)
[237] CDF Collaboration, Abe F *et al* 1998 Observation of the B_c meson in $p\bar{p}$ collisions at $\sqrt{s} = 1.8$ TeV *Phys. Rev. Lett.* **81** 2432–2437 (doi:10.1103/PhysRevLett.81.2432)
[238] CDF Collaboration, Acosta D *et al* 2006 Evidence for the exclusive decay $B_c^{\pm} \to J/\psi\pi^{\pm}$ and measurement of the mass of the B_c meson *Phys. Rev. Lett.* **96** 082002 (doi:10.1103/PhysRevLett.96.082002)
[239] Berezhnoi A V, Kiselev V V, Likhoded A K and Onishchenko A I 1997 B_c meson at LHC *Phys. Atom. Nucl.* **60** 1729–1740 (*Preprint* hep-ph/9703341)
[240] Gouz I P, Kiselev V V, Likhoded A K, Romanovsky V I and Yushchenko O P 2004 Prospects for the B_c studies at LHCb *Phys. Atom. Nucl.* **67** 1559–1570 (doi:10.1134/1.1788046)
[241] Chang C-H and Chen Y-Q 1994 Decays of the B_c meson *Phys. Rev.* D **49** 3399–3411 (doi:10.1103/PhysRevD.49.3399)
[242] Kwong W-K and Rosner J L 1991 Masses of new particles containing b quarks *Phys. Rev.* D **44** 212–219 (doi:10.1103/PhysRevD.44.212)
[243] Eichten E J and Quigg C 1994 Mesons with beauty and charm: Spectroscopy *Phys. Rev.* D **49** 5845–5856 (*Preprint* hep-ph/9402210)
[244] Chen Y-Q and Kuang Y-P 1992 Improved QCD motivated heavy quark potentials with explicit $\Lambda_{\overline{MS}}$ dependence *Phys. Rev.* D **46** 1165–1171 (doi:10.1103/PhysRevD.46.1165)
[245] Chen G, Meng X and Tao J 2006 Feasibility to study the B_c meson at CMS *CMS Note* 2006/118
[246] Sjostrand T, Lonnblad L, Mrenna S and Skands P 2003 PYTHIA 6.3: Physics and manual *Preprint* hep-ph/0308153
[247] Grothe M *et al* 2006 Triggering on Forward Physics *CMS Note* 2006/054. Also available as TOTEM NOTE 2006-01
[248] CMS/TOTEM Collaboration, CMS/TOTEM document on diffractive and forward physics, in preparation 2006
[249] UA8 Collaboration, Bonino R *et al* 1988 Evidence for transverse jets in high mass diffraction *Phys. Lett.* B **211** 239
[250] Arneodo M and Diehl M 2005 Diffraction for non-believers *Preprint* hep-ph/0511047
[251] UA8 Collaboration, Brandt A *et al* 1998 Measurements of single diffraction at $\sqrt{s} = 630$ GeV: Evidence for a non-linear $\alpha(t)$ of the pomeron *Nucl. Phys.* B **514** 3–44 (doi:10.1016/S0550-3213(97)00813-4)
[252] Erhan S and Schlein P E 2000 Inelastic diffraction data and the Pomeron trajectory *Phys. Lett.* B **481** 177–186 (doi:10.1016/S0370-2693(00)00467-6)
[253] Goulianos K 2005 Twenty years of diffraction at the TevatronPresented at 11th international conference on elastic and diffractive scattering: towards high energy frontiers: the 20th anniversary of the blois workshops *Preprint* hep-ph/0510035
[254] FP420 Collaboration, Albrow M G *et al* 2005 FP420: A proposal to investigate the feasibility of installing proton tagging detectors in the 420 m region of the LHC *CERN/LHCC*, 2005-025
[255] CDF Collaboration, Affolder A A *et al* 2000 Diffractive dijets with a leading antiproton in anti-p p collisions at $\sqrt{s}$ = 1800 GeV *Phys. Rev. Lett.* **84** 5043–5048
[256] De Roeck A, Khoze V A, Martin A D, Orava R and Ryskin M G 2002 Ways to detect a light Higgs boson at the LHC *Eur. Phys. J.* C **25** 391–403 (*Preprint* hep-ph/0207042)
[257] Khoze V, Martin A and Ryskin M 2002 Prospects for new physics observations in diffractive processes at the LHC and Tevatron *Eur. Phys. J.* C **23** 311–327 (*Preprint* hep-ph/0111078)
[258] Kisselev A, Petrov V and Ryutin R 2005 5-dimensional quantum gravity effects in exclusive double diffractive events *Phys. Lett.* B **630** 100–107 (doi:10.1016/j.physletb.2005.09.059)
[259] Monk J and Pilkington A 2005 ExHuME: a Monte Carlo event generator for exclusive diffraction *Preprint* hep-ph/0502077
[260] Boonekamp M *et al* 2005 Monte-Carlo generators for central exclusive diffraction *Proceedings of the HERA-LHC Workshop (CERN/DESY, January, 2005)* available at http://www.desy.de/ heralhc/proceedings/wg4montecarlo.pdf
[261] Ryutin R 2004 EDDE Monte Carlo event generator *Preprint* hep-ph/0409180
[262] Kaidalov A, Khoze V A, Martin A D and Ryskin M G 2003 Central exclusive diffractive production as a spin parity analyser: From hadrons to Higgs *Eur. Phys. J.* C **31** 387–396 (*Preprint* hep-ph/0307064)
[263] Carena M, Heinemeyer S, Wagner C E M and Weiglein G 2006 MSSM Higgs boson searches at the Tevatron and the LHC: Impact of different benchmark scenarios *Eur. Phys. J.* C **45** 797–814 (*Preprint* hep-ph/0511023)

[264] Ellis J R, Lee J S and Pilaftsis A 2005 Diffraction as a CP and lineshape analyzer for MSSM Higgs bosons at the LHC *Phys. Rev.* D **71** 075007 (*Preprint* hep-ph/0502251)
[265] Petrov A, Ryutin R, Sobol A and Guillaud J-P 2005 Azimuthal angular distributions in EDDE as spin-parity analyser and glueball filter for LHC *J. High. Energy Phys.* JHEP06(2005)007 (*Preprint* hep-ph/0409118)
[266] Piotrzkowski K 2001 Tagging two-photon production at the LHC *Phys. Rev.* D **63** 071502 (*Preprint* hep-ex/0009065)
[267] Budnev V, Ginzburg I, Meledin G and Serbo V 1974 The Two photon particle production mechanism. physical problems. applications. equivalent photon approximation *Phys. Rept.* **15** 181–281 (doi:10.1016/0370-1573(75)90009-5)
[268] Khoze V, Martin A and Ryskin M 2002 Photon-exchange processes at hadron colliders as a probe of the dynamics of diffraction *Eur. Phys. J.* C **24** 459–468 (*Preprint* hep-ph/0201301) (doi:10.1007/s10052-002-0964-4)
[269] White A R 2005 The physics of a sextet quark sector *Phys. Rev.* D **72** 036007 (*Preprint* hep-ph/0412062)
[270] Piotrzkowski K 2002 High energy two-photon interactions at the LHC *Preprint* hep-ex/0201027
[271] Kalmykov N N, Ostapchenko S S and Pavlov A I 1997 Quark-gluon string model and EAS simulation problems at ultra-high energies *Nucl. Phys. Proc. Suppl.* B **52** 17–28
[272] Engel R, Gaisser T K, Stanev T and Lipari P 1999 Air shower calculations with the new version of SIBYLL *Prepared for 26th International Cosmic Ray Conference* (ICRC 99) (Salt Lake City, Utah, 17–25 August 1999)
[273] Roesler S, Engel R and Ranft J The Event generator DPMJET-III at cosmic ray energies Prepared for 27th International Cosmic Ray Conference (ICRC 2001) (Hamburg, Germany, 7-15 Aug 2001)
[274] Karsch Frithjof 2002 Lattice QCD at high temperature and density *Lect. Notes Phys.* **583** 209–249 (*Preprint* hep-lat/0106019)
[275] Iancu Edmond and Venugopalan Raju 2003 The color glass condensate and high energy scattering in QCD *Preprint* hep-ph/0303204
[276] Schwarz Dominik J 2003 The first second of the universe *Annalen Phys.* **12** 220–270 (*Preprint* astro-ph/0303574)
[277] Starinets Andrei O 2005 Transport coefficients of strongly coupled gauge theories: Insights from string theory *Preprint* nucl-th/0511073
[278] Bonciani Roberto, Catani Stefano, Mangano Michelangelo L and Nason Paolo 1998 NLL resummation of the heavy-quark hadroproduction cross-section *Nucl. Phys.* B **529** 424–450 (*Preprint* hep-ph/9801375)
[279] Davids M *et al* 2006 Measurement of top-pair cross section and top-quark mass in the di-lepton and full-hadronic channels with CMS *CMS Note* http://cms.cern.ch/iCMS/jsp/openfile.jsp?tp=draft&files=2907_ttbar.pdf2006/077
[280] Gennai S *et al* 2006 Tau jet reconstruction and tagging at High Level Trigger and off-line *CMS Note* http://cms.cern.ch/iCMS/jsp/openfile.jsp?type=NOTE&year=2006&files=NOTE2006_028.pdf2006/028
[281] D'Hondt J, Heyninck J and Lowette S 2006 Measurement of the cross section of single leptonic $t\bar{t}$ events *CMS Note* http://cms.cern.ch/iCMS/jsp/openfile.jsp?type=NOTE&year=2006&files=NOTE2006_064.pdf2006/064
[282] Buttar C *et al* 2006 Les Houches Physics at TeV Colliders 2005, Standard Model and Higgs working group: Summary report *Preprint* hep-ph/0604120
[283] Konoplianikov V, Kodolova O and Ulyanov A 2006 Jet calibration using γ+jet events in the CMS Detector *CMS Note* http://cms.cern.ch/iCMS/jsp/openfile.jsp?type=NOTE&year=2006&files=NOTE2006_042.pdf2006/042
[284] D'Hondt J *et al* 2006 Electron and muon reconstruction in single leptonic $t\bar{t}$ events *CMS Note* http://cms.cern.ch/iCMS/jsp/openfile.jsp?type=NOTE&year=2006&files=NOTE2006_024.pdf2006/024
[285] CMS Collaboration, Acosta D *et al* 2006 CMS Coll. Physics TDR Vol. I, Section 12.2.8 *CERN/LHCC* 2006-001
[286] Lowette S, D'Hondt J, Heyninck J and Vanlaer P 2006 Offline calibration of b-jet identification efficiency, *CERN-CMS-NOTE* -2006-013
[287] D'Hondt J, Lowette S, Heyninck J and Kasselmann S 2006 Light quark jet energy scale calibration using the W mass constraint in single-leptonic $t\bar{t}$ events *CERN-CMS-NOTE* -2006-025
[288] The CDF Collaboration, Acosta D *et al* 2005 Measurement of the $t\bar{t}$ cross section in $p\bar{p}$ collisions at $\sqrt{s}$=1.96 TeV using kinematic characteristics of lepton plus jets events *Phys. Rev.* D **71** 072005 (doi:10.1103/PhysRevD.71.072005)
[289] DØ Collaboration, Abazov V M *et al* 2005 Measurement of the $t\bar{t}$ cross section in $p\bar{p}$ collisions at $\sqrt{s}$=1.96 TeV using kinematic characteristics of lepton plus jets events *Phys. Lett.* B **626** 55 (doi:10.1016/j.physletb.2005.08.105)

[290] Vos M and Palla F 2006 B-tagging in the High Level Trigger *CMS Note* http://cmsdoc.cern.ch/documents/06/note06_030.pdf2006-030
[291] CDF and DØ, Wicke D 2005 Top pair production cross-section measurement in the all-hadronic channel at CDF and DØCollaboration *Int. J. Mod. Phys. A* **20** 3183–3186 (*Preprint* hep-ex/0411009) (doi:10.1142/S0217751X05026091)
[292] D'Hondt J, Heyninck J and Lowette S 2006 Top Quark mass measurement in single-leptonic $t\bar{t}$ events *CMS Note* http://cms.cern.ch/iCMS/jsp/openfile.jsp?type=NOTE&year=2006&files=NOTE2006_066.pdf2006/066
[293] CDF Collaboration, Abe F *et al* 1997 First Observation of the All-Hadronic Decay of $t\bar{t}$ pairs *Phys. Rev. Lett.* **79** 1992–1997 (doi:10.1103/PhysRevLett.79.1992)
[294] Tevatron Electroweak Working Group Collaboration 2006 Combination of CDF and DØresults on the mass of the top quark *Preprint* hep-ex/0603039
[295] Kharchilava Avto 2000 Top mass determination in leptonic final states with J/*psi* *Phys. Lett.* **B476** 73–78 (*Preprint* hep-ph/9912320)
[296] Grenier P 2001 *ATLAS Physics Note* 2001-023
[297] Chierici R and Dierlamm A 2006 Determination of the top mass in exclusive JPsi decays *CMS Note* http://cmsdoc.cern.ch/documents/06/note06_058.pdf2006-058
[298] Tevatron Electroweak Working Group Collaboration 2006 Combination of CDF and DØ results on the mass of the top quark *Preprint* hep-ex/0603039
[299] Hill C S, Incandela J R and Lamb J M 2005 A method for measurement of the top quark mass using the mean decay length of *b* hadrons in *t* anti-*t* events *Phys. Rev.* D **71** 054029 (*Preprint* hep-ex/0501043)
[300] Borjanovic I *et al* 2005 Investigation of top mass measurements with the ATLAS detector at LHC *Eur. Phys. J.* **C39S2** 63–90 (*Preprint* hep-ex/0403021)
[301] Lyons Louis, Gibaut Duncan and Clifford Peter 1988 How to combine correlated estimates of a single physical quantity *Nucl. Instrum. Methods* A **270** 110
[302] Valassi A 2003 Combining correlated measurements of several different physical quantities *Nucl. Instrum. Methods* A **500** 391–405
[303] Mahlon G and Parke S 1996 Angular correlation in top quark pair production and decay at hadron collider *Phys. Rev.* D **53** 4886–4896 (*Preprint* hep-ph/9512264)
[304] Stelzer T and Willenbrock S 1996 Spin correlation in top-quark production at hadron collider *Phys. Lett.* B **374** 169–172 (*Preprint* hep-ph/9512292)
[305] Brandenburg A 1996 Spin-spin correlations of top quark pairs at Hadron colliders *Phys. Lett.* B **387** 626–632 (*Preprint* hep-ph/9606379)
[306] Baarmand M, Mermerkaya H and Vodopiyanov I 2006 Measurement of spin correlation in top quark pair production in semi-leptonic final state *CMS Note* 2006/111
[307] Tait T 2000 The tW^- mode of single top production *Phys. Rev.* D **61** 034001 (*Preprint* hep-ph/9909352) (doi:10.1103/PhysRevD.61.034001)
[308] Belyaev A and Boos E 2001 Single top quark t W + X production at the LHC: A closer look *Phys. Rev.* D **63** 034012 (*Preprint* hep-ph/0003260)
[309] Zhu S 2002 Next-to-leading order QCD corrections to b g $\rightarrow$ t W- at the CERN Large Hadron Collider *Phys. Lett.* B **524** 283–288
[310] Boos E, Bunichev V, Dudko L, Savrin V and Sherstnev A 2005 A simulation method of the electroweak top quark production events in the NLO approximation: a Monte-Carlo generator 'singletop'abstract available at http://www.npi.msu.su/eng/science.php3?sec=preprint&ref_pp=1262
[311] CMS Collaboration, Acosta D *et al* 2006 CMS Physics Technical Design Report, Volume 1, Section 9.1.2: Global muon reconstruction *CERN/LHCC*, 2006-001 p 333
[312] CMS Collaboration, Acosta D *et al* 2006 CMS Physics Technical Design Report, Volume 1, Section 9.3: Muon identification *CERN/LHCC*, 2006-001 p 351
[313] CMS Collaboration, Acosta D *et al* 2006 CMS Physics Technical Design Report, Volume 1, Section 10.4: Electron reconstruction and selection *CERN/LHCC*, 2006-001 p 390
[314] CMS Collaboration, Acosta D *et al* 2006 CMS Physics Technical Design Report, Volume 1, Section 11.2.1: Iterative cone *CERN/LHCC*, 2006-001 p 408
[315] CMS Collaboration, Acosta D *et al* 2006 CMS Physics Technical Design Report, Volume 1, Section 11.6.3: γ+jet events *CERN/LHCC*, 2006-001 423
[316] CMS Collaboration, Acosta D *et al* 2006 CMS Physics Technical Design Report, Volume 1, Section 12.2: b-tagging tools *CERN/LHCC*, 2006-001 p 461
[317] Abramov V *et al* 2006 Selection of single top events with the CMS detector at LHC *CMS Note* 2006/084
[318] Yeh P *et al* 2006 Search for W-associated Production of Single Top Quarks in CMS *CMS Note* 2006/086

[319] Campbell J, Ellis R K and Rainwater D L 2003 Next-to-leading order QCD predictions for W + 2jet and Z + 2jet production at the CERN LHC *Phys. Rev.* D **68** 094021 (doi:10.1103/PhysRevD.68.094021)
[320] CMS Collaboration, Acosta D *et al* 2006 CMS Coll. Physics Technical Design Physics, Volume I, Section 11.6.5 *CERN/LHCC*, 2006-001
[321] CMS Collaboration, Acosta D *et al* 2006 CMS Physics Technical Design Physics, Volume I, Section 8.5: Sources of systematic effects *CERN/LHCC*, 2006-001 p 229
[322] Fisher R A 1936 The use of multiple measurements in taxonomic problems *Annuals of Eugenics* **7** 179–188
[323] Mele B, Petrarca S and Soddu A 1998 A new evaluation of the $t \to cH$ decay width in the standard model *Phys. Lett.* B **435** 401–406 (*Preprint* hep-ph/9805498)
[324] Huang C-S, Wu X-H and Zhu S-H 1999 Top-charm associated production at high energy $e^+ e^-$ colliders in standard model *Phys. Lett.* B **452** 143–149 (*Preprint* hep-ph/9901369)
[325] de Divitiis G M, Petronzio R and Silvestrini L 1997 Flavour changing top decays in supersymmetric extensions of the standard model *Nucl. Phys.* B **504** 45–60 (*Preprint* hep-ph/9704244)
[326] Guasch J and Sola J 1999 FCNC top quark decays: A door to SUSY physics in high luminosity colliders? *Nucl. Phys.* B **562** 3–28 (*Preprint* hep-ph/9906268)
[327] Eilam G, Gemintern A, Han T, Yang J M and Zhang X 2001 Top quark rare decay $t \to ch$ in R-parity-violating SUSY *Phys. Lett.* B **510** 227–235 (*Preprint* hep-ph/0102037) (doi:10.1016/S0370-2693(01)00598-6)
[328] Li C S, Zhang X-M and Zhu S H 1999 SUSY-QCD effect on top charm associated production at linear collider *Phys. Rev.* D **60** 077702 (*Preprint* hep-ph/9904273)
[329] Bejar S, Guasch J and Sola J 2001 FCNC top quark decays beyond the standard model *Preprint* hep-ph/0101294
[330] Diaz R A, Martinez R and Alexis Rodriguez J 2001 The rare decay $t \to c\gamma$ in the general 2HDM type III *Preprint* hep-ph/0103307
[331] Han T and Hewett J L 1999 Top charm associated production in high energy $e^+ e^-$ collisions *Phys. Rev.* D **60** 074015 (*Preprint* hep-ph/9811237)
[332] del Aguila F, Aguilar-Saavedra J A and Miquel R 1999 Constraints on top couplings in models with exotic quarks *Phys. Rev. Lett.* **82** 1628–1631 (*Preprint* hep-ph/9808400)
[333] Aguilar-Saavedra J A and Nobre B M 2003 Rare top decays $t \to c\gamma$, $t \to cg$ and CKM unitarity *Phys. Lett.* B **553** 251–260 (*Preprint* hep-ph/0210360)
[334] CDF and DØ Collaboration, Paulini M 1996 Heavy flavor physics from top to bottom *Preprint* hep-ex/9701019
[335] CDF Collaboration, Abe F *et al* 1998 Search for flavor-changing neutral current decays of the top quark in $p\bar{p}$ collisions at $\sqrt{s} = 1.8$ TeV *Phys. Rev. Lett.* **80** 2525–2530 (doi:10.1103/PhysRevLett.80.2525)
[336] Heinson A 1996 Future top physics at the Tevatron and LHC *Preprint* hep-ex/9605010
[337] Aguilar-Saavedra J A and Branco G C 2000 Probing top flavour-changing neutral scalar couplings at the CERN LHC *Phys. Lett.* B **495** 347–356 (*Preprint* hep-ph/0004190)
[338] Aguilar-Saavedra J A 2001 Top flavour-changing neutral coupling signals at a linear collider *Phys. Lett.* B **502** 115–124 (*Preprint* hep-ph/0012305)
[339] Aguilar-Saavedra J A and Riemann T 2001 Probing top flavor-changing neutral couplings at TESLA *Preprint* hep-ph/0102197
[340] Karafasoulis K *et al* 2006 Study of flavour changing neutral currents in top quark decays with the CMS detector *CMS Note* 2006/093
[341] Dissertori G *et al* 2006 How accurately can we count the number of $pp \to ZX$ and $pp \to WX$ events using decays to electrons *CMS Note* 2006/124
[342] Alcaraz J 2006 Measurement of $Z \to \mu^+\mu^-$ and $W \to \mu\nu$ rates in CMS *CMS Note* 2006/082
[343] Frixione S and Webber B R 2006 The MC@NLO 3.2 event generator *Preprint* hep-ph/0601192
[344] For further details see Proceedings of the 2004/2005 HERA-LHC workshop
[345] Dittmar M, Pauss F and Zurcher D 1997 Towards a precise parton luminosity determination at the CERN LHC *Phys. Rev.* D **56** 7284–7290 (*Preprint* hep-ex/9705004)
[346] Drell S D and Yan T-M 1970 Massive lepton pair production in hadron-hadron collisions at high-energies *Phys. Rev. Lett.* **25** 316–320 (doi:10.1103/PhysRevLett.25.316)
[347] Belotelov I *et al* 2006 Study of Drell–Yan di-muon production with the CMS detector *CMS Note* 2006/123
[348] Hamberg R, van Neerven W L and Matsuura T 1991 A Complete calculation of the order α_s^2 correction to the Drell–Yan K-factor *Nucl. Phys.* B **359** 343–405 (doi:10.1016/0550-3213(91)90064-5)
[349] Bourilkov D 2006 Compositeness search with di-muons in CMS *CMS Note* 2006/085
[350] Baur U and Wackeroth D 2003 Electroweak radiative corrections to weak boson production at hadron colliders *Nucl. Phys. Proc. Suppl.* **116** 159–163 (*Preprint* hep-ph/0211089)

[351] Bourilkov D 2003 Study of parton density function uncertainties with LHAPDF and PYTHIA at LHC*Prepared for the LHC/LC Study Group Meeting (Geneva, Switzerland, 9 May 2003) Preprint* hep-ph/0305126
[352] Buege V *et al* 2006 Prospects for the precision measurement of the W mass with the CMS detector *CMS Note* 2006-061
[353] Giele W T and Keller S 1998 Determination of W boson properties at hadron colliders *Phys. Rev.* D **57** 4433–4440 (*Preprint* hep-ph/9704419)
[354] Brigljević V *et al* 2006 Study of di-boson production with the CMS detector at the LHC *CMS Note* 2006/108
[355] Pukhov A *et al* 1999 CompHEP: A package for evaluation of Feynman diagrams and integration over multi-particle phase space. User's manual for version 33 *Preprint* hep-ph/9908288
[356] Higgs P W 1964 Broken symmetries, massless particles and gauge fields *Phys. Lett.* **12** 132–133
[357] Higgs P W 1966 Spontaneous symmetry breakdown without massless bosons *Phys. Rev.* **145** 1156–1163
[358] Englert F and Brout R 1964 Broken symmetry and the mass of gauge vector mesons *Phys. Rev. Lett.* **13** 321–322
[359] Guralnik G S, Hagen C R and Kibble T W B 1964 Global conservation laws and massless particles *Phys. Rev. Lett.* **13** 585–587
[360] Cornwall J M, Levin D N and Tiktopoulos G 1973 Uniqueness of spontaneously broken gauge theories *Phys. Rev. Lett.* **30** 1268–1270 (doi:10.1103/PhysRevLett.30.1268)
[361] Cornwall J M, Levin D N and Tiktopoulos G 1974 Derivation of gauge invariance from high-energy unitarity bounds on the S-Matrix *Phys. Rev.* D **10** 1145
[362] Llewellyn Smith C H 1973 High-energy behavior and gauge symmetry *Phys. Lett.* B **46** 233–236
[363] Joglekar S D 1974 S-matrix derivation of the Weinberg model *Ann. Phys.* **83** 427
[364] Veltman M 1968 Perturbation theory of massive Yang-Mills fields *Nucl. Phys.* B **7** 637–650
[365] 't Hooft G 1971 Renormalization of massless Yang-Mills fields *Nucl. Phys.* B **33** 173–199
[366] 't Hooft G 1971 Renormalizable lagrangians for massive Yang-Mills fields *Nucl. Phys.* B **35** 167–188
[367] 't Hooft G and Veltman M J G 1972 Regularization and renormalization of gauge fields *Nucl. Phys.* B **44** 189–213
[368] 't Hooft G and Veltman M J G 1972 Combinatorics of gauge fields *Nucl. Phys.* B **50** 318–353
[369] Djouadi A 2005 The anatomy of electro-weak symmetry breaking I: The Higgs boson in the standard model *Preprint* hep-ph/0503172
[370] Djouadi A 2005 The anatomy of electro-weak symmetry breaking II: The Higgs bosons in the minimal supersymmetric model *Preprint* hep-ph/0503173
[371] Cabibbo N, Maiani L, Parisi G and Petronzio R 1979 Bounds on the fermions and higgs boson masses in grand unified theories *Nucl. Phys.* B **158** 295
[372] Chanowitz M S, Furman M A and Hinchliffe I 1978 Weak interactions of ultraheavy fermions *Phys. Lett.* B **78** 285
[373] Flores R A and Sher M 1983 Upper limits to fermion masses in the Glashow-Weinberg-Salam model *Phys. Rev.* D **27** 1679
[374] Lindner M 1986 Implications of triviality for the standard model *Zeit. Phys.* C **31** 295
[375] Sher M 1989 Electroweak Higgs potentials and vacuum stability *Phys. Rept.* **179** 273–418
[376] Sher M 1993 Precise vacuum stability bound in the standard model *Phys. Lett.* B **317** 159–163 (*Preprint* hep-ph/9307342)
[377] Altarelli G and Isidori G 1994 Lower limit on the Higgs mass in the standard model: an update *Phys. Lett.* B **337** 141–144
[378] Espinosa J and Quiros M 1995 Improved metastability bounds on the standard model Higgs mass *Phys. Lett.* B **353** 257–266 (*Preprint* hep-ph/9504241)
[379] Hasenfratz A, Jansen K, Lang C B, Neuhaus T and Yoneyama H 1987 The triviality bound of the four component phi**4 model *Phys. Lett.* B **199** 531
[380] Kuti J, Lin L and Shen Y 1988 Upper bound on the Higgs mass in the standard model *Phys. Rev. Lett.* **61** 678
[381] Luscher M and Weisz P 1989 Scaling laws and triviality bounds in the lattice φ^4 theory (III) n-component model *Nucl. Phys.* B **318** 705 (doi:10.1016/0550-3213(89)90637-8)
[382] Higgs Working Group Collaboration, Carena M *et al* 2000 Report of the Tevatron Higgs working group *Preprint* hep-ph/0010338
[383] ATLAS Collaboration, 1994 Technical Design Report *CERN/LHCC*, 94-14, ATLAS TDR 14
[384] Abdullin S *et al* 2005 Summary of the CMS potential for the Higgs boson discovery *Eur. Phys. J.* C **39S2** 41–61 (doi:10.1140/epjcd/s2004-02-003-9)
[385] Braaten E and Leveille J P 1980 Higgs boson decay and the running mass *Phys. Rev.* D **22** 715

[386] Sakai N 1980 Perturbative QCD Corrections to the hadronic decay width of the Higgs boson *Phys. Rev.* D **22** 2220
[387] Inami T and Kubota T 1981 Renormalization group estimate of the Hadronic decay width of the Higgs boson *Nucl. Phys.* B **179** 171
[388] Gorishnii S G, Kataev A L and Larin S A 1984 The width of Higgs Boson decay into Hadrons: three loop corrections of strong interactions *Sov. J. Nucl. Phys.* **40** 329–334
[389] Drees M and Hikasa K-i 1990 Heavy quark thresholds in Higgs physics *Phys. Rev.* D **41** 1547
[390] Drees M and Hikasa K 1990 Note on QCD corrections to Hadronic Higgs decay *Phys. Lett.* B **240** 455
[391] Chetyrkin K G 1997 Correlator of the quark scalar currents and Gamma(tot)(H → hadrons) at O(alpha(s)**3) in pQCD *Phys. Lett.* B **390** 309–317 (*Preprint* hep-ph/9608318)
[392] Fleischer J and Jegerlehner F 1981 Radiative Corrections to Higgs Decays in the Extended Weinberg-Salam Model *Phys. Rev.* D **23** 2001–2026
[393] Bardin D Y, Vilensky B M and Khristova P K 1991 Calculation of the Higgs boson decay width into fermion pairs *Sov. J. Nucl. Phys.* **53** 152–158
[394] Dabelstein A and Hollik W 1992 Electroweak corrections to the fermionic decay width of the standard Higgs boson *Z. Phys.* C **53** 507–516
[395] Kniehl B A 1992 Radiative corrections for $H \to f\bar{f}(\gamma)$ in the standard model *Nucl. Phys.* B **376** 3–28 (doi:10.1016/0550-3213(92)90065)-J
[396] Zheng H-Q and Wu D-D 1990 First order QCD corrections to the decay of the Higgs boson into two photons *Phys. Rev.* D **42** 3760–3763
[397] Djouadi A, Spira M, van der Bij J and Zerwas P 1991 QCD corrections to gamma gamma decays of Higgs particles in the intermediate mass range *Phys. Lett.* B **257** 187–190
[398] Dawson S and Kauffman R P 1993 QCD corrections to H → gamma gamma *Phys. Rev.* D **47** 1264–1267
[399] Djouadi A, Spira M and Zerwas P 1993 Two photon decay widths of Higgs particles *Phys. Lett.* B **311** 255–260 (*Preprint* hep-ph/9305335)
[400] Melnikov K and Yakovlev O I 1993 Higgs → two photon decay: QCD radiative correction *Phys. Lett.* B **312** 179–183 (*Preprint* hep-ph/9302281)
[401] Inoue M, Najima R, Oka T and Saito J 1994 QCD corrections to two photon decay of the Higgs boson and its reverse process *Mod. Phys. Lett.* A **9** 1189–1194
[402] Steinhauser M 1996 Corrections of O(alpha(s)**2) to the decay of an intermediate-mass Higgs boson into two photons *Preprint* hep-ph/9612395
[403] Djouadi A, Gambino P and Kniehl B A 1998 Two-loop electroweak heavy-fermion corrections to Higgs-boson production and decay *Nucl. Phys.* B **523** 17–39 (*Preprint* hep-ph/9712330)
[404] Aglietti U, Bonciani R, Degrassi G and Vicini A 2004 Two-loop light fermion contribution to Higgs production and decays *Phys. Lett.* B **595** 432–441 (*Preprint* hep-ph/0404071)
[405] Degrassi G and Maltoni F 2005 Two-loop electroweak corrections to the Higgs-boson decay H→ gamma gamma *Preprint* hep-ph/0504137
[406] Kniehl B A 1991 Radiative corrections for $H \to ZZ$ in the standard model *Nucl. Phys.* B **352** 1–26 (doi:10.1016/0550-3213(91)90126-I)
[407] Kniehl B A 1991 Radiative corrections for $H \to W^+W^-(\gamma)$ in the standard model *Nucl. Phys.* B **357** 439–466 (doi:10.1016/0550-3213(91)90476-E)
[408] Georgi H, Glashow S, Machacek M and Nanopoulos D 1978 Higgs bosons from two gluon annihilation in proton proton collisions *Phys. Rev. Lett.* **40** 692 (doi:10.1103/PhysRevLett.40.692)
[409] Graudenz D, Spira M and Zerwas P M 1993 QCD corrections to Higgs boson production at proton proton colliders *Phys. Rev. Lett.* **70** 1372–1375 (doi:10.1103/PhysRevLett.70.1372)
[410] Spira M, Djouadi A, Graudenz D and Zerwas P 1993 SUSY Higgs production at proton colliders *Phys. Lett.* B **318** 347–353 (doi:10.1016/0370-2693(93)90138-8)
[411] Spira M, Djouadi A, Graudenz D and Zerwas P 1995 Higgs boson production at the LHC *Nucl. Phys.* B **453** 17–82 (*Preprint* hep-ph/9504378) (doi:10.1016/0550-3213(95)00379-7)
[412] Kramer M, Laenen E and Spira M 1998 Soft gluon radiation in Higgs boson production at the LHC *Nucl. Phys.* B **511** 523–549 (*Preprint* hep-ph/9611272) (doi:10.1016/S0550-3213(97)00679-2)
[413] Djouadi A, Spira M and Zerwas P 1991 Production of Higgs bosons in proton colliders: QCD corrections *Phys. Lett.* B **264** 440–446
[414] Dawson S 1991 Radiative corrections to Higgs boson production *Nucl. Phys.* B **359** 283–300
[415] Kauffman R P and Schaffer W 1994 QCD corrections to production of Higgs pseudoscalars *Phys. Rev.* D **49** 551–554 (*Preprint* hep-ph/9305279)
[416] Dawson S and Kauffman R 1994 QCD corrections to Higgs boson production: nonleading terms in the heavy quark limit *Phys. Rev.* D **49** 2298–2309 (*Preprint* hep-ph/9310281)

[417] Harlander R V and Kilgore W B 2002 Next-to-next-to-leading order Higgs production at hadron colliders *Phys. Rev. Lett.* **88** 201801 (*Preprint* hep-ph/0201206)
[418] Harlander R V and Kilgore W B 2002 Production of a pseudo-scalar Higgs boson at hadron colliders at next-to-next-to leading order *J. High. Energy Phys.* JHEP10(2002)017 (*Preprint* hep-ph/0208096)
[419] Anastasiou C and Melnikov K 2002 Higgs boson production at hadron colliders in NNLO QCD *Nucl. Phys.* B **646** 220–256 (*Preprint* hep-ph/0207004)
[420] Ravindran V, Smith J and van Neerven W L 2003 NNLO corrections to the total cross section for Higgs boson production in hadron hadron collisions *Nucl. Phys.* B **665** 325–366 (*Preprint* hep-ph/0302135)
[421] Catani S, de Florian D, Grazzini M and Nason P 2003 Soft-gluon resummation for Higgs boson production at hadron colliders *J. High. Energy Phys.* JHEP07(2003)028 (*Preprint* hep-ph/0306211)
[422] Djouadi A and Gambino P 1994 Leading electroweak correction to Higgs boson production at proton colliders *Phys. Rev. Lett.* **73** 2528–2531 (*Preprint* hep-ph/9406432)
[423] Chetyrkin K G, Kniehl B A and Steinhauser M 1997 Virtual top-quark effects on the H → b anti-b decay at next-to-leading order in QCD *Phys. Rev. Lett.* **78** 594–597 (*Preprint* hep-ph/9610456)
[424] Chetyrkin K G, Kniehl B A and Steinhauser M 1997 Three-loop O(alpha(s)**2 G(F) M(t)**2) corrections to hadronic Higgs decays *Nucl. Phys.* B **490** 19–39 (*Preprint* hep-ph/9701277)
[425] Ghinculov A and van der Bij J J 1996 The Higgs resonance shape in gluon fusion: Heavy Higgs effects *Nucl. Phys.* B **482** 59–72 (*Preprint* hep-ph/9511414)
[426] Ellis R K, Hinchliffe I, Soldate M and van der Bij J J 1988 Higgs Decay to tau + tau-: A Possible Signature of Intermediate Mass Higgs Bosons at the SSC *Nucl. Phys.* B **297** 221
[427] Baur U and Glover E W N 1990 Higgs Boson Production at Large Transverse Momentum in Hadronic Collisions *Nucl. Phys.* B **339** 38–66
[428] Schmidt C R 1997 $H \to ggg(gq\bar{q})$ at two loops in the large-M_t limit *Phys. Lett.* B **413** 391–395 (doi:10.1016/S0370-2693(97)01102-7)
[429] de Florian D, Grazzini M and Kunszt Z 1999 Higgs production with large transverse momentum in hadronic collisions at next-to-leading order *Phys. Rev. Lett.* **82** 5209–5212 (*Preprint* hep-ph/9902483)
[430] Ravindran V, Smith J and Van Neerven W L 2002 Next-to-leading order QCD corrections to differential distributions of Higgs boson production in hadron hadron collisions *Nucl. Phys.* B **634** 247–290 (*Preprint* hep-ph/0201114)
[431] Glosser C J and Schmidt C R 2002 Next-to-leading corrections to the Higgs boson transverse momentum spectrum in gluon fusion *J. High. Energy Phys.* JHEP12(2002)016 (*Preprint* hep-ph/0209248)
[432] Anastasiou C, Melnikov K and Petriello F 2005 Fully differential Higgs boson production and the di-photon signal through next-to-next-to-leading order *Nucl. Phys.* B **724** 197–246 (*Preprint* hep-ph/0501130)
[433] Catani S, D'Emilio E and Trentadue L 1988 The Gluon Form-Factor to Higher Orders: Gluon Gluon Annihilation at Small Q-Transverse *Phys. Lett.* B **211** 335–342
[434] Hinchliffe I and Novaes S F 1988 On the Mean Transverse Momentum of Higgs Bosons at the SSC *Phys. Rev.* D **38** 3475–3480
[435] Kauffman R P 1991 Higgs boson p(T) in gluon fusion *Phys. Rev.* D **44** 1415–1425
[436] Kauffman R 1992 Higher order corrections to Higgs boson p(T) *Phys. Rev.* D **45** 1512–1517
[437] Balazs C and Yuan C P 2000 Higgs boson production at the LHC with soft gluon effects *Phys. Lett.* B **478** 192–198 (*Preprint* hep-ph/0001103)
[438] Berger E L and Qiu J-w 2003 Differential cross section for Higgs boson production including all-orders soft gluon resummation *Phys. Rev.* D **67** 034026 (*Preprint* hep-ph/0210135)
[439] Kulesza A and Stirling W J 2003 Non-perturbative effects and the resummed Higgs transverse momentum distribution at the LHC *J. High. Energy Phys.* JHEP12(2003)056 (*Preprint* hep-ph/0307208)
[440] Kulesza A, Sterman G and Vogelsang W 2004 Joint resummation for Higgs production *Phys. Rev.* D **69** 014012 (*Preprint* hep-ph/0309264)
[441] Gawron A and Kwiecinski J 2004 Resummation effects in Higgs boson transverse momentum distribution within the framework of unintegrated parton distributions *Phys. Rev.* D **70** 014003 (*Preprint* hep-ph/0309303)
[442] Watt G, Martin A and Ryskin M 2004 Unintegrated parton distributions and electroweak boson production at hadron colliders *Phys. Rev.* D **70** 014012 (*Preprint* hep-ph/0309096)
[443] Lipatov A and Zotov N 2005 Higgs boson production at hadron colliders in the k(T)-factorization approach *Eur. Phys. J.* C **44** 559–566 (*Preprint* hep-ph/0501172)
[444] de Florian D and Grazzini M 2000 Next-to-next-to-leading logarithmic corrections at small transverse momentum in hadronic collisions *Phys. Rev. Lett.* **85** 4678–4681 (*Preprint* hep-ph/0008152)

[445] Catani S, De Florian D and Grazzini M 2001 Higgs production at hadron colliders in (almost) NNLO QCD *Bologna 2001, Deep Inelastic Scattering (Bologna, Italy, April, 2001)* pp 518–521 *Preprint* hep-ph/0106049
[446] Catani S, de Florian D and Grazzini M 2001 Universality of non-leading logarithmic contributions in transverse momentum distributions *Nucl. Phys.* B **596** 299–312 (*Preprint* hep-ph/0008184)
[447] Bozzi G, Catani S, de Florian D and Grazzini M 2003 The q(T) spectrum of the Higgs boson at the LHC in QCD perturbation theory *Phys. Lett.* B **564** 65–72 (*Preprint* hep-ph/0302104)
[448] Bozzi G, Catani S, de Florian D and Grazzini M 2006 Transverse-momentum resummation and the spectrum of the Higgs boson at the LHC *Nucl. Phys.* B **737** 73–120 (*Preprint* hep-ph/0508068)
[449] Cahn R N and Dawson S 1984 Production of Very Massive Higgs Bosons *Phys. Lett.* B **136** 196
[450] Hikasa K-i 1985 Heavy Higgs Production in e+ e- and e- e- Collisions *Phys. Lett.* B **164** 385
[451] Altarelli G, Mele B and Pitolli F 1987 Heavy Higgs production at future colliders *Nucl. Phys.* B **287** 205–224
[452] Han T, Valencia G and Willenbrock S 1992 Structure function approach to vector boson scattering in p p collisions *Phys. Rev. Lett.* **69** 3274–3277 (*Preprint* hep-ph/9206246)
[453] Figy T, Oleari C and Zeppenfeld D 2003 Next-to-leading order jet distributions for Higgs boson production via weak-boson fusion *Phys. Rev.* D **68** 073005 (*Preprint* hep-ph/0306109)
[454] Glashow S, Nanopoulos D and Yildiz A 1978 Associated production of Higgs bosons and Z particles *Phys. Rev.* D **18** 1724–1727
[455] Kunszt Z, Trocsanyi Z and Stirling W J 1991 Clear signal of intermediate mass Higgs boson production at LHC and SSC *Phys. Lett.* B **271** 247–255
[456] Han T and Willenbrock S 1991 QCD correction to the p p → W H and Z H total cross- sections *Phys. Lett.* B **273** 167–172
[457] Brein O, Djouadi A and Harlander R 2004 NNLO QCD corrections to the Higgs-strahlung processes at hadron colliders *Phys. Lett.* B **579** 149–156 (*Preprint* hep-ph/0307206)
[458] Ciccolini M L, Dittmaier S and Kramer M 2003 Electroweak radiative corrections to associated W H and Z H production at hadron colliders *Phys. Rev.* D **68** 073003 (*Preprint* hep-ph/0306234)
[459] Raitio R and Wada W W 1979 Higgs Boson production at large transverse momentum in QCD *Phys. Rev.* D **19** 941
[460] Ng J N and Zakarauskas P 1984 A QCD Parton calculation of conjoined production of Higgs Bosons and heavy flavors in p anti-p collision *Phys. Rev.* D **29** 876
[461] Kunszt Z 1984 Associated production of heavy Higgs boson with top quarks *Nucl. Phys.* B **247** 339
[462] Gunion J F 1991 Associated top anti-top Higgs production as a large source of W H events: Implications for Higgs detection in the lepton neutrino gamma gamma final state *Phys. Lett.* B **261** 510–517
[463] Marciano W J and Paige F E 1991 Associated production of Higgs bosons with t anti-t pairs *Phys. Rev. Lett.* **66** 2433–2435
[464] Beenakker W, Dittmaier S, Kraemer M, Pluemper B, Spira M and Zerwas P 2001 Higgs radiation off top quarks at the Tevatron and the LHC *Phys. Rev. Lett.* **87** 201805 (*Preprint* hep-ph/0107081)
[465] Dawson S, Orr L H, Reina L and Wackeroth D 2003 Associated top quark Higgs boson production at the LHC *Phys. Rev.* D **67** 071503 (*Preprint* hep-ph/0211438)
[466] Dawson S and Reina L 1998 QCD corrections to associated Higgs boson production *Phys. Rev.* D **57** 5851–5859 (*Preprint* hep-ph/9712400)
[467] Futyan D, Fortin D and Giordano D 2006 Search for the Standard Model Higgs Boson in the Two-Electron and Two-Muon Final State with CMS *CMS Note* 2006/136
[468] Bartalini P *et al* 2006 NLO vs. LO: kinematical differences for signal and background in the $H \to ZZ^{(*)} \to 4\mu$ analysis *CMS Note* 2006/130
[469] Baffioni S *et al* 2006 Discovery potential for the SM Higgs boson in the $H \to ZZ^{(*)} \to e^+e^-e^+e^-$ decay channel *CMS Note* 2006/115
[470] Dittmar M and Dreiner H K 1997 How to find a Higgs boson with a mass between 155-GeV to 180-GeV at the LHC *Phys. Rev.* D **55** 167–172 (*Preprint* hep-ph/9608317)
[471] Davatz G, Dittmar M and Giolo-Nicollerat A-S 2006 Standard Model Higgs Discovery Potential of CMS in H→WW→ $\ell\nu\ell\nu$ Channel *CMS Note* 2006/047
[472] Davatz G, Dissertori G, Dittmar M, Grazzini M and Pauss F 2004 Effective K-factors for $gg \to H \to WW \to \ell\nu\ell\nu$ at the LHC *J. High. Energy Phys.* JHEP05(2004)009 (*Preprint* hep-ph/0402218)
[473] Campbell J and Tramontano F 2005 Next-to-leading order corrections to W t production and decay *Nucl. Phys.* B **726** 109–130 (*Preprint* hep-ph/0506289)
[474] CMS Collaboration, Beaudette F *et al* 2006 Search for a Light Standard Model Higgs Boson in the $H \to WW^{(*)} \to e^+\nu e^-\bar{\nu}$ Channel *CMS Note* 2006/114

[475] Plehn T, Rainwater D L and Zeppenfeld D 2000 A method for identifying $H \to \tau\tau \to e^{\pm}\mu^{\mp}_{P_{\mathrm{T}}}$ at the CERN LHC *Phys. Rev.* D **61** 093005 (doi:10.1103/PhysRevD.61.093005)

[476] Rainwater D L, Zeppenfeld D and Hagiwara K 1999 Searching for $H \to \tau\tau$ in weak boson fusion at the LHC *Phys. Rev.* D **59** 014037 (doi:10.1103/PhysRevD.59.014037)

[477] Cavalli D *et al* 2002 The Higgs working group: Summary report *Preprint* hep-ph/0203056

[478] Zeppenfeld D, Kinnunen R, Nikitenko A and Richter-Was E 2000 Measuring Higgs boson couplings at the LHC *Phys. Rev.* D **62** 013009 (*Preprint* hep-ph/0002036)

[479] Duhrssen M *et al* 2004 Extracting Higgs boson couplings from LHC data *Phys. Rev.* D **70** 113009 (*Preprint* hep-ph/0406323)

[480] Plehn T, Rainwater D L and Zeppenfeld D 1999 Probing the MSSM Higgs sector via weak boson fusion at the LHC *Phys. Lett.* B **454** 297–303 (*Preprint* hep-ph/9902434)

[481] Foudas C, Nikitenko A and Takahashi M 2006 Observation of the Standard Model Higgs boson via H$\to \tau\tau \to$ lepton+jet Channel *CMS Note* 2006/088

[482] Pi H, Avery P, Rohlf J, Tully C and Kunori S 2006 Search for Standard Model Higgs Boson via Vector Boson Fusion in the H$\to$W^{+}W^{-} to $\ell^{\pm}\nu$jj with $120 < \mathrm{m_H} < 250\,\mathrm{GeV}/c^2$ *CMS Note* 2006/092

[483] Dubinin M, Litvin V, Ma Y, Newman H and Pieri M 2006 Vector Boson Fusion Production with H$\to \gamma\gamma$ *CMS Note* 2006/097

[484] Delaere C 2006 Study of associated WH production with H$\to$WW* in the 3 leptons final state *CMS Note* 2006/053

[485] CDF Collaboration, Acosta D *et al* 2005 Measurement of the ttbar Production Cross Section in ppbar Collisions at sqrt(s) = 1.96 TeV using Lepton + Jets Events with Secondary Vertex b-tagging *Phys. Rev.* D **71** 052003

[486] Djouadi A and Ferrag S 2003 PDF Uncertainties In Higgs Production At Hadron Colliders *Preprint* hep-ph/0310209

[487] Higgs Working Group Collaboration, Assamagan K *et al* 2004 The Higgs working group: Summary report 2003 *Preprint* hep-ph/0406152

[488] Belanger G, Boudjema F and Sridhar K 2000 SUSY Higgs at the LHC: Large stop mixing effects and associated production *Nucl. Phys.* B **568** 3–39 (*Preprint* hep-ph/9904348)

[489] Dubinin M, Ilyin V and Savrin V 1997 Light Higgs Boson Signal at LHC in the reaction pp $\to \gamma\gamma$+jet and pp $\to \gamma\gamma$+lepton *CMS Note* 1997/101

[490] Kinnunen R and Denegri D 1997 Expected SM/SUSY Higgs Observability in CMS *CMS Note* 1997/057

[491] ATLAS Collaboration, 1999 ATLAS Detector and Physics Performance. Technical Design Report. Vol. 2 *CERN/LHCC, CERN-LHCC* -99-15

[492] Beauchemin P, Azuelos G and Burgess C 2004 Dimensionless coupling of bulk scalars at the LHC *J. Phys.* **G30** N17 (doi:10.1088/0954-3899/30/10/N01)

[493] Stelzer T and Long W F 1994 Automatic generation of tree level helicity amplitudes *Comput. Phys. Commun.* **81** 357–371 (doi:10.1016/0010-4655(94)90084-1)

[494] Murayama H, Watanabe I and Hagiwara K HELAS: HELicity amplitude subroutines for Feynman diagram evaluations KEK-91-11

[495] Mangano M, Moretti M and Pittau R 2002 Multijet matrix elements and shower evolution in hadronic collisions: $Wb\bar{b}+n$-jets as a case study *Nucl. Phys.* B **632** 343–362 (*Preprint* hep-ph/0108069) (doi:10.1016/S0550-3213(02)00249-3)

[496] Caravaglios F, Mangano M, Moretti M and Pittau R 1999 A new approach to multi-jet calculations in hadron collisions *Nucl. Phys.* B **539** 215–232 (*Preprint* hep-ph/9807570)

[497] Buttar C *et al* Les Houches physics at TeV colliders 2005, standard model, QCD, EW, and Higgs working group: Summary report 2006 *Preprint* hep-ph/0604120

[498] Bityukov S, Erofeeva S, Krasnikov N and Nikitenko A 2005 Program for evaluation of significance, confidence intervals and limits by direct calculation of probabilities *Proceedings of PhyStat 2005*

[499] Lethuillier M *et al* 2006 Search for a neutral Higgs boson with WH / ZH, H$\to \gamma\gamma$ channel *CMS Note* 2006/110

[500] Ravat O 2004 Etude du Calorimètre électromagnétique de l'expérience CMS et recherche de bosons de Higgs neutres dans le canal de production associée PhD Thesis, IPN, Lyon, 2004. LYCEN-T2004-29

[501] Graham D J 1995 An algorithm using tracks to locate the two photon vertex at high luminosity *CMS TN* 1995/115

[502] Djouadi A 1998 Squark effects on Higgs boson production and decay at the LHC *Phys. Lett.* B **435** 101–108 (*Preprint* hep-ph/9806315)

[503] Eynard G 1998 Study of associated Higgs boson production HW, Ht$\bar{\mathrm{t}}$, HZ $\to \gamma\gamma + \mathrm{e}^{\pm}/\mu^{\pm} + \mathrm{X}$ with the ATLAS detector at LHC. (In French) PhD Thesis, Annecy, *CERN-THESIS* -2000-036

[504] Beauchemin P-H and Azuelos G 2004 Search for the Standard Model Higgs Boson in the $\gamma\gamma + E_{\mathrm{T}}^{miss}$ channel *ATL-PHYS-2004-028*
[505] Lethuillier M, Agram J-L, Baty C, Gascon-Shotkin S, Perries S and Ravat O 2006 Search for a Neutral Higgs Boson with WH/ZH, H→ $\gamma\gamma$ Channel *CMS Note* 2006/110
[506] CMS Collaboration 2000 The TriDAS Project Technical Design Report, Volume 1: The Trigger Systems *CERN/LHCC*, 2000-38, CMS TDR 6.1
[507] CMS Collaboration, Acosta D *et al* 2006 CMS Physics Technical Design Report, Volume 1, Section 10.3.2: Photon isolation *CERN/LHCC*, 2006-001 p 376
[508] Read A L 2002 Presentation of search results: The CL(s) technique *J. Phys.* G **28** 2693–2704
[509] Junk T 1999 Confidence level computation for combining searches with small statistics *Nucl. Instrum. Meth.* A **434** 435–443 (*Preprint* hep-ex/9902006)
[510] Djouadi A and Ferrag S 2004 PDF uncertainties in Higgs production at hadron colliders *Phys. Lett.* B **586** 345–352 (*Preprint* hep-ph/0310209)
[511] Dell'Aquila J R and Nelson C A 1986 Simple tests for CP or P violation by sequential decays: V_1V_2 modes with decays into $\bar{\ell}_A\ell_B$ and/or $\bar{q}_Aq_B$ *Phys. Rev.* D **33** 101 (doi:10.1103/PhysRevD.33.101)
[512] Skjold A and Osland P 1994 Signals of CP violation in Higgs decay *Phys. Lett.* B **329** 305–311 (*Preprint* hep-ph/9402358)
[513] Choi S Y, Miller D J, Muhlleitner M M and Zerwas P M 2003 Identifying the Higgs spin and parity in decays to Z pairs *Phys. Lett.* B **553** 61–71 (*Preprint* hep-ph/0210077)
[514] Buszello C P, Fleck I, Marquard P and van der Bij J J 2004 Prospective analysis of spin- and CP-sensitive variables in H → ZZ → l(1)+ l(1)- l(2)+ l(2)- at the LHC *Eur. Phys. J.* C **32** 209–219 (*Preprint* hep-ph/0212396)
[515] Bluj M 2006 A Study of Angular Correlations in H→ZZ→2e2μ *CMS Note* 2006/094
[516] Wess J and Zumino B 1974 Supergauge transformations in four-dimensions *Nucl. Phys.* B **70** 39–50
[517] Fayet P and Ferrara S 1977 Supersymmetry *Phys. Rept.* **32** 249–334
[518] Nilles H P 1984 Supersymmetry, supergravity and particle physics *Phys. Rept.* **110** 1
[519] Barbieri R 1988 Looking beyond the standard model: the supersymmetric option *Riv. Nuovo Cim.* **11N4** 1–45
[520] Haber H E and Kane G L 1985 The search for supersymmetry: probing physics beyond the standard model *Phys. Rept.* **117** 75
[521] Witten E 1981 Mass hierarchies in supersymmetric theories *Phys. Lett.* B **105** 267
[522] Dimopoulos S, Raby S and Wilczek F 1981 Supersymmetry and the scale of unification *Phys. Rev.* D **24** 1681–1683
[523] Ibanez L E and Ross G G 1981 Low-energy predictions in supersymmetric grand unified theories *Phys. Lett.* B **105** 439
[524] Ibanez L E and Ross G G 1982 $SU(2)_L \times U(1)$ Symmetry breaking as a radiative effect of supersymmetry breaking in GUTs *Phys. Lett.* B **110** 215–220 (doi:10.1016/0370-2693(82)91239-4)
[525] Inoue K, Kakuto A, Komatsu H and Takeshita S 1982 Aspects of grand unified models with softly broken supersymmetry *Prog. Theor. Phys.* **68** 927
[526] Alvarez-Gaume L, Claudson M and Wise M B 1982 Low-energy supersymmetry *Nucl. Phys.* B **207** 96
[527] Ellis J R, Nanopoulos D V and Tamvakis K 1983 Grand unification in simple supergravity *Phys. Lett.* B **121** 123
[528] Dimopoulos S and Georgi H 1981 Softly broken supersymmetry and SU(5) *Nucl. Phys.* B **193** 150
[529] Sakai N 1981 Naturalness in supersymmetric 'GUTS' *Zeit. Phys.* C **11** 153
[530] Okada Y, Yamaguchi M and Yanagida T 1991 Upper bound of the lightest Higgs boson mass in the minimal supersymmetric standard model *Prog. Theor. Phys.* **85** 1–6
[531] Haber H E and Hempfling R 1991 Can the mass of the lightest Higgs boson of the minimal supersymmetric model be larger than m(Z)? *Phys. Rev. Lett.* **66** 1815–1818
[532] Ellis J R, Ridolfi G and Zwirner F 1991 Radiative corrections to the masses of supersymmetric Higgs bosons *Phys. Lett.* B **257** 83–91
[533] Barbieri R, Frigeni M and Caravaglios F 1991 The supersymmetric Higgs for heavy superpartners *Phys. Lett.* B **258** 167–170
[534] Yamada A 1991 Radiative corrections to the Higgs masses in the minimal supersymmetric standard model *Phys. Lett.* B **263** 233–238
[535] Brignole A, Ellis J R, Ridolfi G and Zwirner F 1991 The supersymmetric charged Higgs boson mass and LEP phenomenology *Phys. Lett.* B **271** 123–132
[536] Chankowski P H, Pokorski S and Rosiek J 1992 Charged and neutral supersymmetric Higgs boson masses: Complete one loop analysis *Phys. Lett.* B **274** 191–198

[537] Espinosa J R and Quiros M 1991 Two loop radiative corrections to the mass of the lightest Higgs boson in supersymmetric standard models *Phys. Lett.* B **266** 389–396
[538] Hempfling R and Hoang A H 1994 Two loop radiative corrections to the upper limit of the lightest Higgs boson mass in the minimal supersymmetric model *Phys. Lett.* B **331** 99–106 (*Preprint* hep-ph/9401219)
[539] Casas J A, Espinosa J R, Quiros M and Riotto A 1995 The lightest Higgs boson mass in the minimal supersymmetric standard model *Nucl. Phys.* B **436** 3–29 (*Preprint* hep-ph/9407389)
[540] Carena M, Espinosa J R, Quiros M and Wagner C 1995 Analytical expressions for radiatively corrected Higgs masses and couplings in the MSSM *Phys. Lett.* B **355** 209–221 (*Preprint* hep-ph/9504316)
[541] Carena M, Quiros M and Wagner C E M 1996 Effective potential methods and the Higgs mass spectrum in the MSSM *Nucl. Phys.* B **461** 407–36 (*Preprint* hep-ph/9508343)
[542] Heinemeyer S, Hollik W and Weiglein G 1998 QCD corrections to the masses of the neutral CP-even Higgs bosons in the MSSM *Phys. Rev.* D **58** 091701 (*Preprint* hep-ph/9803277)
[543] Heinemeyer S, Hollik W and Weiglein G 1998 Precise prediction for the mass of the lightest Higgs boson in the MSSM *Phys. Lett.* B **440** 296–304 (*Preprint* hep-ph/9807423)
[544] Heinemeyer S, Hollik W and Weiglein G 2000 Constraints on tan(beta) in the MSSM from the upper bound on the mass of the lightest Higgs boson *J. High. Energy Phys.* JHEP06(2000)009 (*Preprint* hep-ph/9909540)
[545] Espinosa J R and Zhang R-J 2000 Complete two-loop dominant corrections to the mass of the lightest CP-even Higgs boson in the minimal supersymmetric standard model *Nucl. Phys.* B **586** 3–38 (*Preprint* hep-ph/0003246)
[546] Brignole A, Degrassi G, Slavich P and Zwirner F 2002 On the $\mathcal{O}(\alpha_t^2)$ two-loop corrections to the neutral Higgs boson masses in the MSSM *Nucl. Phys.* B **631** 195–218 (doi:10.1016/S0550-3213(02)00184-0)
[547] Brignole A, Degrassi G, Slavich P and Zwirner F 2002 On the two-loop sbottom corrections to the neutral Higgs boson masses in the MSSM *Nucl. Phys.* B **643** 79–92 (*Preprint* hep-ph/0206101)
[548] Heinemeyer S, Hollik W, Rzehak H and Weiglein G 2005 High-precision predictions for the MSSM Higgs sector at $\mathcal{O}(\alpha_b\alpha_s)$ *Eur. Phys. J.* C **39** 465–481 (doi:10.1140/epjc/s2005-02112-6)
[549] Coarasa J A, Jimenez R A and Sola J 1996 Strong effects on the hadronic widths of the neutral Higgs Bosons in the MSSM *Phys. Lett.* B **389** 312–320 (*Preprint* hep-ph/9511402)
[550] Chankowski P H, Pokorski S and Rosiek J 1994 Complete on-shell renormalization scheme for the minimal supersymmetric Higgs sector *Nucl. Phys.* B **423** 437–496 (*Preprint* hep-ph/9303309)
[551] Dabelstein A 1995 The One loop renormalization of the MSSM Higgs sector and its application to the neutral scalar Higgs masses *Z. Phys.* C **67** 495–512 (*Preprint* hep-ph/9409375)
[552] Brignole A 1992 Radiative corrections to the supersymmetric neutral Higgs boson masses *Phys. Lett.* B **281** 284–294
[553] Haber H E, Hempfling R and Hoang A H 1997 Approximating the radiatively corrected Higgs mass in the minimal supersymmetric model *Z. Phys.* C **75** 539–554 (*Preprint* hep-ph/9609331)
[554] Zhang R-J 1999 Two-loop effective potential calculation of the lightest CP-even Higgs-boson mass in the MSSM *Phys. Lett.* B **447** 89–97 (*Preprint* hep-ph/9808299)
[555] Espinosa J R and Zhang R-J 2000 MSSM lightest CP-even Higgs boson mass to O(alpha(s) alpha(t)): The effective potential approach *J. High. Energy Phys.* JHEP03(2000)026 (*Preprint* hep-ph/9912236)
[556] Degrassi G, Slavich P and Zwirner F 2001 On the neutral Higgs boson masses in the MSSM for arbitrary stop mixing *Nucl. Phys.* B **611** 403–422 (*Preprint* hep-ph/0105096)
[557] Hempfling R 1994 Yukawa coupling unification with supersymmetric threshold corrections *Phys. Rev.* D **49** 6168–6172
[558] Hall L J, Rattazzi R and Sarid U 1994 The Top quark mass in supersymmetric SO(10) unification *Phys. Rev.* D **50** 7048–7065 (*Preprint* hep-ph/9306309)
[559] Carena M, Olechowski M, Pokorski S and Wagner C 1994 Electroweak symmetry breaking and bottom-top Yukawa unification *Nucl. Phys.* B **426** 269–300 (*Preprint* hep-ph/9402253)
[560] Guasch J, Hafliger P and Spira M 2003 MSSM Higgs decays to bottom quark pairs revisited *Phys. Rev.* D **68** 115001 (*Preprint* hep-ph/0305101)
[561] Dedes A, Degrassi G and Slavich P 2003 On the two-loop Yukawa corrections to the MSSM Higgs boson masses at large tan(beta) *Nucl. Phys.* B **672** 144–162 (*Preprint* hep-ph/0305127)
[562] Eberl H, Hidaka K, Kraml S, Majerotto W and Yamada Y 2000 Improved SUSY QCD corrections to Higgs boson decays into quarks and squarks *Phys. Rev.* D **62** 055006 (*Preprint* hep-ph/9912463)
[563] Carena M, Garcia D, Nierste U and Wagner C 2000 Effective Lagrangian for the $\bar{t}bH^+$ interaction in the MSSM and charged Higgs phenomenology *Nucl. Phys.* B **577** 88–120 (doi:0.1016/S0550-3213(00)00146-2)

[564] Heinemeyer S, Hollik W and Weiglein G 2006 Electroweak precision observables in the minimal supersymmetric standard model *Phys. Rept.* **425** 265–368 (*Preprint* hep-ph/0412214)
[565] Carena M and Haber H E 2003 Higgs boson theory and phenomenology. ((V)) *Prog. Part. Nucl. Phys.* **50** 63–152 (*Preprint* hep-ph/0208209)
[566] ALEPH, DELPHI, L3, OPAL Collaboration 2006 LEP Working Group for Higgs Boson Searches, Search for neutral MSSM Higgs bosons at LEP *Preprint* hep-ex/0602042
[567] LEP Higgs Working Group for Higgs boson searches Collaboration 2001 Search for charged Higgs bosons: Preliminary combined results using LEP data collected at energies up to 209 GeV *Preprint* hep-ex/0107031
[568] Dabelstein A 1995 Fermionic decays of neutral MSSM Higgs bosons at the one loop level *Nucl. Phys.* B **456** 25–56 (*Preprint* hep-ph/9503443)
[569] Heinemeyer S, Hollik W and Weiglein G 2000 Decay widths of the neutral CP-even MSSM Higgs bosons in the Feynman-diagrammatic approach *Eur. Phys. J.* C **16** 139–153 (*Preprint* hep-ph/0003022)
[570] Djouadi A, Janot P, Kalinowski J and Zerwas P M 1996 SUSY Decays of Higgs Particles *Phys. Lett.* B **376** 220–226 (*Preprint* hep-ph/9603368)
[571] Djouadi A, Kalinowski J, Ohmann P and Zerwas P M 1997 Heavy SUSY Higgs bosons at e+ e- linear colliders *Z. Phys.* C **74** 93–111 (*Preprint* hep-ph/9605339)
[572] Dawson S, Djouadi A and Spira M 1996 QCD Corrections to SUSY Higgs Production: The Role of Squark Loops *Phys. Rev. Lett.* **77** 16–19 (*Preprint* hep-ph/9603423)
[573] Harlander R V and Steinhauser M 2003 Hadronic Higgs production and decay in supersymmetry at next-to-leading order *Phys. Lett.* B **574** 258–268 (*Preprint* hep-ph/0307346)
[574] Harlander R and Steinhauser M 2003 Effects of SUSY-QCD in hadronic Higgs production at next-to-next-to-leading order *Phys. Rev.* D **68** 111701 (*Preprint* hep-ph/0308210)
[575] Harlander R V and Steinhauser M 2004 Supersymmetric Higgs production in gluon fusion at next-to-leading order *J. High. Energy Phys.* JHEP09(2004)066 (*Preprint* hep-ph/0409010)
[576] Harlander R V and Hofmann F 2005 Pseudo-scalar Higgs production at next-to-leading order SUSY-QCD *Preprint* hep-ph/0507041
[577] Langenegger U, Spira M, Starodumov A and Trueb P 2006 SM and MSSM Higgs boson production: spectra at large transverse momentum *Preprint* hep-ph/0604156
[578] Djouadi A and Spira M 2000 SUSY-QCD corrections to Higgs boson production at hadron colliders *Phys. Rev.* D **62** 014004 (*Preprint* hep-ph/9912476)
[579] Wu P *et al* 2005 NLO supersymmetric QCD corrections to t anti-t h0 associated production at hadron colliders *Preprint* hep-ph/0505086
[580] Dittmaier S, Kramer M and Spira M 2004 Higgs radiation off bottom quarks at the Tevatron and the LHC *Phys. Rev.* D **70** 074010 (*Preprint* hep-ph/0309204)
[581] Dawson S, Jackson C B, Reina L and Wackeroth D 2004 Exclusive Higgs boson production with bottom quarks at hadron colliders *Phys. Rev.* D **69** 074027 (*Preprint* hep-ph/0311067)
[582] Dicus D A and Willenbrock S 1989 Higgs boson production from heavy quark fusion *Phys. Rev.* D **39** 751
[583] Dicus D, Stelzer T, Sullivan Z and Willenbrock S 1999 Higgs boson production in association with bottom quarks at next-to-leading order *Phys. Rev.* D **59** 094016 (*Preprint* hep-ph/9811492)
[584] Balazs C, He H-J and Yuan C P 1999 QCD corrections to scalar production via heavy quark fusion at hadron colliders *Phys. Rev.* D **60** 114001 (*Preprint* hep-ph/9812263)
[585] Harlander R V and Kilgore W B 2003 Higgs boson production in bottom quark fusion at next-to-next-to-leading order *Phys. Rev.* D **68** 013001 (*Preprint* hep-ph/0304035)
[586] Aivazis M A G, Olness F I and Tung W-K 1994 Leptoproduction of heavy quarks. 1. General formalism and kinematics of charged current and neutral current production processes *Phys. Rev.* D **50** 3085–3101 (*Preprint* hep-ph/9312318)
[587] Aivazis M A G, Collins J C, Olness F I and Tung W-K 1994 Leptoproduction of heavy quarks. 2. A unified QCD formulation of charged and neutral current processes from fixed target to collider energies *Phys. Rev.* D **50** 3102–3118 (*Preprint* hep-ph/9312319)
[588] Campbell J *et al* 2004 Higgs boson production in association with bottom quarks *Preprint* hep-ph/0405302 Contributed to 3rd Les Houches Workshop: Physics at TeV Colliders, Les Houches, France, 26 May–6 June 2003
[589] Campbell J, Ellis R K, Maltoni F and Willenbrock S 2003 Higgs boson production in association with a single bottom quark *Phys. Rev.* D **67** 095002 (*Preprint* hep-ph/0204093)
[590] Dawson S, Jackson C B, Reina L and Wackeroth D 2005 Higgs boson production with one bottom quark jet at hadron colliders *Phys. Rev. Lett.* **94** 031802 (doi:10.1103/PhysRevLett.94.031802)
[591] Bawa A C, Kim C S and Martin A D 1990 Charged Higgs production at hadron colliders *Z. Phys.* C **47** 75–82

[592] Borzumati F, Kneur J-L and Polonsky N 1999 Higgs-strahlung and R-parity violating slepton-strahlung at hadron colliders *Phys. Rev.* D **60** 115011 (*Preprint* hep-ph/9905443)
[593] Belyaev A, Garcia D, Guasch J and Sola J 2002 Prospects for heavy supersymmetric charged Higgs boson searches at hadron colliders *J. High. Energy Phys.* JHEP06(2002)059 (*Preprint* hep-ph/0203031)
[594] Wu P *et al* 2006 NLO supersymmetric QCD corrections to the t anti-b H-associated production at hadron colliders *Phys. Rev.* D **73** 015012 (*Preprint* hep-ph/0601069) (doi:10.1103/PhysRevD.73.015012)
[595] Zhu S-H 2003 Complete next-to-leading order QCD corrections to charged Higgs boson associated production with top quark at the CERN large hadron collider *Phys. Rev.* D **67** 075006 (doi:10.1103/PhysRevD.67.075006)
[596] Plehn T Charged Higgs boson production in bottom-gluon fusion Prepared for 10th International Conference on Supersymmetry and Unification of Fundamental Interactions (SUSY02), Hamburg, Germany, 17–23 June 2002
[597] Berger E L, Han T, Jiang J and Plehn T 2005 Associated production of a top quark and a charged Higgs boson *Phys. Rev.* D **71** 115012 (*Preprint* hep-ph/0312286)
[598] Gao G, Lu G, Xiong Z and Yang J M 2002 Loop effects and non-decoupling property of SUSY QCD in $gb \to t H^-$ *Phys. Rev.* D **66** 015007 (doi:10.1103/PhysRevD.66.015007)
[599] Willenbrock S S D 1987 Pair production of supersymmetric charged Higgs bosons *Phys. Rev.* D **35** 173
[600] Krause A, Plehn T, Spira M and Zerwas P M 1998 Production of charged Higgs boson pairs in gluon–gluon collisions *Nucl. Phys.* B **519** 85–100 (*Preprint* hep-ph/9707430)
[601] Jiang Y, Han L, Ma W-G, Yu Z-H and Han M 1997 Pair production of charged Higgs bosons in gluon–gluon collisions *J. Phys.* **G23** 385–400 (*Preprint* hep-ph/9703275)
[602] Brein O and Hollik W 2000 Pair production of charged MSSM Higgs bosons by gluon fusion *Eur. Phys. J.* C **13** 175–184 (*Preprint* hep-ph/9908529)
[603] Barrientos Bendezu A A and Kniehl B A 2000 H^+H^- pair production at the large hadron collider *Nucl. Phys.* B **568** 305–318 (doi:10.1016/S0550-3213(99)00732-4)
[604] Hou H-S *et al* 2005 Pair production of charged Higgs bosons from bottom-quark fusion *Phys. Rev.* D **71** 075014 (doi:10.1103/PhysRevD.71.075014)
[605] Barrientos Bendezu A A and Kniehl B A 1999 $W^\pm H^\mp$ associated production at the large hadron collider *Phys. Rev.* D **59** 015009 (*Preprint* hep-ph/9807480) (doi:10.1103/PhysRevD.59.015009)
[606] Brein O, Hollik W and Kanemura S 2001 The MSSM prediction for $W^\pm H^\mp$ production by gluon fusion *Phys. Rev.* D **63** 095001 (*Preprint* hep-ph/0008308)
[607] Barrientos Bendezu A A and Kniehl B A 2001 Squark loop correction to $W^\pm H^\mp$ associated hadroproduction *Phys. Rev.* D **63** 015009 (*Preprint* hep-ph/0007336)
[608] Dicus D, Hewett J, Kao C and Rizzo T G 1989 $W^\pm H^\mp$ production at hadron colliders *Phys. Rev.* D **40** 787
[609] Hollik W and Zhu S-h 2002 $\mathcal{O}(\alpha_s)$ corrections to $b\bar{b} \to W^\pm H^\mp$ at the CERN large hadron collider *Phys. Rev.* D **65** 075015 (*Preprint* hep-ph/0109103) (doi:10.1103/PhysRevD.65.075015)
[610] Zhao J, Li C S and Li Q 2005 SUSY-QCD corrections to $W^\pm H^\mp$ associated production at the CERN large hadron collider *Phys. Rev.* D **72** 114008 (*Preprint* hep-ph/0509369)
[611] Lehti S 2006 Study of H/A$\to \tau\tau \to e\mu$+X in CMS *CMS Note* 2006/101
[612] Lehti S 2002 Study of $gg \to b\bar{b}H_{SUSY}$, $H_{SUSY} \to \tau\tau \to \ell\ell + X$ *CMS Note* 2002/035
[613] Bloch D private communication
[614] Boos E, Djouadi A, Muhlleitner M and Vologdin A 2002 The MSSM Higgs bosons in the intense-coupling regime *Phys. Rev.* D **66** 055004 (*Preprint* hep-ph/0205160)
[615] Boos E, Djouadi A and Nikitenko A 2004 Detection of the neutral MSSM Higgs bosons in the intense-coupling regime at the LHC *Phys. Lett.* B **578** 384–393 (*Preprint* hep-ph/0307079)
[616] CMS Collaboration, Acosta D *et al* 2006 CMS Physics Technical Design Report, Volume 1, Section 12.2.3: Combined secondary vertex tag *CERN/LHCC*, 2006-001 p 466
[617] Fernandez J 2006 Search for MSSM heavy neutral Higgs bosons in the four-b final state *CMS Note* 2006/080
[618] CMS Collaboration, Acosta D *et al* 2006 CMS Physics Technical Design Report, Volume 1, Section 12.2.6: HLT b tag *CERN/LHCC*, 2006-001 p 474
[619] CMS Collaboration, Acosta D *et al* 2006 CMS Physics Technical Design Report, Volume 1, Section 11.6.4: Parton-level corrections *CERN/LHCC*, 2006-001 p 428
[620] DØ Collaboration, Abazov V M *et al* 2005 Search for neutral supersymmetric Higgs bosons in multijet events at $\sqrt{s}$ =1.96 TeV *Phys. Rev. Lett.* **95** 151801 (doi:10.1103/PhysRevLett.95.151801)
[621] Baarmand M, Hashemi M and Nikitenko A 2006 Light Charged Higgs Discovery Potential of CMS in the $H^+ \to \tau\nu$ with single lepton trigger *CMS Note* 2006/056
[622] Roy D 1999 The hadronic tau decay signature of a heavy charged Higgs boson at LHC *Phys. Lett.* B **459** 607–614 (*Preprint* hep-ph/9905542)

[623] Kinnunen R 2004 Study of $A/H \to \tau\tau$ and $H^{\pm} \to \tau\nu$ in CMS *Czech. J. Phys.* **54** A93–A101
[624] Assamagan K A and Coadou Y 2002 The hadronic tau decay of a heavy $H^{\pm}$ in ATLAS *Acta Phys. Polon.* B **33** 707–720
[625] Baarmand M, Hashemi M and Nikitenko A 2006 Search for the heavy charged MSSM Higgs bosons with the $H^{+} \to \tau\nu$ decay mode in fully hadronic final state *CMS Note* 2006/100
[626] Roy D P 2004 Looking for the charged Higgs boson *Mod. Phys. Lett.* A **19** 1813–1828 (*Preprint* hep-ph/0406102)
[627] Alwall J and Rathsman J 2004 Improved description of charged Higgs boson production at hadron colliders *J. High Energy Phys.* JHEP12(2004)050 (*Preprint* hep-ph/0409094)
[628] Plehn T 2003 Charged Higgs boson production in bottom gluon fusion *Phys. Rev.* D **67** 014018 (*Preprint* hep-ph/0206121)
[629] Lowette S, D'Hondt J and Vanlaer P 2006 Charged MSSM Higgs boson observability in the $H^{\pm} \to tb$ Decay *CMS Note* 2006/109
[630] CMS Collaboration, Anagnostou G and Daskalakis G 2006 Search for the MSSM A → Zh decay with Z → $\ell^{+}\ell^{-}$, h → bb *CMS Note* 2006/063
[631] CMS Collaboration, Charlot C, Salerno R and Sirois Y 2006 Observability of the heavy neutral SUSY Higgs Bosons decaying into neutralinos *CMS Note* 2006/125
[632] Allanach B C *et al* 2002 The snowmass points and slopes: benchmarks for SUSY searches *Eur. Phys. J.* C **25** 113–123 (*Preprint* hep-ph/0202233)
[633] Battaglia M *et al* 2004 Updated post-WMAP benchmarks for supersymmetry *Eur. Phys. J.* C **33** 273–296 (*Preprint* hep-ph/0306219)
[634] Carena M, Heinemeyer S, Wagner C and Weiglein G 1999 Suggestions for improved benchmark scenarios for Higgs-boson searches at LEP2 *Preprint* hep-ph/9912223
[635] Carena M, Heinemeyer S, Wagner C and Weiglein G 2003 Suggestions for benchmark scenarios for MSSM Higgs boson searches at hadron colliders *Eur. Phys. J.* C **26** 601–607 (*Preprint* hep-ph/0202167)
[636] ECFA/DESY LC Physics Working Group Collaboration, Aguilar-Saavedra J A *et al* 2001 TESLA Technical Design Report Part III: Physics at an e+e- Linear Collider *Preprint* hep-ph/0106315
[637] Bennett C L *et al* 2003 First year Wilkinson Microwave Anisotropy Probe (WMAP) observations: preliminary maps and basic results *Astrophys. J. Suppl.* **148** 1 (*Preprint* astro-ph/0302207)
[638] WMAP Collaboration, Spergel D N *et al* 2003 First year Wilkinson Microwave Anisotropy Probe (WMAP) observations: determination of cosmological parameters *Astrophys. J. Suppl.* **148** 175 (*Preprint* astro-ph/0302209)
[639] Goldberg H 1983 Constraint on the photino mass from cosmology *Phys. Rev. Lett.* **50** 1419
[640] Ellis J R, Hagelin J, Nanopoulos D, Olive K A and Srednicki M 1984 Supersymmetric relics from the big bang *Nucl. Phys.* B **238** 453–476
[641] Heavy Flavor Averaging Group Collaboration, Barberio E *et al* 2006 Averages of b-hadron properties at the end of 2005 *Preprint* hep-ex/0603003
[642] Asatrian H M, Hovhannisyan A, Poghosyan V, Greub C and Hurth T 2005 Towards the NNLL precision in anti-B→X/s gamma *Preprint* hep-ph/0512097
[643] Muon Collaboration, Bennett G W 2006 Final report of the muon E821 anomalous magnetic moment measurement at BNL *Preprint* hep-ex/0602035
[644] Czarnecki A and Marciano W J 2001 The muon anomalous magnetic moment: A harbinger for 'new physics' *Phys. Rev.* D **64** 013014 (*Preprint* hep-ph/0102122)
[645] Carena M *et al* 2000 Reconciling the two-loop diagrammatic and effective field theory computations of the mass of the lightest CP-even Higgs boson in the MSSM *Nucl. Phys.* B **580** 29–57 (*Preprint* hep-ph/0001002)
[646] Randall L and Sundrum R 1999 An alternative to compactification *Phys. Rev. Lett.* **83** 4690–4693 (doi:10.1103/PhysRevLett.83.4690)
[647] Giudice G F, Rattazzi R and Wells J D 2001 Graviscalars from higher-dimensional metrics and curvature- Higgs mixing *Nucl. Phys.* B **595** 250–276 (*Preprint* hep-ph/0002178)
[648] Chaichian M, Datta A, Huitu K and Yu Z-h 2002 Radion and Higgs mixing at the LHC *Phys. Lett.* B **524** 161–169 (*Preprint* hep-ph/0110035)
[649] Hewett J L and Rizzo T G 2003 Shifts in the properties of the Higgs boson from radion mixing *J. High. Energy Phys.* JHEP08(2003)028 (*Preprint* hep-ph/0202155)
[650] Dominici D, Grzadkowski B, Gunion J F and Toharia M 2003 The scalar sector of the Randall-Sundrum model *Nucl. Phys.* B **671** 243–292 (*Preprint* hep-ph/0206192)
[651] Battaglia M, De Curtis S, De Roeck A, Dominici D and Gunion J F 2003 On the complementarity of Higgs and radion searches at LHC *Phys. Lett.* B **568** 92–102 (*Preprint* hep-ph/0304245)

[652] Azuelos G, Cavalli D, Przysiezniak H and Vacavant L 2002 Search for the radion using the ATLAS detector *Eur. Phys. J. direct* C **4** 16
[653] Dominici D, Dewhirst G, Nikitenko A, Gennai S and Fanò L 2005 Search for radion decays into Higgs boson pairs in the $\gamma\gamma b\bar{b}$, $\tau\tau b\bar{b}$ and $b\bar{b}b\bar{b}$ final states *CMS Note* 2005/007
[654] Arkani-Hamed N, Cohen A G and Georgi H 2001 (De)constructing dimensions *Phys. Rev. Lett.* **86** 4757–4761 (*Preprint* hep-th/0104005)
[655] Cheng H-C, Hill C T, Pokorski S and Wang J 2001 The standard model in the latticized bulk *Phys. Rev.* D **64** 065007 (*Preprint* hep-th/0104179)
[656] Arkani-Hamed N, Cohen A G and Georgi H 2001 Electroweak symmetry breaking from dimensional deconstruction *Phys. Lett.* B **513** 232–240 (*Preprint* hep-ph/0105239)
[657] Arkani-Hamed N, Cohen A G, Katz E and Nelson A E 2002 The littlest Higgs *J. High Energy Phys.* JHEP07(2002)034 (*Preprint* hep-ph/0206021)
[658] Schechter J and Valle J 1980 Neutrino masses in $SU(2) \times U(1)$ Theories *Phys. Rev.* D **22** 2227 (doi:10.1103/PhysRevD.22.2227)
[659] Ma E and Sarkar U 1998 Neutrino masses and leptogenesis with heavy Higgs triplets *Phys. Rev. Lett.* **80** 5716–5719 (*Preprint* hep-ph/9802445)
[660] Ma E, Raidal M and Sarkar U 2000 Verifiable model of neutrino masses from large extra dimensions *Phys. Rev. Lett.* **85** 3769–3772 (*Preprint* hep-ph/0006046)
[661] Ma E, Raidal M and Sarkar U 2001 Phenomenology of the neutrino-mass-giving Higgs triplet and the low-energy seesaw violation of lepton number *Nucl. Phys.* B **615** 313–330 (*Preprint* hep-ph/0012101)
[662] Ma E and Sarkar U 2006 Connecting dark energy to neutrinos with an observable Higgs triplet *Preprint* hep-ph/0602116
[663] Marandella G, Schappacher C and Strumia A 2005 Little-Higgs corrections to precision data after LEP2 *Phys. Rev.* D **72** 035014 (*Preprint* hep-ph/0502096)
[664] Huitu K, Maalampi J, Pietila A and Raidal M 1997 Doubly charged Higgs at LHC *Nucl. Phys.* B **487** 27–42 (*Preprint* hep-ph/9606311)
[665] Han T, Logan H E and Wang L-T 2005 Smoking-gun signatures of little Higgs models *Preprint* hep-ph/0506313
[666] Azuelos G *et al* 2005 Exploring little Higgs models with ATLAS at the LHC *Eur. Phys. J.* C **39S2** 13–24 (*Preprint* hep-ph/0402037)
[667] Gunion J F, Grifols J, Mendez A, Kayser B and Olness F I 1989 Higgs bosons in left-right symmetric models *Phys. Rev.* D **40** 1546 (doi:10.1103/PhysRevD.40.1546)
[668] Muhlleitner M and Spira M 2003 A note on doubly-charged Higgs pair production at hadron colliders *Phys. Rev.* D **68** 117701 (*Preprint* hep-ph/0305288)
[669] Bityukov S, Krasnikov N and Taperechkina V 2001 Confidence intervals for Poisson distribution parameter *Preprint* hep-ex/0108020
[670] Martin S P 1997 A supersymmetry primer *Perspectives in Supersymmetry* ed G. Kane (World Scientific) *Preprint* hep-ph/9709356
[671] CMS Collaboration Abdullin S *et al* 2002 Discovery potential for supersymmetry in CMS *J. Phys.* G **28** 469 (doi:10.1088/0954-3899/28/3/401)
[672] Paige F E, Protopopescu S D, Baer H and Tata X 2003 ISAJET 7.69: A Monte Carlo Event Generator for pp, $\bar{p}p$, and e^+e^- Reactions (*Preprint* hep-ph/0312045)
[673] De Roeck A *et al* 2005 Supersymmetric benchmarks with non-universal scalar masses or gravitino dark matter *Preprint* hep-ph/0508198
[674] de Boer W *et al* 2004 Excess of EGRET galactic gamma ray data interpreted as dark matter annihilation *Preprint* astro-ph/0408272
[675] Acosta D *et al* 2006 Potential to Discover SUSY in Events with Muons Jets and Large Missing Transverse Energy in pp Collisions at $\sqrt{s} = 14$ TeV *CMS Note* 2006/134
[676] Acosta D *et al* 2006 CMS Discovery Potential for mSUGRA in Same Sign Di-muon Events with Jets and Large Missing Transverse Energy in pp collisions at $\sqrt{s} = 14$ TeV*CMS Note*
[677] Chiorboli M, Galanti M and Tricomi A 2006 Leptons + Jets + Missing Energy analysis at LM1 *CMS Note* 2006/133
[678] Mangeol D and Goerlach U 2006 Search for $\tilde{\tau}$ production in di-tau final states and measurements of SUSY masses in mSUGRA cascade decays *CMS Note* 2006/096
[679] Bityukov S I 2005 Uncertainty, Systematics, Limits Available at http://cmsdoc.cern.ch/bityukov
[680] Kyriazopoulou S and Markou C 2006 Search for SUSY in Final States with Z Bosons *CMS Note* 2006/116
[681] Nikitenko A, Quast G and Ciulli V Minimal requirements for significance estimates of the physics resultInfo located at http://cmsdoc.cern.ch/ anikiten/cms-higgs/stat.txt

[682] Beenakker W, Hopker R and Spira M 1996 PROSPINO: A program for the PROduction of Supersymmetric Particles In Next-to-leading Order QCD *Preprint* hep-ph/9611232
[683] Allanach B C, Lester C G, Parker M A and Webber B R 2000 Measuring sparticle masses in non-universal string inspired models at the LHC *J. High. Energy Phys.* JHEP09(2000)004 (*Preprint* hep-ph/0007009)
[684] Beenakker W *et al* 1999 The production of charginos/neutralinos and sleptons at hadron colliders *Phys. Rev. Lett.* **83** 3780–3783 (doi:10.1103/PhysRevLett.83.3780)
[685] del Aguila F and Ametller L 1991 On the detectability of sleptons at large hadron colliders *Phys. Lett.* B **261** 326–333 (doi:10.1016/0370-2693(91)90336-O)
[686] Baer H, Chen C-h, Paige F and Tata X 1994 Detecting sleptons at hadron colliders and supercolliders *Phys. Rev.* D **49** 3283–3290 (*Preprint* hep-ph/9311248)
[687] Denegri D, Rurua L and Stepanov N 1996 Detection of Sleptons in CMS, Mass Reach *CMS TN* 96-059
[688] Andreev Y M, Bityukov S I and Krasnikov N V 2005 Sleptons at post-WMAP benchmark points at LHC(CMS) *Phys. Atom. Nucl.* **68** 340–347 (*Preprint* hep-ph/0402229)
[689] Bityukov S I and Krasnikov N V 1999 The search for sleptons and lepton-flavor-number violation at LHC (CMS) *Phys. Atom. Nucl.* **62** 1213–1225 (*Preprint* hep-ph/9712358)
[690] Krasnikov N 1994 Flavor lepton number violation at LEP-2 *Mod. Phys. Lett.* A **9** 791–794
[691] Arkani-Hamed N, Cheng H-C, Feng J L and Hall L J 1996 Probing lepton flavor violation at future colliders *Phys. Rev. Lett.* **77** 1937–1940 (*Preprint* hep-ph/9603431) (doi:10.1103/PhysRevLett.77.1937)
[692] Krasnikov N V 1997 Search for flavor lepton number violation in slepton decays at LHC *JETP Lett.* **65** 148 (doi:10.1134/1.567315)
[693] Agashe K and Graesser M 2000 Signals of supersymmetric lepton flavor violation at the LHC *Phys. Rev.* D **61** 075008 (*Preprint* hep-ph/9904422)
[694] Hisano J, Kitano R and Nojiri M M 2002 Flavor mixing in slepton production at the large hadron collider *Phys. Rev.* D **65** 116002
[695] Baer H, Chen C-h, Paige F and Tata X 1994 Trileptons from chargino - neutralino production at the CERN Large Hadron Collider *Phys. Rev.* D **50** 4508–4516 (*Preprint* hep-ph/9404212) (doi:10.1103/PhysRevD.50.4508)
[696] Ellis J R, Olive K A and Santoso Y 2002 The MSSM parameter space with non-universal Higgs masses *Phys. Lett.* B **539** 107–118 (*Preprint* hep-ph/0204192)
[697] Altarelli G, Mele B and Ruiz-Altaba M 1989 Searching for new heavy vector bosons in $p\bar{p}$ colliders *Z. Phys.* C **45** 109 (doi:10.1007/BF01556677)
[698] Arkani-Hamed N, Dimopoulos S and Dvali G R 1998 The hierarchy problem and new dimensions at a millimeter *Phys. Lett.* B **429** 263–272 (*Preprint* hep-ph/9803315)
[699] Lykken J D, Poppitz E and Trivedi S P 1999 Branes with GUTs and supersymmetry breaking *Nucl. Phys.* B **543** 105–121 (*Preprint* hep-th/9806080)
[700] Antoniadis I 1990 A possible new dimension at a few TeV *Phys. Lett.* B **246** 377–384 (doi:10.1016/0370-2693(90)90617-F)
[701] Lykken J D 1996 Weak scale superstrings *Phys. Rev.* D **54** 3693–3697 (*Preprint* hep-th/9603133) (doi:10.1103/PhysRevD.54.R3693)
[702] Giudice G F, Rattazzi R and Wells J D 1999 Quantum gravity and extra dimensions at high-energy colliders *Nucl. Phys.* B **544** 3–38 (*Preprint* hep-ph/9811291)
[703] Han T, Lykken J D and Zhang R-J 1999 On Kaluza-Klein states from large extra dimensions *Phys. Rev.* D **59** 105006 (*Preprint* hep-ph/9811350) (doi:10.1103/PhysRevD.59.105006)
[704] Cullen S, Perelstein M and Peskin M E 2000 TeV strings and collider probes of large extra dimensions *Phys. Rev.* D **62** 055012 (*Preprint* hep-ph/0001166)
[705] Lykken J D and Randall L 2000 The shape of gravity *J. High. Energy Phys.* JHEP06(2000)014 (*Preprint* hep-th/9908076)
[706] Vacavant L and Hinchliffe I 2001 Signals of models with large extra dimensions in ATLAS *J. Phys.* G **27** 1839–1850
[707] Ruppert J, Rahmede C and Bleicher M 2005 Determination of the fundamental scale of gravity and the number of space-time dimensions from high energetic particle interactions *Phys. Lett.* B **608** 240–243 (*Preprint* hep-ph/0501028)
[708] Dudas E and Mourad J 2000 String theory predictions for future accelerators *Nucl. Phys.* B **575** 3–34 (doi:10.1016/S0550-3213(00)00082-1)
[709] Chialva D, Iengo R and Russo J G 2005 Cross sections for production of closed superstrings at high energy colliders in brane world models *Phys. Rev.* D **71** 106009 (*Preprint* hep-ph/0503125)
[710] Bando M, Kugo T, Noguchi T and Yoshioka K 1999 Brane fluctuation and suppression of Kaluza-Klein mode couplings *Phys. Rev. Lett.* **83** 3601–3604 (doi:10.1103/PhysRevLett.83.3601)

[711] Hewett J L 1999 Indirect collider signals for extra dimensions *Phys. Rev. Lett.* **82** 4765–4768 (doi:10.1103/PhysRevLett.82.4765)
[712] Davoudiasl H, Hewett J L and Rizzo T G 2000 Phenomenology of the Randall-Sundrum gauge hierarchy model *Phys. Rev. Lett.* **84** 2080 (doi:10.1103/PhysRevLett.84.2080)
[713] Hewett J and Spiropulu M 2002 Particle physics probes of extra spacetime dimensions *Ann. Rev. Nucl. Part. Sci.* **52** 397–424 (doi:10.1146/annurev.nucl.52.050102.090706)
[714] Clerbaux B, Mahmoud T, Collard C and Miné P 2006 Search with the CMS detector for heavy resonances decaying into an electron pair *CMS Note* 2006/083
[715] Collard C and Lemaire M-C 2004 Search with the CMS Detector for Randall-Sundrum Excitations of Gravitons Decaying Into Electron Pairs *CMS Note* 2004/024
[716] CMS Collaboration, Acosta D *et al* 2006 CMS Physics Technical Design Report Volume 1, Section 10 *CERN/LHCC*, 2006-001
[717] Clerbaux B, Mahmoud T, Collard C, Lemaire M-C and Litvin V 2006 TeV electron and photon saturation studies *CMS Note* 2006/004
[718] CDF Collaboration, Affolder T *et al* 2001 Measurement of ds/dM and Forward-Backward charge asymmetry for high-mass Drell–Yan e $^{+}$e $^{-}$ pairs from collisions at $\sqrt{s} = 1.8$ TeV *Phys. Rev. Lett.* **87** 131802
[719] CTEQ Collaboration, Lai H L *et al* 2000 Global QCD analysis of parton structure of the nucleon: CTEQ5 parton distributions *Eur. Phys. J.* C **12** 375–392 (doi:10.1007/s100529900196)
[720] CTEQ Collaboration, Stump D *et al* 2003 Inclusive jet production, parton distributions, and the search for new physics *J. High. Energy Phys.* JHEP0310(2003)046 (*Preprint* hep-ph/0303013)
[721] Davoudiasl H, Hewett J L and Rizzo T G 2001 Experimental probes of localized gravity: on and off the wall *Phys. Rev.* D **63** 075004 (*Preprint* hep-ph/0006041)
[722] Cheung K-m and Landsberg G 2000 Drell–Yan and diphoton production at hadron colliders and low scale gravity model *Phys. Rev.* D **62** 076003 (*Preprint* hep-ph/9909218)
[723] Belotelov I, Golutvin I, Bourilkov D, Lanyov A, Rogalev E, Savina M and Shmatov S 2006 Search for ADD extra dimensional gravity in di-muon channel with the CMS Detector *CMS Note* 2006/076
[724] Mohapatra R and Pati J 1975 Left-right gauge symmetry and an 'isoconjugate' model of CP violation *Phys. Rev.* D **11** 566–571 (doi:10.1103/PhysRevD.11.566)
[725] Senjanovic G and Mohapatra R 1975 Exact left-right symmetry and spontaneous violation of parity *Phys. Rev.* D **12** 1502 (doi:10.1103/PhysRevD.12.1502)
[726] Mohapatra R and Senjanovic G 1980 Neutrino mass and spontaneous parity nonconservation *Phys. Rev. Lett.* **44** 912 (doi:10.1103/PhysRevLett.44.912)
[727] Pati J and Salam A 1974 Lepton number as the fourth color *Phys. Rev.* D **10** 275–289
[728] CDF Collaboration, Affolder T *et al* 2001 Search for quark lepton compositeness and a heavy W' boson using the e nu channel in p anti-p collisions at s $^{**}(1/2) = 1.8$-TeV *Phys. Rev. Lett.* **87** 231803 (*Preprint* hep-ex/0107008)
[729] Hof C, Hebbeker T and Hoepfner K 2006 Detection of New Heavy Charged Gauge Bosons in the Muon Plus Neutrino Channel *CMS Note* 2006/117
[730] Gumus K, Akchurin N, Esen S and Harris R M 2006 CMS sensitivity to dijet resonances *CMS Note* 2006/070
[731] Baur U, Hinchliffe I and Zeppenfeld D 1987 Excited quark production at Hadron colliders *Int. J. Mod. Phys.* A **2** 1285
[732] Bagger J, Schmidt C and King S 1988 Axigluon production in hadronic collisions *Phys. Rev.* D **37** 1188
[733] Chivukula R S, Cohen A G and Simmons E H 1996 New strong interactions at the Tevatron? *Phys. Lett.* B **380** 92–98 (*Preprint* hep-ph/9603311)
[734] Hewett J L and Rizzo T G 1989 Low-energy phenomenology of superstring inspired E(6) models *Phys. Rept.* **183** 193
[735] Lane K and Mrenna S 2003 The collider phenomenology of technihadrons in the technicolor Straw man model *Phys. Rev.* D **67** 115011 (doi:10.1103/PhysRevD.67.115011)
[736] Eichten E, Hinchliffe I, Lane K D and Quigg C 1984 Super collider physics *Rev. Mod. Phys.* **56** 579–707
[737] CMS Collaboration, Lemaire M-C, Newman H and Litvin V 2006 Search for Randall-Sundrum excitations of gravitons decaying into two photons for CMS at LHC *CMS Note* 2006/051
[738] CMS Collaboration, Clerbaux B, Mahmoud T, Collard C, Lemaire M-C and Litvin V 2006 TeV electron and photon saturation studies *CMS Note* 2006/004
[739] Acosta D *et al* 2005 Measurement of the Cross Section for Prompt Diphoton Production in $p\bar{p}$ Collisions at $\sqrt{s} = 1.96$ TeV *Phys. Rev. Lett.* **95** 022003 (doi:10.1103/PhysRevLett.95.022003)
[740] Weng J *et al* 2006 Search for ADD Direct Graviton Emission in Photon plus Missing Transverse Energy Final States at CMS *CMS Note* 2006/129
[741] Myers R C and Perry M J 1986 Black holes in higher dimensional space-times *Ann. Phys.* **172** 304

[742] Hawking S W 1975 Particle creation by black holes *Commun. Math. Phys.* **43** 199–220
[743] Argyres P C, Dimopoulos S and March-Russell J 1998 Black holes and sub-millimeter dimensions *Phys. Lett.* B **441** 96–104 (*Preprint* hep-th/9808138)
[744] Harris C M, Richardson P and Webber B R 2003 CHARYBDIS: A black hole event generator *J. High. Energy Phys.* JHEP08(2003)033 (*Preprint* hep-ph/0307305)
[745] Mathews P, Ravindran V and Sridhar K 2005 NLO-QCD corrections to dilepton production in the Randall-Sundrum model *J. High. Energy Phys.* JHEP10(2005)031 (*Preprint* hep-ph/0506158)
[746] Lane K D 2000 Technicolor 2000 *Preprint* hep-ph/0007304
[747] Kreuzer P 2006 Search for Technicolour at CMS in the $\rho_{TC} \to WZ$ channel *CMS Note* 2006/135
[748] Betev B, Bourilkov D and Mavrodiev S. Shch Structure functions of pion and nucleon determined from high mass muon pair production JINR-E2-85-312
[749] Super-Kamiokande Collaboration, Fukuda Y *et al* 1998 Evidence for oscillation of atmospheric neutrinos *Phys. Rev. Lett.* **81** 1562–1567 (*Preprint* hep-ex/9807003)
[750] Esen S and Harris R 2006 CMS sensitivity to quark contact interactions using dijets *CMS Note* 2006/071
[751] Pati J C and Salam A 1975 Anomalous lepton-hadron interactions and gauge models *Phys. Rev.* D **11** 1137–1154 (doi:10.1103/PhysRevD.11.1137)
[752] CMS Collaboration, Gninenko N, Kirsanov M, Krasnikov N and Matveev N 2006 Detection of Heavy Majorana Neutrinos and Right-Handed Bosons *CMS Note* 2006/098
[753] Particle Data Group, Hagiwara K *et al* 2002 Review of Particle Physics *Phys. Rev.* D **66** 010001
[754] Barenboim G, Bernabeu J, Prades J and Raidal M 1997 Constraints on the W(R) mass and CP-violation in left-right models *Phys. Rev.* D **55** 4213–4221 (*Preprint* hep-ph/9611347)
[755] DØ Collaboration, Abachi S *et al* 1996 Search for right-handed W bosons and heavy W' in $p\bar{p}$ collisions at $\sqrt{s}$ =1.8 TeV *Phys. Rev. Lett.* **76** 3271–3276 (*Preprint* hep-ex/9512007)
[756] Datta A, Guchait M and Roy D P 1993 Prospect of heavy right-handed neutrino search at SSC/LHC energies *Phys. Rev.* D **47** 961–966 (*Preprint* hep-ph/9208228)
[757] CMS Collaboration, Karafasoulis K, Kyriakis A, Petrakou H and Mazumdar K 2006 Little Higgs model and top-like heavy quark at CMS *CMS Note* 2006/079
[758] D'Hondt J, Lowette S, Hammad G, Heyninck J and Van Mulders P 2006 Observability of same-charge lepton topology in di-leptonic ttbar events *CMS Note* 2006/065
[759] Larios F and Penunuri F 2004 FCNC production of same sign top quark pairs at the LHC *J. Phys.* G **30** 895–904 (*Preprint* hep-ph/0311056)
[760] Gouz Y P and Slabospitsky S R 1999 Double top production at hadronic colliders *Phys. Lett.* B **457** 177–185 (doi:10.1016/S0370-2693(99)00516-X)
[761] Yue C-X, Zong Z-J, Xu L-L and Chen J-X 2006 Associated production of the top-pions and single top at hadron colliders *Phys. Rev.* D **73** 015006 (*Preprint* hep-ph/0601058)
[762] Kraml S and Raklev A R 2006 Same-sign top quarks as signature of light stops at the LHC *Phys. Rev.* D **73** 075002 (*Preprint* hep-ph/0512284)
[763] Bityukov S I and Krasnikov N V 2000 On the observability of a signal above background *Nucl. Instrum. and Methods* A **452** 518–524 (doi:10.1016/S0168-9002(00)00454-X)
[764] Lehmann E L 1957 A theory of some multiple decision problems *The Annals of Mathematical Statistics* **28 1**
[765] O'Neill R and Wetherill G B 1971 The present state of multiple comparison methods *Journal of the Royal Statistical Society, Series B (Methodological)* **33 2**
[766] Hauser J 2006 Search for new physics in tails of distributionsPrivate communications, paper in preparation
[767] DØ Collaboration, Abazov V M *et al* 2005 Measurement of the $t\bar{t}$ production cross section in $p\bar{p}$ collisions at $\sqrt{s} = 1.96$ TeV using kinematic characteristics of lepton + jets events *Phys. Lett.* B **626** 45–54 (*Preprint* hep-ex/0504043) (doi:10.1016/j.physletb.2005.08.104)
[768] Abbott B *et al* 2000 Search for New physics in $e\mu X$ data at DØ Using Sleuth: a quasi-model-independent search strategy for new physics *Phys. Rev.* D **62** (doi:10.1103/PhysRevD.62.092004)
[769] Abbott B *et al* 2001 A Quasi-Model-Independent search for new physics at large transverse momentum *Phys. Rev.* D **64** (*Preprint* hep-ex/0011067)
[770] Finley C *et al* 2004 On the evidence for clustering in the arrival directions of AGASA's ultrahigh energy cosmic rays *Astroparticle Physics* **21**
[771] Frixione S, Nason P and Webber B R 2003 Matching NLO QCD and parton showers in heavy flavour production *J. High. Energy Phys.* JHEP08(2003)007 (*Preprint* hep-ph/0305252)
[772] Lonnblad L 2002 Correcting the colour-dipole cascade model with fixed order matrix elements *J. High. Energy Phys.* JHEP05(2002)046 (*Preprint* hep-ph/0112284)
[773] Frixione S and Webber B R 2002 Matching NLO QCD computations and parton shower simulations *J. High. Energy Phys.* JHEP06(2002)029 (*Preprint* hep-ph/0204244)

[774] Krauss F 2002 Matrix elements and parton showers in hadronic interactions *J. High. Energy Phys.* JHEP08(2002)015 (*Preprint* hep-ph/0205283)

[775] Mrenna S and Richardson P 2004 Matching matrix elements and parton showers with HERWIG and PYTHIA *J. High. Energy Phys.* JHEP05(2004)040 (*Preprint* hep-ph/0312274)

[776] Butterworth J, Butterworth S, Waugh B, Stirling W and Whalley M 2004 The CEDAR project *Preprint* hep-ph/0412139

[777] LEP Collaboration, 2004 A combination of preliminary electroweak measurements and constraints on the standard model *Preprint* hep-ex/0412015

[778] Stump D R 2002 A new generation of CTEQ parton distribution functions with uncertainty analysis Prepared for 31st International Conference on High Energy Physics (ICHEP 2002), (*Amsterdam, The Netherlands, 24–31 July 2002*)

[779] Stirling W J, Martin A D, Roberts R G and Thorne R S 2005 MRST parton distributions *AIP Conf. Proc.* **747** 16–21

[780] Botje M 2000 A QCD analysis of HERA and fixed target structure function data *Eur. Phys. J.* C **14** 285–297 (*Preprint* hep-ph/9912439)

[781] Alekhin S I 2001 Global fit to the charged leptons DIS data: alpha(s), parton distributions, and high twists *Phys. Rev.* D **63** 094022 (*Preprint* hep-ph/0011002)

[782] Altarelli G and Parisi G 1977 Asymptotic freedom in parton language *Nucl. Phys.* B **126** 298

[783] Lonnblad L 1992 ARIADNE version 4: A program for simulation of QCD cascades implementing the color dipole model *Comput. Phys. Commun.* **71** 15–31

[784] CDF Collaboration, Abe F *et al* 1994 Evidence for color coherence in $p\bar{p}$ collisions at $\sqrt{s} = 1.8$ TeV *Phys. Rev.* D **50** 5562–5579 (doi:10.1103/PhysRevD.50.5562)

[785] DØ Collaboration, Abbott B *et al* 1997 Color coherent radiation in multijet events from $p\bar{p}$ collisions at $\sqrt{s} = 1.8$ TeV *Phys. Lett.* B **414** 419–427 (doi:10.1016/S0370-2693(97)01190-8)

[786] Knowles I G *et al* 1995 QCD event generators *Preprint* hep-ph/9601212

[787] ALEPH Collaboration, Buskulic D *et al* 1992 Properties of hadronic Z decays and test of QCD generators *Z. Phys.* C **55** 209–234

[788] DELPHI Collaboration, Abreu P *et al* 1996 Tuning and test of fragmentation models based on identified particles and precision event shape data *Z. Phys.* C **73** 11–60 (doi:10.1007/s002880050295)

[789] OPAL Collaboration, Alexander G *et al* 1996 A Comparison of b and (u d s) quark jets to gluon jets *Z. Phys.* C **69** 543–560

[790] Andersson B, Gustafson G and Soderberg B 1983 A general model for jet fragmentation *Z. Phys.* C **20** 317

[791] ALEPH Collaboration, Heister A *et al* 2001 Study of the fragmentation of b quarks into B mesons at the Z peak *Phys. Lett.* B **512** 30–48 (*Preprint* hep-ex/0106051)

[792] OPAL Collaboration, Abbiendi G *et al* 2003 Inclusive analysis of the b quark fragmentation function in Z decays at LEP ((B)) *Eur. Phys. J.* C **29** 463–478 (*Preprint* hep-ex/0210031)

[793] SLD Collaboration, Abe K *et al* 2002 Measurement of the b-quark fragmentation function in Z^0 decays *Phys. Rev.* D **65** 092006 (doi:10.1103/PhysRevD.65.092006)

[794] Bowler M G 1981 e+ e- Production of heavy quarks in the String Model *Zeit. Phys.* C **11** 169

[795] Peterson C, Schlatter D, Schmitt I and Zerwas P M 1983 Scaling violations in inclusive e^+e^- annihilation spectra *Phys. Rev.* D **27** 105

[796] Kartvelishvili V, Likhoded A and Petrov V 1978 On the fragmentation functions of heavy quarks into hadrons *Phys. Lett.* B **78** 615

[797] Norrbin E and Sjostrand T 2000 Production and hadronization of heavy quarks *Eur. Phys. J.* C **17** 137–161 (*Preprint* hep-ph/0005110)

[798] Engel R and Ranft J 1999 Color singlet exchange between jets and the PHOJET Monte Carlo *Nucl. Phys. Proc. Suppl.* A **75** 272–274 (doi:10.1016/S0920-5632(99)00263-7)

[799] CDF Collaboration, Affolder T *et al* 2002 Charged jet evolution and the underlying event in proton anti-proton collisions at 1.8 TeV *Phys. Rev.* D **65** 092009 (doi:10.1103/PhysRevD.65.092009)

[800] Nason P *et al* 1999 Bottom production *Preprint* hep-ph/0003142

[801] Sjostrand T and Skands P Z 2005 Transverse-momentum-ordered showers and interleaved multiple interactions *Eur. Phys. J.* C **39** 129–154 (*Preprint* hep-ph/0408302) (doi:10.1140/epjc/s2004-02084-y)

[802] Sapeta S and Golec-Biernat K 2005 Total, elastic and diffractive cross sections at LHC in the Miettinen-Pumplin model *Phys. Lett.* B **613** 154–161 (*Preprint* hep-ph/0502229)

[803] Lange D J 2001 The EvtGen particle decay simulation package *Nucl. Instrum. Methods* A **462** 152–155

[804] Bartalini P 2005 Supporting Monte Carlo Generators at the LHC *Proceedings of the 10th International Conference on B-Physics at Hadron Machines* (Assisi Perugia, Italy June, 2005) ed M Biasini and S Erhan volume 156, *Published in Nucl. Phys B - Proceedings Supplements 1* (doi:10.1016/j.nuclphysbps.2006.02.123)
[805] Sullivan Z 2002 Fully differential W production and decay at next-to- leading order in QCD *Phys. Rev.* D **66** 075011 (*Preprint* hep-ph/0207290)
[806] Dobbs M A *et al* 2004 Les Houches guidebook to Monte Carlo generators for hadron collider physics *Preprint* hep-ph/0403045
[807] HIJING Web Site Located at http://www-nsdth.lbl.gov/ xnwang/hijing/index.html
[808] Gleisberg T *et al* 2005 Event generator for the LHC *Preprint* hep-ph/0508315
[809] Boos E *et al* 2001 Generic user process interface for event generators *Preprint* hep-ph/0109068
[810] Lokhtin I P and Snigirev A M 2000 Nuclear geometry of jet quenching *Eur. Phys. J.* C **16** 527–536 (*Preprint* hep-ph/0004176) (doi:10.1007/s100520000437)
[811] Lokhtin I P and Snigirev A M 2004 Fast simulation of jet quenching in ultrarelativistic heavy ion collisions SINP MSU-13/752 *Preprint* hep-ph/0406038
[812] Lokhtin I P and Snigirev A M 2003 Fast simulation of flow effects in central and semi-central heavy ion collisions at LHC *Preprint* hep-ph/0312204
[813] CDF Collaboration, Field R D 2001 The underlying event in hard scattering processes *eConf* C **010630** P501 (*Preprint* hep-ph/0201192)
[814] CompHEP Collaboration, Boos E, Bunichev V, Dubinin M, Dudko L, Edneral V, Ilyin V, Kryukov A, Savrin V, Semenov A and Sherstnev A 2004 Web site at http://theory.sinp.msu.ru/comphep. See also [355]
[815] Lokhtin I P, Sarycheva L I and Snigirev A M 2002 The method for analysing jet azimuthal anisotropy in ultrarelativistic heavy ion collisions *Phys. Lett.* B **537** 261–267 (*Preprint* hep-ph/0203144) (doi:10.1016/S0370-2693(02)01913-5)
[816] Carena M, Daleo A, Dobrescu B A and Tait T M P 2004 Z' gauge bosons at the Tevatron *Phys. Rev.* D **70** 093009 (doi:10.1103/PhysRevD.70.093009)
[817] Balazs C, Qiu J-w and Yuan C P 1995 Effects of QCD resummation on distributions of leptons from the decay of electroweak vector bosons *Phys. Lett.* B **355** 548–554 (doi:10.1016/0370-2693(95)00726-2)
[818] Balazs C and Yuan C P 1997 Soft gluon effects on lepton pairs at hadron colliders *Phys. Rev.* D **56** 5558–5583 (doi:10.1103/PhysRevD.56.5558)
[819] Martin A D, Roberts R G, Stirling W J and Thorne R S 2003 Uncertainties of predictions from parton distributions I: Experimental errors *Eur. Phys. J.* C **28** 455–473 (*Preprint* hep-ph/0211080)
[820] Holland J H 1975 Adaptation in natural and artificial systems (The University of Michigan Press, Ann Arbor)
[821] Goldberg D E 1989 Genetic algorithms in search, optimization and machine learning (Addison: Wesley)
[822] Abdullin S 2003 Genetic algorithm for SUSY trigger optimization in CMS detector at LHC *NIM A* **502** 693–695 (doi:10.1016/S0168-9002(03)00546-1)
[823] TOTEM Collaboration, 2004 TOTEM Technical Design Report *CERN/LHCC*, 2004-002
[824] TOTEM Collaboration, 2004 Addendum to the TOTEM-TDR *CERN/LHCC*, 2004-020
[825] Avati V and Österberg K 2005 TOTEM forward measurements: leading proton acceptance *Proceedings of the HERA-LHC Workshop* (CERN/DESY: January, 2005) Available at http://www.desy.de/ heralhc/proceedings/wg4avati.pdf
[826] Kalliopuska J *et al* 2005 TOTEM forward measurements: exclusive central diffraction *Proceedings of the HERA-LHC Workshop* (CERN/DESY: January, 2005) Available at http://www.desy.de/ heralhc/proceedings/wg4pXp_heralhc.pdf
[827] The MAD-X Program, Methodical Accelerator Design Information available at http://www.cern.ch/mad
[828] Arneodo M *et al* 2005 Diffractive Higgs: CMS/TOTEM Level-1 Trigger Studies *Proceedings of the HERA-LHC Workshop* (CERN/DESY: January, 2005) Available at http://www.desy.de/ heralhc/proceedings/wg4arneodo.pdf
[829] Croft R 2006 (In preparation) PhD Thesis, University of Bristol
[830] Oljemark F 2006 First level triggering of diffractively produced low-mass Higgs at The Large Hadron Collider, University of Helsinki
[831] Bruni G *et al* 2005 Leading proton production in ep and pp, experiments: how well do high-energy physics Monte Carlos reproduce the data? *Proceedings of the HERA-LHC Workshop* (CERN/DESY: January, 2005) Available at http://www.desy.de/ heralhc/proceedings/wg5lps.pdf
[832] Ferro F 2005 Diffractive Higgs in CMS/TOTEM: study of L1 trigger conditions from T1 and T2 *TOTEM Note* **04-2005**
[833] Cox B and Forshaw J 2002 Herwig for diffractive interactions *Comput. Phys. Commun.* **144** 104–110 (doi:10.1016/S0010-4655(01)00467-2)

[834] Collins J C 1997 Light-cone variables, rapidity and all that *Preprint* hep-ph/9705393
[835] Albrow M G and Rostovtsev A 2000 Searching for the Higgs at hadron colliders using the missing mass method *Preprint* hep-ph/0009336
[836] Albrow M G 2005 Double pomeron physics at the LHC *AIP Conf. Proc.* **792** 509–514 (*Preprint* hep-ex/0507095)

Colour plates CP1–CP9

Various figures are in colour throughout the online edition but only plates CP1–CP9 are in colour in both the print and online editions.

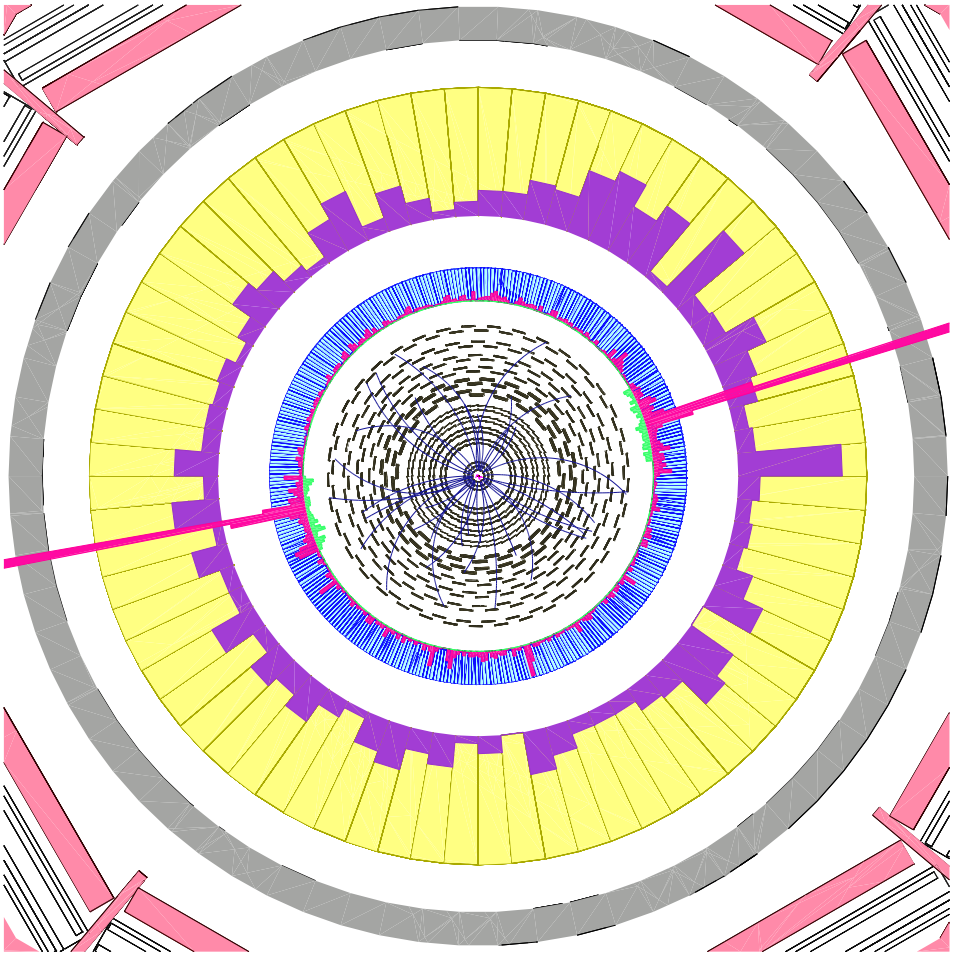

Figure CP1. Example of a $pp \to H + X$ event with Higgs particle decay $H \to \gamma\gamma$. (See section 2.1.)

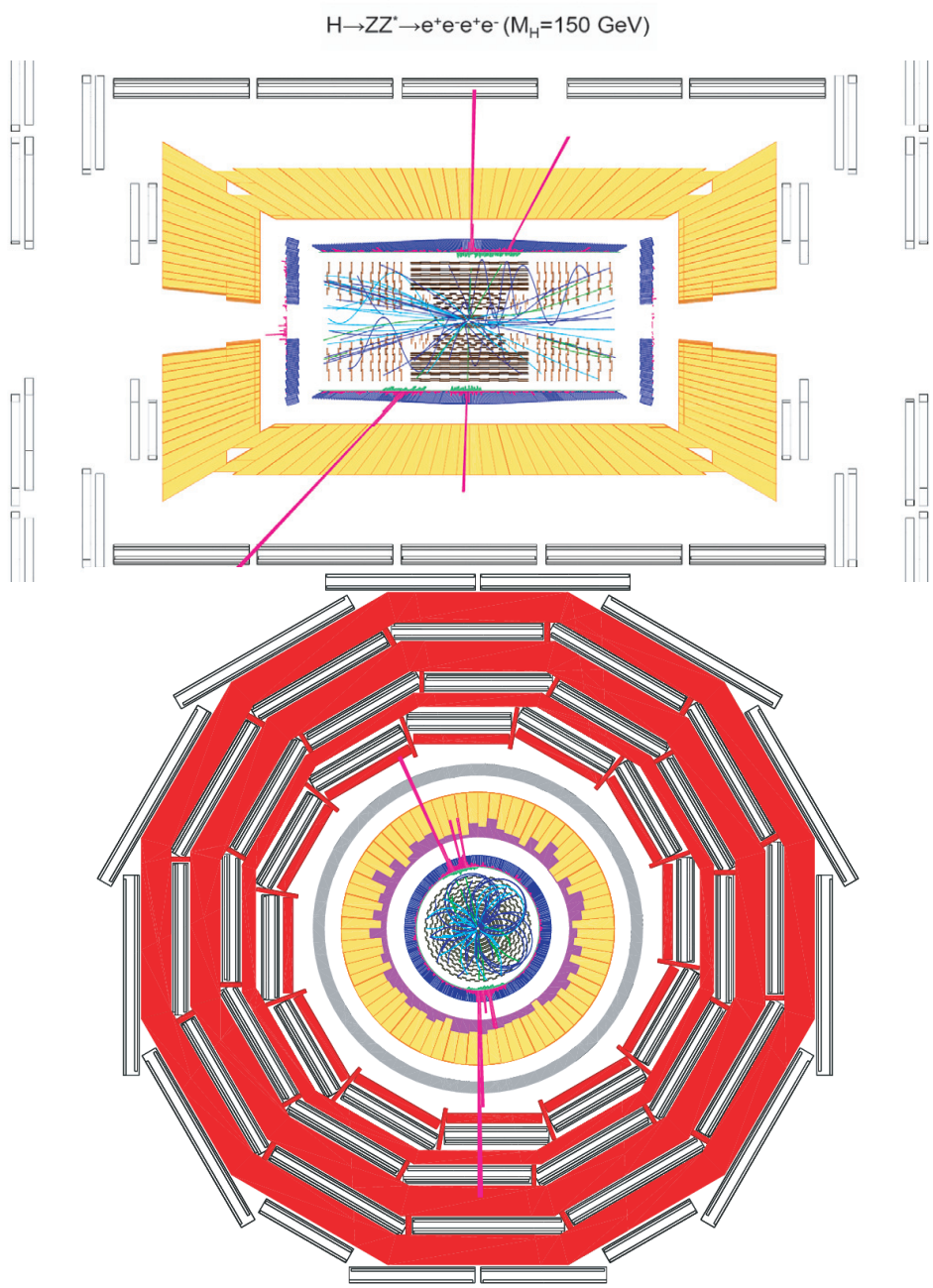

Figure CP2. Display of an event candidate in the CMS detector at the LHC for the Standard Model Higgs boson decay channel $H \to ZZ^* \to 4e$. The event is shown in a longitudinal (top) and transversal (bottom) projection of the detector. A mass of $150\,\mathrm{GeV/c^2}$ is measured from the reconstructed electrons. (See section 2.2.)

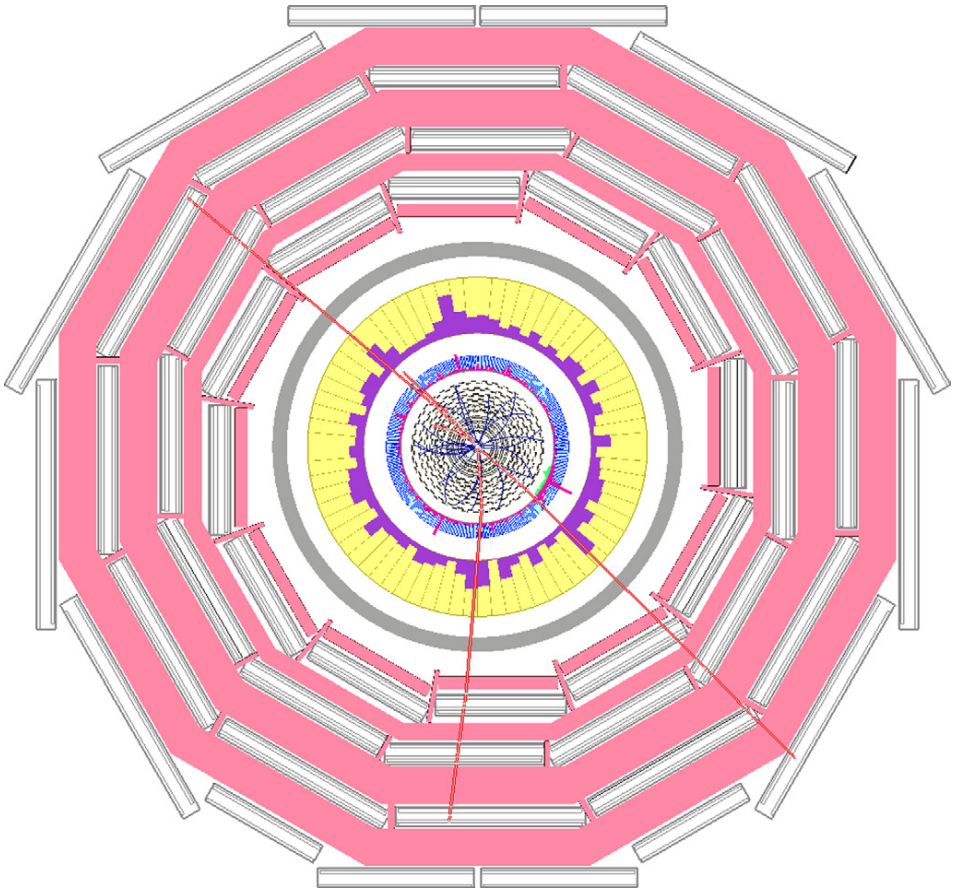

Figure CP3. Example of a $H \rightarrow ZZ \rightarrow 4\mu$ event showing only the reconstructed tracks. One muon goes in the endcap detectors. (See section 3.1.1.)

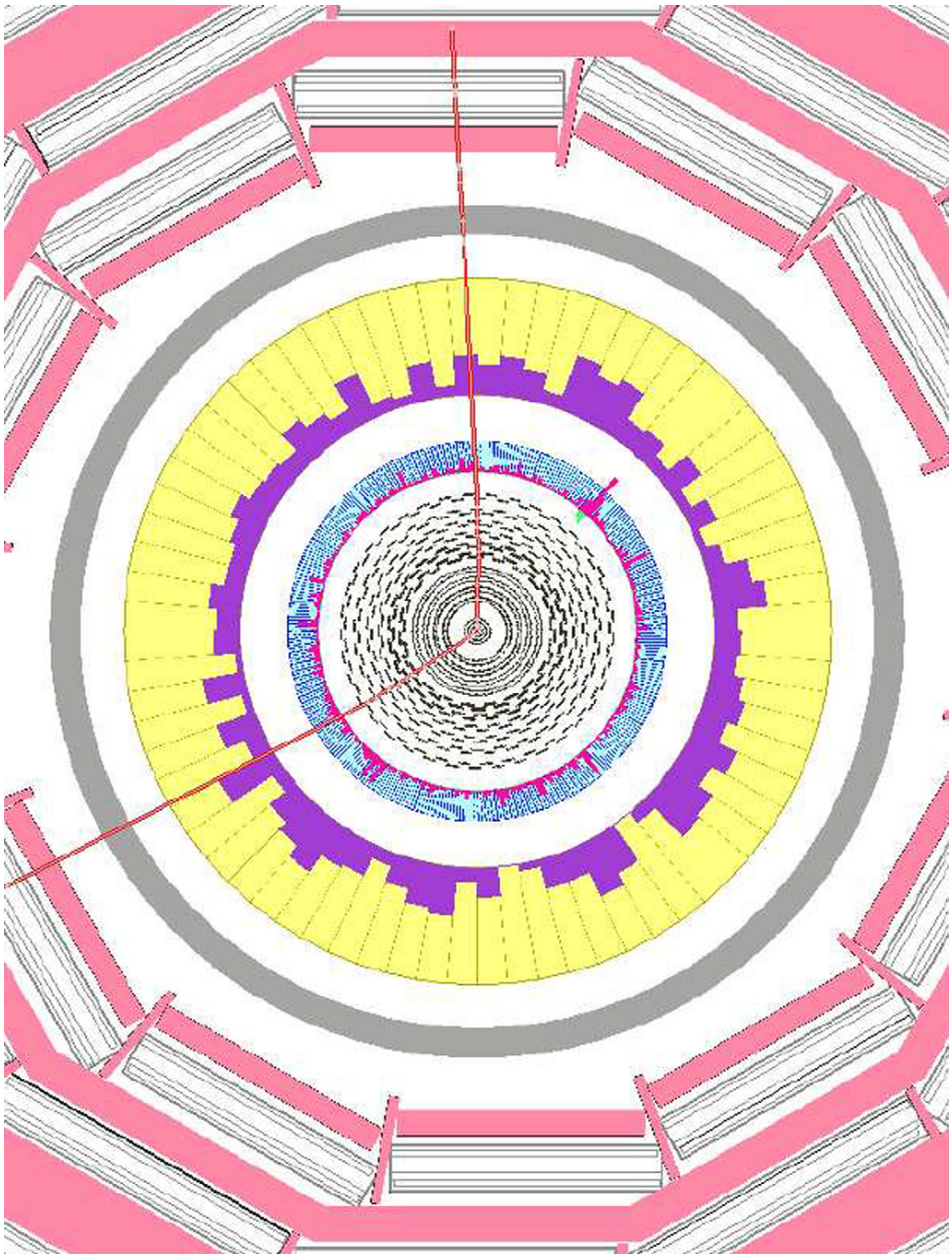

Figure CP4. Example of a pp $\rightarrow$ H + X event with H $\rightarrow$ WW $\rightarrow \mu\nu\mu\nu$. (See section 3.2.2.1.)

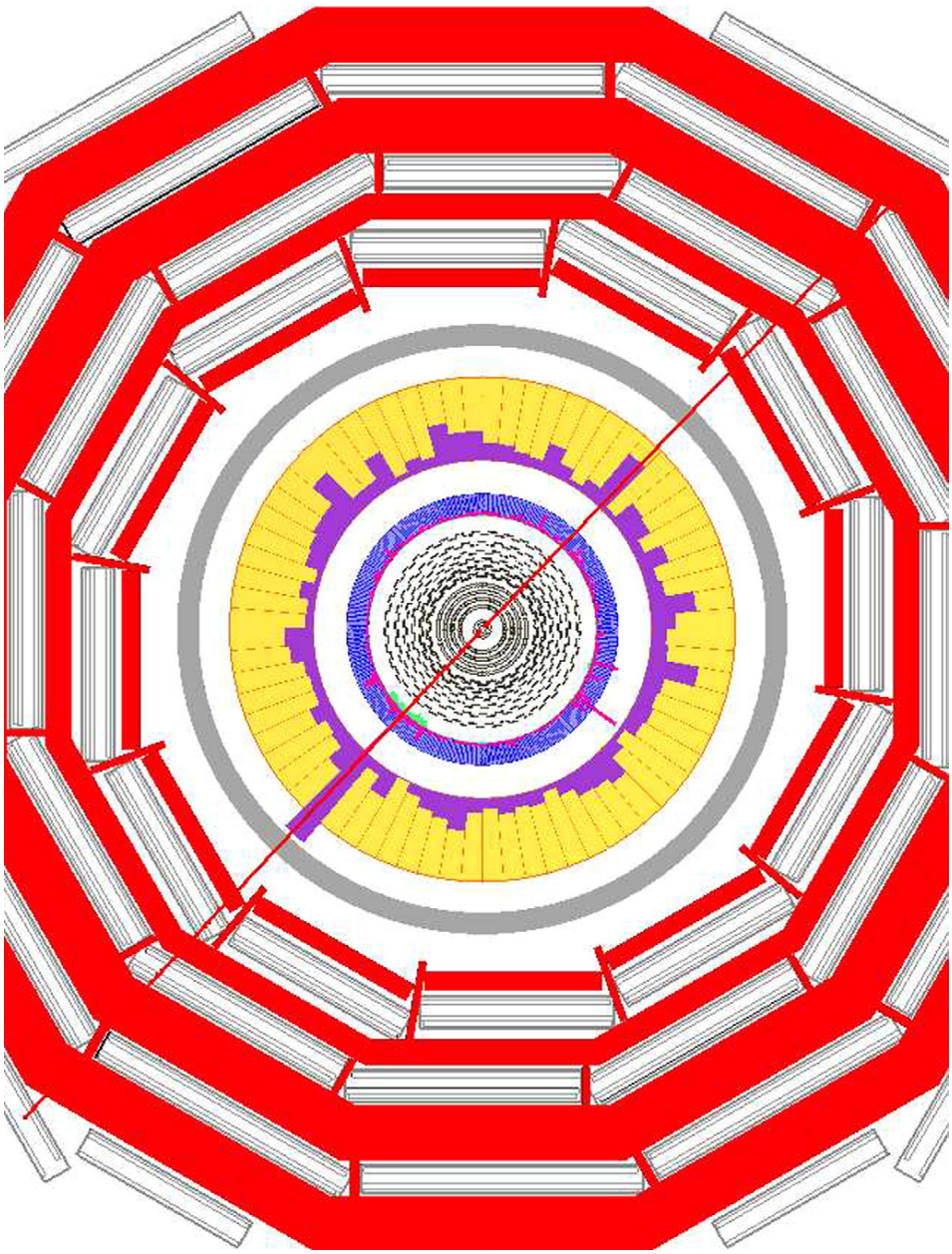

Figure CP5. Typical simulated event of a dimuon decay of $3\,\mathrm{TeV/c^2}$ Z′ produced at $\mathcal{L} = 2 \times 10^{33}\,\mathrm{cm^{-2}\,s^{-1}}$, showing the muon tracks only. (See section 3.3.1.)

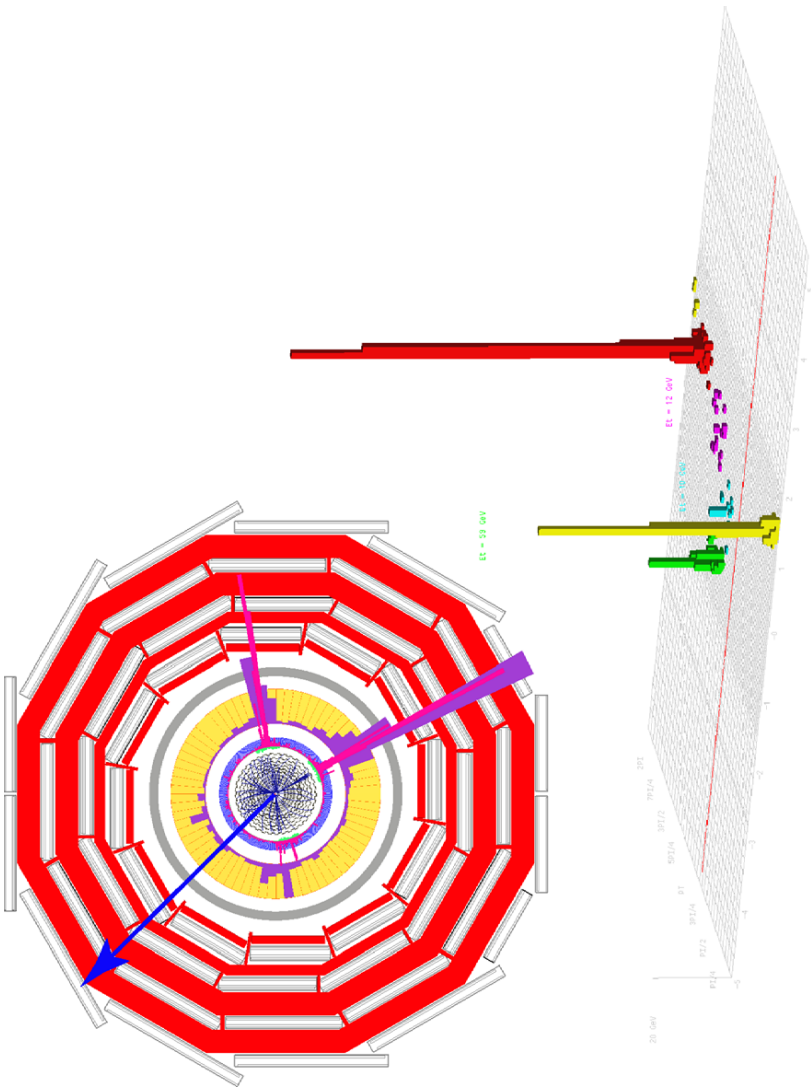

Figure CP6. Event display of SUSY candidate event that survives the requirements of the multijet+missing energy analysis of section 13.5. The three highest E_T jets are 330, 140 and 60 GeV while the missing transverse energy is 360 GeV. The Lego $\eta - \phi$ calorimeter display shows the three leading jets, colour coded red-yellow-green, while the missing energy ϕ is indicated with the red line. The transverse $x - y$ view shows relative depositions of the jets in the calorimeter systems as well as the reconstructed tracks and the missing energy vector direction (in blue).

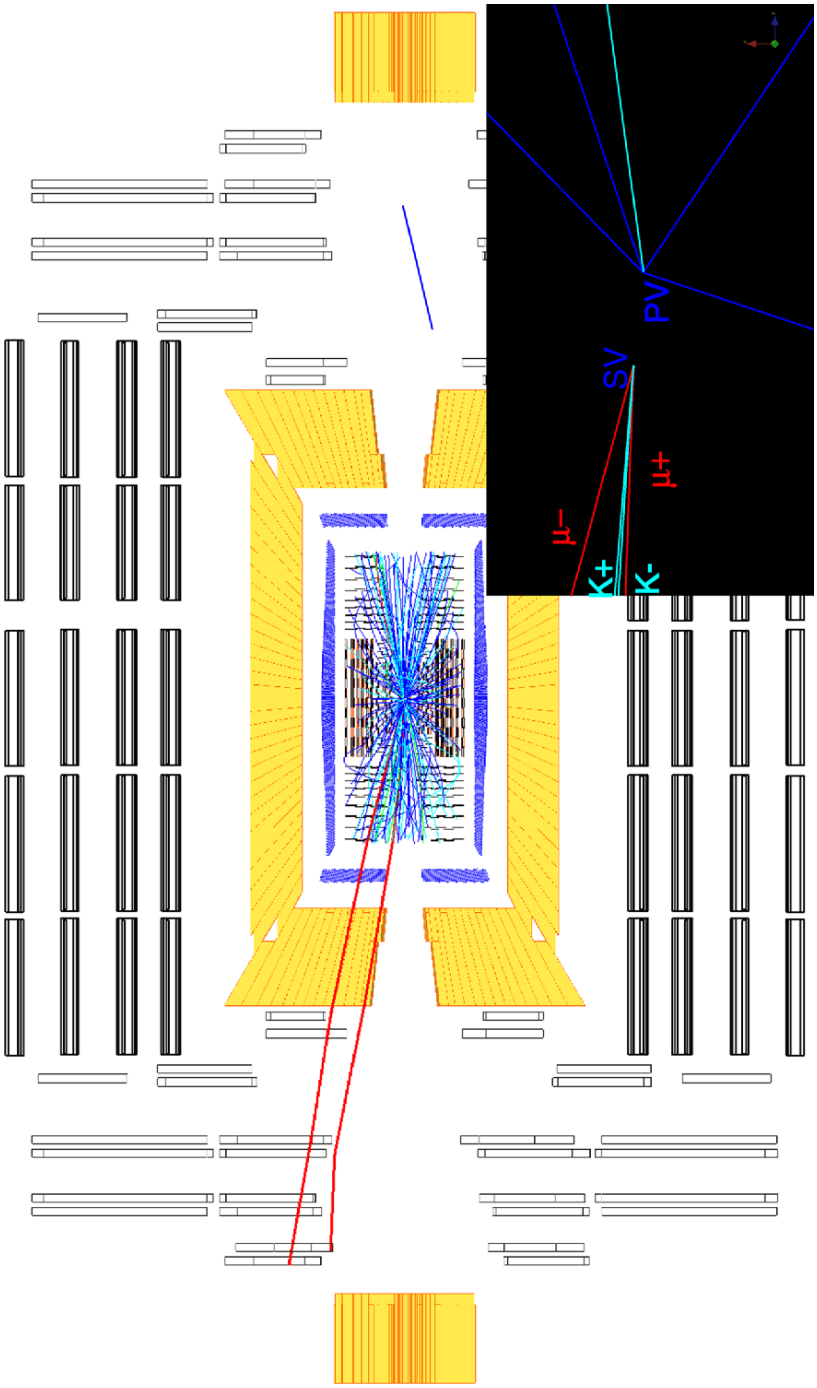

Figure CP7. Example of a $pp \to B_s + X$ event with $B_s \to J/\psi\phi$. (See section 5.1.1.)

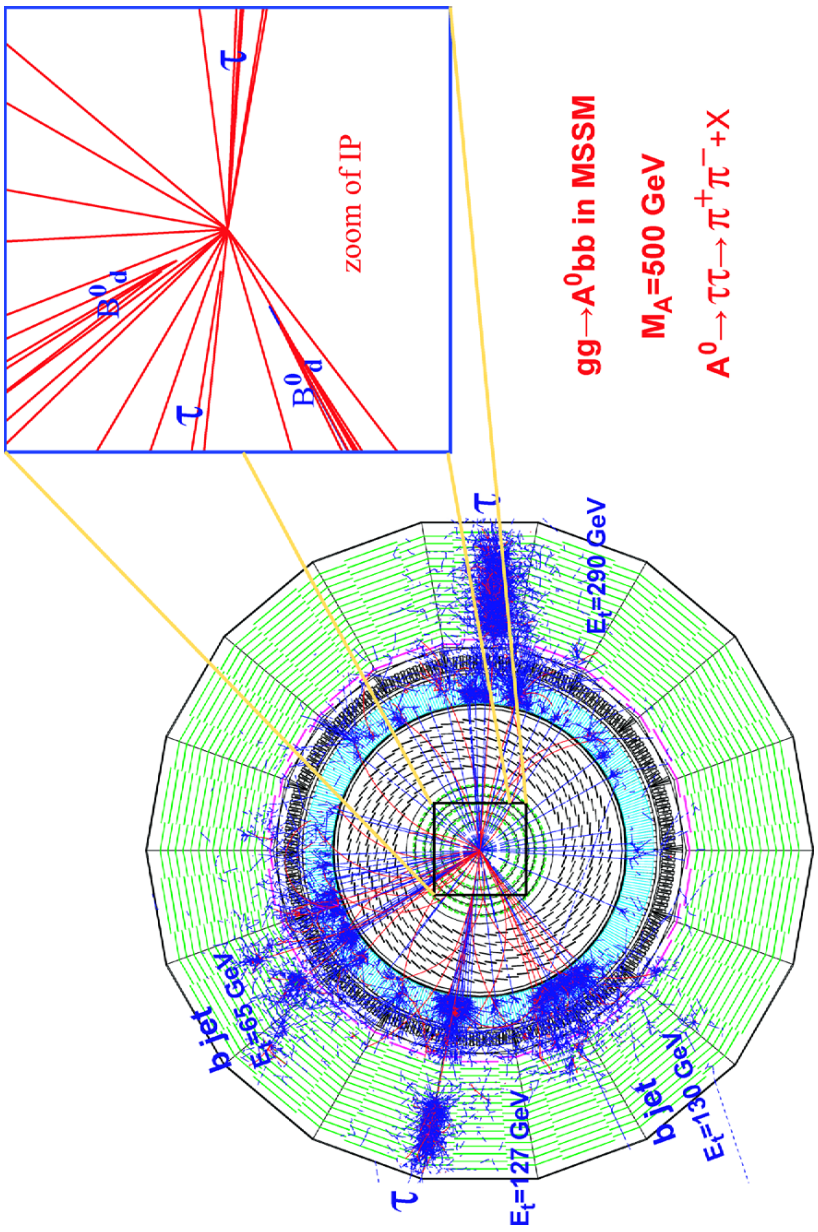

Figure CP8. Example of a pp → H + X event with H → $\tau\nu\tau\nu$. (See section 5.2.1.)

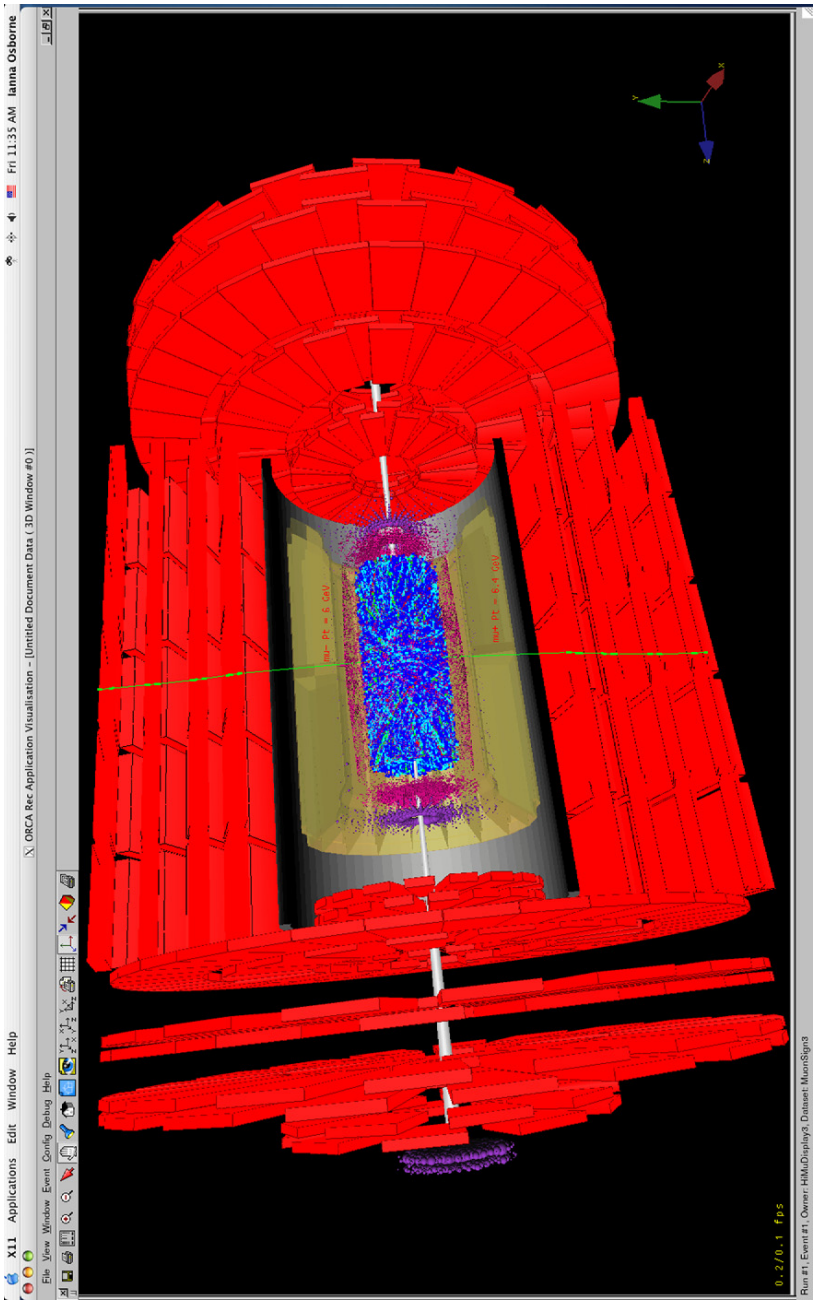

Figure CP9. $\Upsilon \to \mu^+\mu^-$ event embedded in a PbPb collision at $\sqrt{s_{NN}} = 5.5$ TeV with charged multiplicities at mid-rapidity $dN_{ch}/d\eta|_{\eta=0} = 3500$. (See section 6.1.)